



**California Traffic Control Devices Committee (CTCDC)  
Agenda Item Report**



<b>Meeting Date:</b> November 02, 2023 <b>Item Number:</b> 20-12	<b>From:</b> Florencia Allenger, PE, Caltrans
<b>Sponsored By:</b> Yue Wang, PE, Caltrans	<b>Presented By:</b> Barbara S. Linke, Dr.-Ing. habil., Professor, Department of Mechanical and Aerospace Engineering, University of California Davis
<b>Description:</b> Request for Closure of Experiment on "Orange Contrast Temporary Pavement Delineation in Construction Zones"	

**Recommendation**

Motion by committee to approve closure of CTCDC Experiment 20-12 – "Orange Contrasted Temporary Pavement Delineation in Construction Zones" [and FHWA experiment 6(09)-59(E) - Orange Contrast Temporary Pavement Markings - CA DOT] after receipt of final report dated September 30, 2023.

**Agency Making Request/Sponsor:**

AHMCT Research Center at UC Davis for Caltrans DRISl and District 11 / Yue Wang, CTCDC Member

**Background:**

The final report for CTCDC Experiment 20-12 – Orange Contrasted Temporary Pavement Delineation in Construction Zones [and FHWA experiment 6(09)-59(E) - Orange Contrast Temporary Pavement Markings - CA DOT] has been completed by the Advanced Highway Maintenance and Construction Technology (AHMCT) Research Center of the Department of Mechanical and Aerospace Engineering at University of California (UC) Davis. The research was conducted and Report Number CA23-3836 prepared under a task order with Caltrans Division of Research, Innovation and System Information (DRISl).

**Attachment:**

Attachment A – Technical Report for Orange Contrast Temporary Pavement Delineation in Construction Zones



# ATTACHMENT A



California Traffic Control Devices Committee (CTCDC)  
Agenda Item Report



**Attachment A –**

**Technical Report for Orange Contrast Temporary Pavement Delineation in Construction Zones**

**ADA Notice**  
 For individuals with sensory disabilities, this document is available in alternate formats. For information call (916) 654-6410 or TDD (916) 654-3880 or write Records and Forms Management, 1120 N Street, MS-89, Sacramento, CA 95814.

1. REPORT NUMBER <b>CA23-3836</b>	2. GOVERNMENT ASSOCIATION NUMBER <b>N/A</b>	3. RECIPIENT'S CATALOG NUMBER <b>N/A</b>
4. TITLE AND SUBTITLE <b>Orange Contrasted Temporary Pavement Delineation in Construction Zones</b>		5. REPORT DATE <b>09/30/2023</b>
		6. PERFORMING ORGANIZATION CODE <b>AHMCT Research Center, UC Davis</b>
7. AUTHOR <b>Barbara Linke, Wilderich White, Kin Yen, Felicia Fashanu, Nathan Byrd</b>		8. PERFORMING ORGANIZATION REPORT NO. <b>UCD-ARR-23-09-30</b>
9. PERFORMING ORGANIZATION NAME AND ADDRESS <b>AHMCT Research Center UCD Dept. of Mechanical &amp; Aerospace Engineering Davis, California 95616-5294</b>		10. WORK UNIT NUMBER <b>N/A</b>
		11. CONTRACT OR GRANT NUMBER <b>65A0749 Task 3836</b>
		13. TYPE OF REPORT AND PERIOD COVERED <b>Final report 04/01/21 -09/30/23</b>
12. SPONSORING AGENCY AND ADDRESS <b>California Department of Transportation P.O. Box 942873, MS #83 Sacramento, CA 94273-0001</b>		14. SPONSORING AGENCY CODE <b>Caltrans</b>
15. SUPPLEMENTARY NOTES <b>N/A</b>		
16. ABSTRACT <p>The California Department of Transportation (Caltrans) needs to maintain safety on its roads, including during construction in work zones. Orange temporary striping promises to increase driver awareness of construction work zones. This project collected and analyzed quantitative and subjective data about driver behavior and traffic incidents to understand the effectiveness of orange temporary delineations in work zones. A survey with 1,185 responses showed a clear preference of drivers for the temporary orange striping. A positive effect of orange temporary striping with slightly reduced average vehicle speeds was found. Retroreflectivity and color measurements showed expected trends of fading colors and diminishing retroreflectivity, and the findings will help with setting quality requirements for potential future installations.</p>		
17. KEY WORDS <b>Work zone safety; lane striping</b>	18. DISTRIBUTION STATEMENT <b>No restrictions. This document is available to the public through the National Technical Information Service, Springfield, Virginia 22161.</b>	
19. SECURITY CLASSIFICATION (of this report) <b>Unclassified</b>	20. NUMBER OF PAGES <b>130</b>	21. COST OF REPORT CHARGED <b>N/A</b>

# DISCLAIMER

The research reported herein was performed by the Advanced Highway Maintenance and Construction Technology (AHMCT) Research Center, within the Department of Mechanical and Aerospace Engineering at the University of California – Davis, for the Division of Research, Innovation and System Information (DRISI) at the California Department of Transportation. AHMCT and DRISI work collaboratively to complete valuable research for the California Department of Transportation.

This document is disseminated in the interest of information exchange. The contents of this report reflect the views of the authors who are responsible for the facts and accuracy of the data presented herein. The contents do not necessarily reflect the official views or policies of the State of California or the Federal Highway Administration. This publication does not constitute a standard, specification or regulation. This report does not constitute an endorsement by the Department of any product described herein.

The contents of this report do not necessarily reflect the official views or policies of the University of California. This report does not constitute an endorsement by the University of California of any product described herein.

For individuals with sensory disabilities, this document is available in alternate formats. For information, call (916) 654-8899, TTY 711, or write to California Department of Transportation, Division of Research, Innovation and System Information, MS-83, P.O. Box 942873, Sacramento, CA 94273-0001.



# **Advanced Highway Maintenance and Construction Technology Research Center**

Department of Mechanical and Aerospace Engineering  
University of California at Davis

## **Orange Contrasted Temporary Pavement Delineation in Construction Zones**

Barbara Linke, Wilderich White, Kin Yen, Felicia Fashanu, Nathan Byrd

Report Number: CA23-3836  
AHMCT Research Report: UCD-ARR-23-09-30  
Interim Task Report of Contract: 65A0749 Task 3836

09/30/2023

## **California Department of Transportation**

Division of Research, Innovation and System Information

# Table of Contents

Table of Contents	ii
List of Figures	iv
List of Tables	ix
List of Acronyms and Abbreviations	x
Chapter 1: Background	1
State of the Art	2
Chapter 2: Assessment of driver behavior in the work zones with orange delineation	4
Visually observed driver behavior	4
Analysis of video recordings from temporarily installed cameras	7
Camera system specification and installation	8
Camera locations	10
Road markings to support video analysis	15
Video analysis	17
Findings on lane keeping behavior	26
Interim conclusion	30
Chapter 3: Assessment of driver perception	31
Survey results	31
Time progression of responses	33
Additional participant comments	34
Interim conclusion	35
Chapter 4: Evaluation of visibility of orange temporary striping	37
State of the art	37
Measurement of retroreflectivity	38
Methodology	38
Results for orange temporary striping in the work zone	40
Measurement of striping color	44
Test measurements	45
Results for orange temporary striping in the work zone	46
Dashboard camera recordings	51
Striping quality evaluation for orange tape striping	52
Interim conclusion	56
Chapter 5: Analysis of Influence on speed and accidents	58

State of the Art_____	58
Traffic incidents in the work zones _____	58
Comparison of data bases _____	61
Localized PeMS accident data analysis _____	63
TIMS accident data analysis _____	67
Vehicle Speed in the Work zone _____	68
General findings and interim conclusions _____	74
Chapter 6: Conclusions _____	76
References _____	79
Appendix A – Details on camera system design and installation _____	82
Power system including batteries and solar panel _____	82
Component Installation Details _____	86
General findings for camera installation _____	89
Appendix B – Feasibility study of use of Light Detection and Ranging sensors _____	90
Introduction _____	90
Objectives and Requirements _____	90
State of the Art_____	90
LiDAR Systems Hardware _____	91
Software _____	92
Use of LiDAR technology for driver behavior evaluation _____	94
Proof of Concept _____	95
General findings and future work _____	103
Appendix C – Survey on orange striping perception _____	104
Survey questions _____	104
Survey results _____	108



# List of Figures

Figure 1.1: Workers in a work zone in the I-5 NCC project \_\_\_\_\_ 1

Figure 1.2: Orange preceding white striping in southbound (SB) direction (left); orange along both sides of white striping in northbound (NB) direction (right) (photos: courtesy of Caltrans) \_\_\_\_\_ 2

Figure 2.1: Left: Visual observation of driver lane keeping on Palomar Airport Rd Overcrossing over I-5, south view on SB traffic. Right: Using the three-part clicker for recording and smartphone as timer on Las Flores Overcrossing over I-5, south view on SB traffic. \_\_\_\_\_ 4

Figure 2.2: Lane keeping observation from Las Flores Overcrossing, south view, SB traffic, Thursday, 1/13/ 2022, start 9:43 am \_\_\_\_\_ 5

Figure 2.3: Bias observation from Las Flores Overcrossing, south view, NB traffic, Thursday, 1/13/2022, start 10:05 am \_\_\_\_\_ 6

Figure 2.4: Comparison of bias from Las Flores Overcrossing, south view, for SB and NB traffic, 3 minutes per lane \_\_\_\_\_ 6

Figure 2.5: Examples for lane keeping and pavement joints, left: Las Flores, I-5 south view, lane 2, SB traffic; right: I-5, Tustin, CA, NB traffic; both pictures taken on 1/13/2022 \_\_\_\_\_ 7

Figure 2.6: Diagram of the camera system. \_\_\_\_\_ 8

Figure 2.7: Diagram of camera position with relationship to freeway lanes and vehicles. \_\_\_\_\_ 10

Figure 2.8: Camera locations on I-5 (map obtained from [www.google.com/maps](http://www.google.com/maps)). \_\_\_\_\_ 12

Figure 2.9: Road marking; Left: photo; Right: diagram of freeway and road markings with nominal values (black) and measured values (red) \_\_\_\_\_ 16

Figure 2.10: Road marking application with spray paint \_\_\_\_\_ 16

Figure 2.11: Positioning of road markings; left: with laser perpendicular to road (x1, x2, x3); right: with wheel along the road (yi) \_\_\_\_\_ 17

Figure 2.12: Definition of Mean of vehicle distance from lane center (MLP) and Standard deviation of lateral position (SDLP) \_\_\_\_\_ 18

Figure 2.13: Video screenshots with different views, from Las Flores Overcrossing, south view, SB traffic; left: close view; middle: intermediate view; right: far view \_\_\_\_\_ 18

Figure 2.14: Video screenshots at night with different numbers of cars, left: from Jefferson Overcrossing, north view, NB traffic, night time; right: from Las Flores Overcrossing, S view, SB traffic \_\_\_\_\_ 19

Figure 2.15: Video screenshots at night from Jefferson Overcrossing, north view, NB traffic; left: color video; right black & white video \_\_\_\_\_ 19

Figure 2.16: Lane distance measurement (example video from Richards Blvd Overcrossing over I-80, Davis, CA), left: line tool, right: marker tool \_\_\_\_\_ 20

Figure 2.17: Analysis of Figure 2.16 left measurements: (a) lane distance measurement in pixel and (b) resolution measurement for a lane width of 12 ft _____	21
Figure 2.18: Transformation of region of interest _____	22
Figure 2.19: Automated Yolo vehicle center analysis _____	23
Figure 2.20: Manual vehicle center measurement _____	23
Figure 2.21: Trendline of errors at Las Flores, NB and SB direction; in the morning (11 am and 10 am) and night (10 pm) for 10 cars each _____	24
Figure 2.22: Trendlines of errors per CCTV camera (10 cars per video) _____	25
Figure 2.23: Automated Yolo vehicle center analysis for 1,604 vehicles on 1/26/22 (Wednesday) at 10 am, 10-min video, Jefferson Overcrossing, NB traffic _____	26
Figure 2.24: Lane keeping behavior for lanes 1 to 4 from automated Yolo vehicle center analysis, Jefferson Overcrossing, selected weekdays at 10 am, 10-min videos; average speed from HERE Technologies data for 1 h at Las Flores Dr/Exit 51A (closest location to Jefferson Overcrossing) _____	27
Figure 2.25: Lane keeping behavior for lane 2 from automated Yolo vehicle center analysis, Las Flores Overcrossing, selected Wednesdays at 10 am, 10-min videos (Mean is not weighted by car count); average speed from HERE Technologies data for 1 h at Las Flores Dr/Exit 51A _____	28
Figure 2.26: Lane keeping behavior from automated Yolo vehicle center analysis, Cassidy Overcrossing, SB direction, selected Wednesdays at 10 am, 10-min videos; average speed from HERE Technologies data for 1 h at Cassidy St/Exit 51C _____	29
Figure 3.1: Visual for question Q5 on pattern preference. _____	32
Figure 3.2: Change of responses and ratio of yes to no answers to question Q3 _____	34
Figure 3.3: Change of responses and ratio of yes to no answers to question Q8 _____	35
Figure 4.1: Test locations _____	39
Figure 4.2: Left: Striping quality measurements performed by AHMCT researcher and Caltrans staff days after orange striping installation; Right: Retroreflectivity and nighttime color measurements on tape striping on I-5, _____	39
Figure 4.3: Measurement routine per stripe pattern _____	40
Figure 4.4: Retroreflectivity measurements at 0 months after orange striping installation; Left: on northbound stripe (Orange left, white middle, orange right stripes); Right: on southbound orange preceding stripe (Orange and white stripes); n = 48 measurements per bar _____	41
Figure 4.5: Average retroreflectivity values Av. RL over time after orange striping installation; error bars show standard deviation $\sigma_{RL}$ (n = 48 measurements for NB White, SB Orange, and SB White; n = 96 measurements for NB Orange) _____	42
Figure 4.6: Microscope pictures from orange (left) and white (right) temporary striping on Nov. 14, 2022 _____	43
Figure 4.7: Average retroreflectivity values Av. RL over time after orange striping installation for NB orange left and right stripes separately; error bars show	

standard deviation $\sigma_{RL}$ (n = 48 measurements for NB O-Left and NB-O-Right each)	44
Figure 4.8: Test daytime color measurements, n=5 to 13 measurements per sample type	45
Figure 4.9: Test nighttime color measurements, n= 6 to 20 measurements per sample type	46
Figure 4.10: Daytime color measurements on measurements at 0 months after orange striping installation, compared with ASTM Standard D6628 (n =48 measurements per stripe type)	47
Figure 4.11: Nighttime color measurements on measurements at 0 months after orange striping installation, compared with ASTM Standard D6628 (48 measurements per stripe type)	48
Figure 4.12: Average daytime color coordinates over time after orange striping installation, compared with regions in ASTM Standard D6628 (n = 48 measurements for NB White, SB Orange, SB White (except for 12.6 months, $n_{SB\ Orange} = 27$ and $n_{SB\ White} = 24$ ); n = 96 measurements for NB Orange); arrows indicate increasing number of months	49
Figure 4.13: Average nighttime color coordinates over time after orange striping installation, compared with regions in ASTM Standard D6628 (n = 48 measurements for NB White, SB Orange, SB White; n = 96 measurements for NB Orange); arrows indicate increasing number of months	50
Figure 4.14: Screenshots from dashboard camera videos from June 14 and 15, 2021 of work zones with temporary white striping; Left: I-5 northbound during the day; Right: I-5 southbound at night.	51
Figure 4.15: Screenshots from dashboard camera videos in southbound direction, at Las Flores exit, daytime versus nighttime, lane 3, May 2022	52
Figure 4.16: Screenshots from dashboard camera videos in northbound direction, at Cannon Rd exit, daytime versus nighttime, lanes 3 and 4, May 2022	52
Figure 4.17: Tape on freeway concrete surface with grinding grooves (left); Orange tape striping worn (at 5 months) and new	53
Figure 4.18: Daytime color measurements on new and worn orange tape, 3 worn stripes after 5 months of installation, 1 new stripe	53
Figure 4.19: Nighttime color and retroreflectivity measurements on new and worn orange tape, 3 worn stripes after 5 months of installation, 1 new stripe	54
Figure 4.20: Color degradation of orange along both sides of white tape after exposure to sunlight	54
Figure 4.21: Retroreflectivity measurements of orange tape, left in the sunshine after installation on May 22, 2022, 4 stripes, measured 3x each	55
Figure 4.22: Daytime color measurements of orange tape, left in the sunshine after installation on May 22, 2022; 4 stripes, measured 3x each; white, yellow and red color areas from ASTM D6628-16	55

Figure 4.23: Nighttime color measurements of orange tape, left in the sunshine after installation on May 22, 2022; 4 stripes, measured 3x each; white and yellow color areas from ASTM D6628-16, _____	56
Figure 5.1: Vehicle Miles Traveled for 5-month periods in NB and SB direction, Abs PM 46 – 52, from PeMS database _____	60
Figure 5.2: Vehicle Miles Traveled per month for 2022 in NB and SB direction, Abs PM 46 - 52, from PeMS database _____	60
Figure 5.3: PeMS and SWITRS NB accidents between Abs PM 46 – 52 in 5-month periods, normalized by VMT _____	62
Figure 5.4: PeMS and SWITRS SB accidents between Abs PM 46 – 52 in 5-month periods, normalized by VMT _____	62
Figure 5.5: Northbound accident counts with linear continuous trendlines in WZ and corridor excluding WZ, PeMS data _____	64
Figure 5.6: Southbound accident counts with linear continuous trendlines in WZ and corridor excluding WZ, PeMS data _____	64
Figure 5.7: Northbound weekly accidents normalized by the weekly VMT with linear trendlines (bold lines for WZ, dotted lines for corridor excluding WZ), divided into three time periods, PeMS data _____	65
Figure 5.8: Southbound weekly accidents normalized by the weekly VMT with linear trendlines (bold lines for WZ, dotted lines for corridor excluding WZ), divided into three time periods, PeMS data _____	66
Figure 5.9: TIMS accident type numbers and distribution for Abs PM 46 – 51 during selected 5-month periods (data downloaded on 7/31/23) _____	67
Figure 5.10: HERE average speed data at 10:00 am to 10:59 am from Abs PM 47 to 51, only Wednesdays _____	70
Figure 5.11: Average speed from HERE data, per day, at 10:00 am, Las Flores ramps, with linear trendlines _____	71
Figure 5.12: Average speed from HERE data, per day, at 10:00 AM, Tamarack ramps, with linear trendlines _____	72
Figure 5.13: Average speed from HERE data, per day, at 10:00 pm, Las Flores ramps, with linear trendlines _____	73
Figure 5.14: Median average speed from HERE data, per day, at 10:00 pm, Las Flores ramps, with linear trendlines _____	74
Figure A1.1: Comparing the effect of panel tilt (20°, 40°, 60°) on energy output – San Diego and Sacramento _____	83
Figure A1.2: Comparing the effect of panel tilt on energy output – San Diego_	83
Figure A1.3: Comparing the effect of azimuth angle (Vertical scale different than prior figures) _____	84
Figure A1.4: Solar panel and electronics box installation _____	85
Figure A1.5: Pictures of electronics box and solar panel _____	85
Figure A1.6: Camera installation on Jefferson Overcrossing (left) and Las Flores Overcrossing (right) _____	86
Figure A1.7: Details of camera mounting and cabling at Las Flores Overcrossing _____	87

Figure A1.8: Left: Installation of electronics box at Jefferson Overcrossing with a bucket truck; right: straps around the steel pole.	88
Figure A1.9: Access to electronics box: Left: at Jefferson Overcrossing, Right: at Las Flores Overcrossing.	88
Figure A2.1: Multi-beams 360 degree LiDAR sensor	91
Figure A2.1: Velodyne VLP16 LiDAR sensor with a 30 degree tilt from horizontal	95
Figure A2.2: Example of a single frame point cloud from C1 (Top image shows roadside view; middle image shows top view; bottom image shows roadway view along the direction of vehicle travel.)	97
Figure A2.3: Example of a single frame point cloud from C3 (Top image shows roadside view; middle image shows top view; bottom image shows roadway view along the direction of vehicle travel)	98
Figure A2.4: Example of a single frame point cloud from C3 (Top image shows roadside view; middle image shows top view; bottom image shows roadway view along the direction of vehicle travel)	99
Figure A2.5: Example of a single frame point cloud from C4 (Top image shows roadside view; middle image shows top view; bottom image shows roadway view along the direction of vehicle travel)	100
Figure A2.6: High level conceptual point cloud post-processing steps	102

# List of Tables

Table 2.1: Cameras at Jefferson Overcrossing (installed January 2022) \_\_\_\_\_ 13

Table 2.2: Cameras at Las Flores Overcrossing (installed January 2022) \_\_\_\_\_ 13

Table 2.3: Camera at Cassidy Overcrossing (installed June 2022) \_\_\_\_\_ 14

Table 2.4: Camera at Palomar Airport Rd Overcrossing (installed June 2022) \_\_\_\_\_ 14

Table 2.5: Cameras at La Costa Overcrossing (installed June 2022) \_\_\_\_\_ 15

Table 4.1: Manufacturer orange color coordinates (X,Y) for WZ Orange Fast Dry Waterborne (TT-P-1952F Type I & II), by 2020 Ennis-Flint, Inc, 2020 \_\_\_\_\_ 48

Table 5.1: Locations of interest \_\_\_\_\_ 59

Table 5.2: Examined 5-month periods \_\_\_\_\_ 59

Table 5.3: Total accident count (NB and SB) for the 9 first 5-months periods from 04/14/18 to 9/14/2022 (as defined in Table 5.2) for Abs PM 46 – 52; data downloaded in June and July 2023 \_\_\_\_\_ 61

Table 5.5: Northbound Trendline Equations and R<sup>2</sup> value \_\_\_\_\_ 66

Table 5.6: Southbound Trendline Equations and R<sup>2</sup> value \_\_\_\_\_ 66

Table 5.7: Comparison of data source quality for average vehicle speed \_\_\_\_\_ 69

Table 5.8: Median average speeds (mph) from HERE data for different time periods and locations \_\_\_\_\_ 74

Table A2.1: LiDAR experiment configuration descriptions and their name \_\_\_\_\_ 96

# List of Acronyms and Abbreviations

<b>Acronym</b>	<b>Definition</b>
Abs	Absolute
AHMCT	Advanced Highway Maintenance and Construction Technology Research Center
Av. RL	Average retroreflectivity
CA	California
Caltrans	California Department of Transportation
CCTV	Closed-circuit television
CHP	California Highway Patrol
DOT	Department of Transportation
DRISI	Caltrans Division of Research, Innovation and System Information
E	East
FOV	Field of view
fps	Frames per second
GB	Giga byte
I	Interstate
JF	Jefferson Overcrossing
LF	Las Flores Overcrossing
LiDAR	Light Detection and Ranging
MLP	Mean of vehicle distance from lane center
N	Sample size

<b>Acronym</b>	<b>Definition</b>
NB	Northbound
NCC	North Coast Corridor
PDO	Personal damage only
PeMS	Caltrans Performance Measurement System
PIOs	Public Information Offices
PM	Postmile
R	Realigned
RL	Coefficient of retroreflected luminance
ROS	Robotic Operating System
SANDAG	San Diego Association of Governments
SB	Southbound
SDLP	Standard deviation of lateral position
SWITRS	Statewide Integrated Traffic Records System
TIMS	Transportation Injury Mapping System
USB	Universal Serial Bus
VMT	Vehicle miles traveled
W	West
WDR	Wide dynamic range
WZ	Work zone
Yolo	"You Only Look Once", video processing algorithm
$\sigma$ RL	Standard deviation of RL



# Chapter 1: Background

The California Department of Transportation (Caltrans) needs to maintain safety on its roads, including during construction in work zones. Replacement of pavement delineation with temporary striping and lane shifts during construction often leave behind ghost lines and pavement removal scarring, which can confuse drivers. Practices in other countries and testing in three U.S. states indicated that orange temporary delineation can reduce driver confusion and improve worker safety, but this had not yet been tested in California.

This project assessed the influence of orange pavement delineation in a work zone in Caltrans District 11 in the Interstate 5 (I-5) North Coast Corridor (NCC) Construction Project in San Diego County (Figure 1.1). The construction started with standard temporary white striping and then temporary orange contrast striping was added later. The different time periods with white and orange temporary striping allowed the researchers to compare driver behavior and evaluate the effectiveness of the orange temporary delineation. There were two alternatives used for orange striping with lane lines. The southbound (SB) direction had orange preceding white temporary striping (Figure 1.2 left); the northbound (NB) direction had orange along both sides of white striping (Figure 1.2 right). The orange contrast with the right edge line, lane drop, and gores was the same in both directions.



**Figure 1.1: Workers in a work zone in the I-5 NCC project**



**Figure 1.2: Orange preceding white striping in southbound (SB) direction (left); orange along both sides of white striping in northbound (NB) direction (right) (photos: courtesy of Caltrans)**

This project collected measurable and subjective data about driver behavior and traffic incidents. In particular, the following assessments were performed and will be discussed in the succeeding chapters:

- Assessment of driver behavior in the work zones with orange delineation as compared to work zones with standard temporary white delineation,
- Assessment of driver perception of effectiveness of orange delineation,
- Evaluation of visibility of orange temporary striping,
- Analysis of influence on traffic incidents and speed.

## **State of the Art**

Several countries and U.S. states have experimented with using orange temporary striping. Orange is one of the most salient colors in human perception as Shaw et al. (2017) pointed out in their review of international use of orange striping (Shaw et al., 2017).

A study in Wisconsin with orange pavement marking tapes in a work zone did not demonstrate statistically significant differences between the distributions of vehicle lane position data for the test and control sites. Speed data also showed similar driver behavior for both sites. Driver surveys with 60 participants indicated a better visibility of orange markings. (Shaw et al., 2018)

Researchers at the Kentucky Transportation Center tested several combinations of paint and glass bead variations. Acknowledging challenges in controlling all variables, the researchers found that waterborne paint had low retroreflectivity and wore off quickly. Spray thermoplastic had higher retroreflectivity and was more durable than waterborne paint. High-build waterborne paint markings were best to see at night. Average speeds in the work zone with orange striping, control work zones, and regular highway did not

show any differences. Unfortunately, it seemed that very few drivers lowered their speed as they travelled through a work zone; however, wet and nighttime crashes were reduced with orange temporary striping. (Lammers-Staats et al., 2021)

There are several current studies in progress. In Texas, the effectiveness of orange temporary striping is assessed through vehicle lateral position, retroreflectivity and color values of the striping, as well as driver opinions (Finley, 2020). Lane shifts in and out of the work zone are being evaluated in the Texas study. In Indiana, orange tape and paint stripes with different bead packages were evaluated for their visibility, color, and wear (Williamson, 2023). Findings suggested that orange pavement markings reduce crashes in work zones. A survey confirmed higher driver awareness of work zones when orange striping was present and higher visibility of orange temporary striping over white or yellow striping (Williamson, 2023). The Washington State Department of Transportation (DOT) is planning to investigate the effectiveness of orange temporary (n/a, 2023).

# Chapter 2:

## Assessment of driver behavior in the work zones with orange delineation

Driver behavior in work zones with orange delineation was evaluated using three means: visual observation, video recordings from temporarily installed closed-circuit television (CCTV) cameras, and Light Detection and Ranging (LiDAR) sensors. The visual observation will be discussed in the next section followed by the video analysis. Appendix A gives more details on camera system design and installation. The LiDAR measurements were preliminary feasibility studies and are described in Appendix B.

### Visually observed driver behavior

Initial visual observations of driver behavior were performed from Palomar Airport Road Overcrossing over I-5 with tally marks (Figure 2.1 left). This location was not yet a work zone but provided a good and safe observation location. A protocol to record lane keeping was developed by counting cars that were either in the middle, drifted to the left, or drifted to the right for a given time per lane with tally marks on paper. The initial protocol was refined with a longer recording time and the use of a clicker (Figure 2.1 right).



**Figure 2.1: Left: Visual observation of driver lane keeping on Palomar Airport Rd Overcrossing over I-5, south view on SB traffic. Right: Using the three-part clicker for recording and smartphone as timer on Las Flores Overcrossing over I-5, south view on SB traffic.**

The protocol to perform visual observation was:

1. Find a safe location, preferably on an overcrossing to be able to stand above a particular lane.
2. Note time, date, location, direction of view, and direction of traffic.
3. Move over lane 1.
4. Set timer for 3 minutes and start timer.
5. Count all vehicles with clicker until timer alarm goes off:
  - a. Left clicker for left biased vehicle,
  - b. Middle clicker for vehicle in lane center,
  - c. Right clicker for right biased vehicle.
6. Note all numbers and reset clickers and timer.
7. Move to next lane and repeat steps 4, 5, 6 until all lanes in this traffic direction were covered.

Note that the left clicker counts bias towards the K-rail / inner shoulder for outgoing traffic or bias towards outside shoulder for incoming traffic.

The SB traffic under the Las Flores Overcrossing came after a right on-ramp from State Route 78 (SR-78), and most cars were in lanes 2, 3, and 4 (Figure 2.2). The NB traffic came from a curve and approaching an off-ramp to SR-78, so the largest number of cars accumulated in lane 4 (Figure 2.3). The traffic density for SB and NB was close with 230 and 237 cars respectively for 3 minutes.

Las Flores bridge, south view, southbound traffic

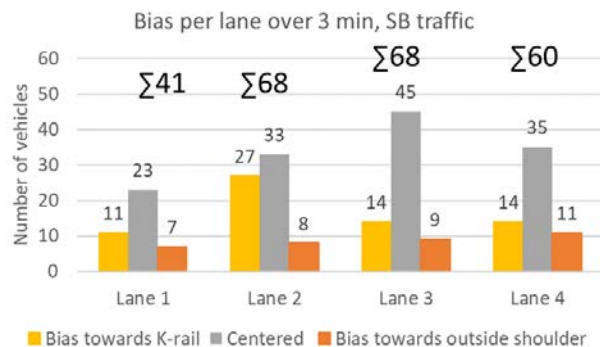


**Figure 2.2: Lane keeping observation from Las Flores Overcrossing, south view, SB traffic, Thursday, 1/13/ 2022, start 9:43 am**

Las Flores bridge, south view, northbound traffic

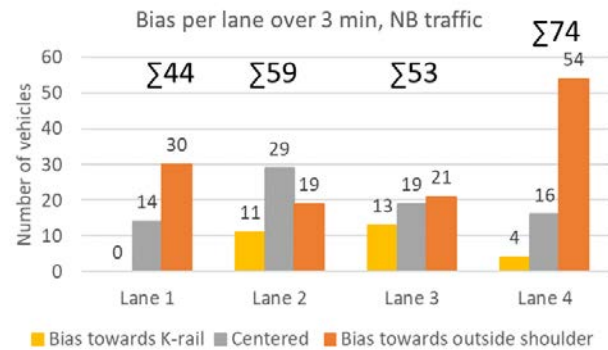


**Figure 2.3: Bias observation from Las Flores Overcrossing, south view, NB traffic, Thursday, 1/13/2022, start 10:05 am**

Most of the SB traffic was centered, with a proportion of 49% and higher, and more vehicles were biased towards the K-rail than the outside shoulder on any lane (Figure 2.4 left). The NB traffic had a very strong bias towards the outside shoulder on lanes 1 (68%) and 4 (73%), which also followed the drift from the curve (Figure 2.4 right). Lanes 2 and 3 had more cars in the center of each lane, but in general, the bias towards the outside shoulder was bigger than towards the K-rail. The curve seemed to have a significant impact on the lane position of the cars.

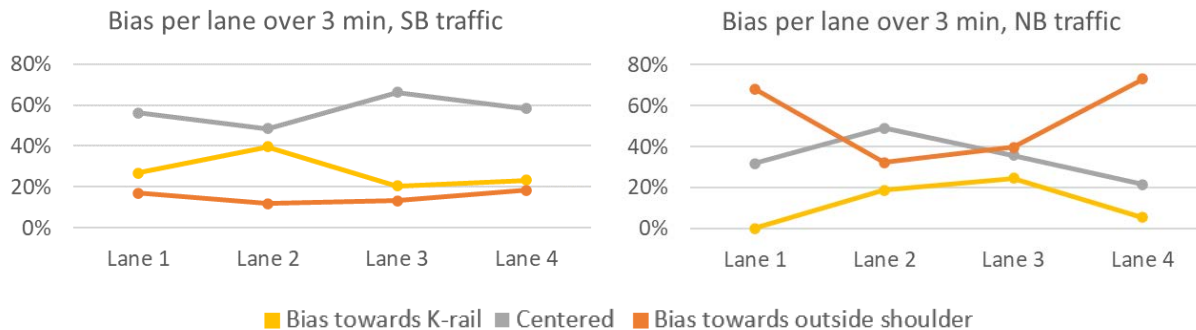


**Figure 2.4: Comparison of bias from Las Flores Overcrossing, south view, for SB and NB traffic, 3 minutes per lane**

The slabs of the concrete added additional features to the lanes and might have also affected driver behavior. For example, a straight slab seam, as in Figure 2.5 left, tempted drivers to stay on one side, especially drivers in smaller cars. Figure 2.4 left shows a larger bias of lane 2 towards the K-rail than for all other lanes. Figure 2.5 right shows slab seams moving across lane markings, which might have confused drivers. No quantitative measurements were taken in this study, but the influence of pavement joints and vehicles ahead on driver behavior need to be considered.



**Figure 2.5: Examples for lane keeping and pavement joints, left: Las Flores, I-5 south view, lane 2, SB traffic; right: I-5, Tustin, CA, NB traffic; both pictures taken on 1/13/2022**

Some findings include:

- Positioning the observer directly above the lane is helpful to make a good decision on vehicle lane keeping. Video recordings from a fixed camera position will have distorted views on lanes to the left and right of the camera.
- Visual observations are based on quick and ternary decisions, which are sometimes hard to make.
- Instead of left/middle/right, a five-part decision with very left/little left/middle/little right/very right would give more detailed results.
- Traffic coming towards the observer was easier to evaluate because there is longer time to watch each vehicle.
- Lane keeping was impacted by curves and large road defects.
- The clicker method for bias observation does not allow for recording lane changes or lane hits easily.

It was decided to rely on video recordings instead of visual observations to have more data points and a less subjective analysis.

## **Analysis of video recordings from temporarily installed cameras**

Any video analysis needs careful consideration of camera specification, camera location, and automated analysis routines, which will be discussed in the following subsections before showing results on lane keeping behavior in the work zone.

# Camera system specification and installation

The specifications of the CCTV camera system were chosen with regard to overall power need for the system, solar energy input, battery storage capacity, camera specifications (pixel size, zoom, pan and tilt options), data transmission over mobile phone networks and direct Ethernet connection, and mounting. The camera operation needed a system of cameras, solar chargers, batteries, modems, further electronics, and housing (Figure 2.6).

AHMCT and Caltrans decided that the electronics box, solar panels, and cameras did not need to be on the same pole, which led to higher installation effort but increased flexibility for component placing. The camera location prioritized video information; the electronics box location prioritized accessibility for AHMCT researchers to trouble-shoot and download data; and the solar panel location prioritized maximum solar energy intake.

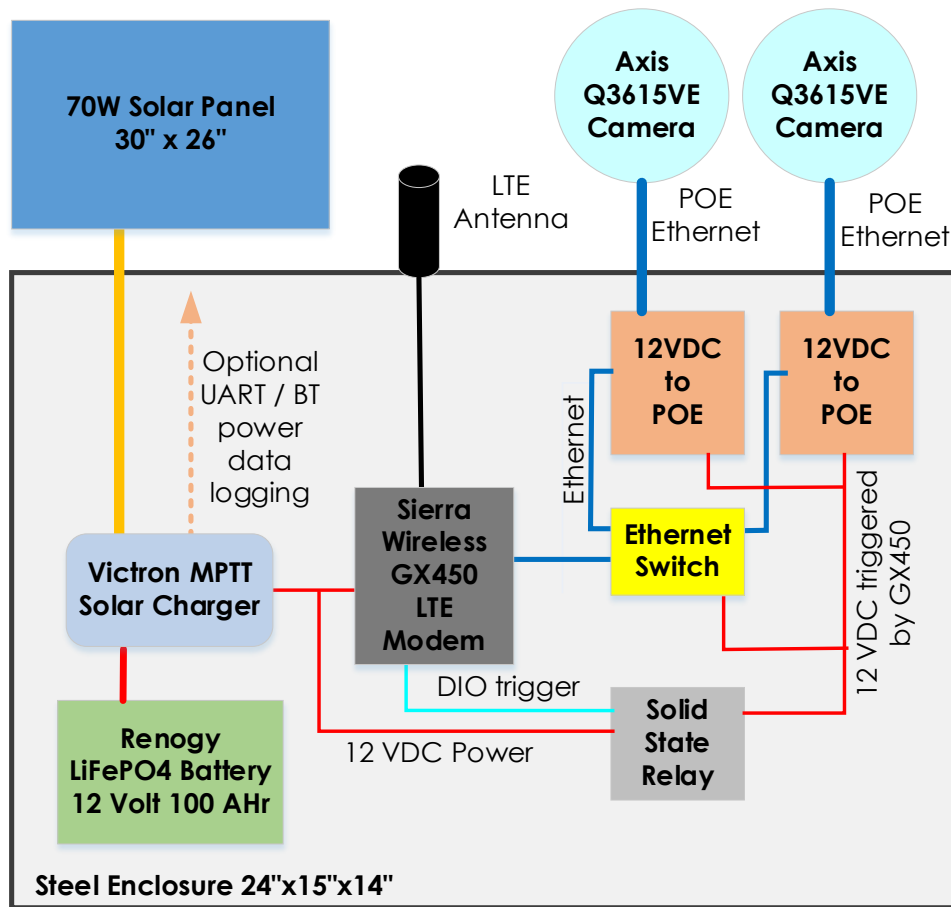


Figure 2.6: Diagram of the camera system.

The cameras were mounted on overcrossings, which allowed for an ideal top view of one lane and low distortion views of more lanes compared to pole



mounting in the median or on the side of the freeway where all lanes would be distorted in the camera view.

The camera system was designed based on the following requirements:

- The CCTV video must be of high quality for observation of vehicle speeds and lane keeping.
- The cameras must be accessible via internet because the AHMCT researchers were not local and needed to collect videos on different days and at different times and seasons.
- The video file size is related to the video quality but consumes local storage space and data transmission rates.
- All components need to be powered.
- Tampering with components by random pedestrians should be avoided.
- The cameras should be installed as high as possible.

The Axis Communications Q3615VE camera was chosen for the CCTV camera based on high video quality, remote accessibility, and the additional functions of pan, tilt, and zoom. It supported a 256 Gigabyte (GB) micro-SD card for video recording storage internally. The video quality was defined by the following criteria:

- Resolution – The resolution of the video is defined by the pixel size of the CCTV sensor. The chosen camera could record video up to 1920 x 1080 resolution with 60 frames per second (fps) or 30 fps with wide dynamic range (WDR) video.
- Frame rate – The frame rate defines the number of pictures per second, which is related to the information content and the smoothness of the video.
- Color versus black and white video – The color impacts the information density. While black and white videos used less storage and were sufficient for most computer video analysis routines, the color videos were preferred for human analysis.
- Video compression – Depending on the activity level in the video, the video size is impacted. For example, more moving vehicles produced larger video files than stationary vehicles or empty roads.
- Additional camera functions – The pan and tilt abilities increased the possible field of view. From prior experience, the pan and tilt option was deemed necessary in case the camera view moved over time. Zoom

allowed for enlarging an area of interest.

The entire CCTV system was solar powered (70 Watt solar panel) with a 12 Volt 100 AHr LiFePO<sub>4</sub> battery. The Sierra Wireless GX450 modem had a digital output port that could be remotely triggered by a solid state relay to turn the cameras on and off to conserve power. The cameras could be controlled over mobile phone networks and direct Ethernet connection. Figure 2.6 shows a diagram of the final system components. The battery voltage and temperature inside the enclosure could also be monitored remotely. The battery charge state could be estimated based on the battery voltage. The system design was minimized with regard to size and weight to minimize the mounting requirement. Appendix A details the selection process for the solar panel and battery as well as the system installation efforts.

## Camera locations

Initially, different camera locations were considered, including mounting on overcrossings, existing lamp posts, and temporary wood poles in the median or at the side of the road. The camera location was examined in connection with camera optimal mount height and vehicle distance in the different lanes (Figure 2.7).

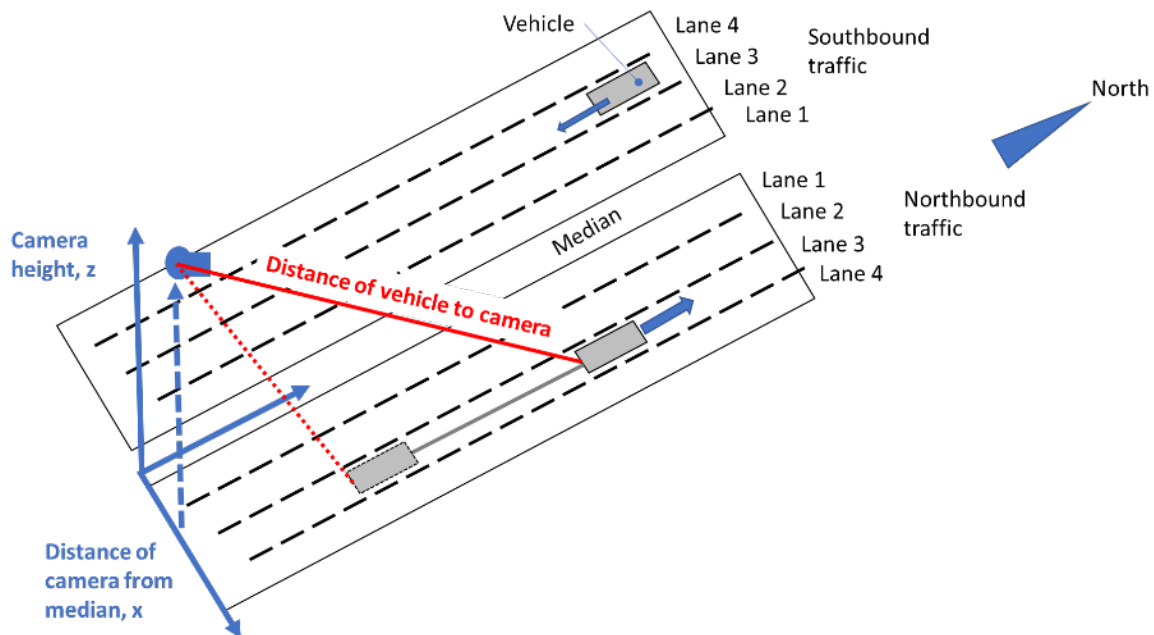


**Figure 2.7: Diagram of camera position with relationship to freeway lanes and vehicles.**

There was a desired camera location from the information standpoint, but this location might not be feasible for safety and access; for example, the median gives a broad field of view, but the camera would not be easily

accessible for AHMCT researchers. The manual observation and test videos showed that the camera positioned as centrally as possible over a lane would minimize shadow effects and allow for finding the vehicle center within the lane.

The camera locations needed to have a large field of view and should include important road features, such as curves, marking schemes, or ramps. Initially, observing vehicle behavior at on- or off-ramps was discussed but was omitted to focus on the striping effect within the work zone. It was decided to focus on the following general conditions and locations, as shown in Figure 2.8:

- Taper shift between regular traffic zone with normal striping and work zone with orange temporary striping (Cassidy Overcrossing and Palomar Airport Rd Overcrossing),
- Straight road in work zone with orange temporary striping (Jefferson Overcrossing),
- Curve in work zone with orange temporary striping (Las Flores Overcrossing),
- Curve in regular traffic zone with normal striping (La Costa Overcrossing).

Due to construction ending, the taper shift between normal striping and white temporary striping in prior work zones was not monitored. The cameras were mounted on the overcrossings over lane 2. With cameras for SB and NB traffic, there was traffic going towards the camera and traffic going away from the camera. Traffic coming towards the camera created higher contrast at night between the road, vehicles, and their headlights. In general, the presence of lighted traffic signs creates optical artifacts.

Tables 2.1 and 2.2 show the first sets of two cameras each in a straight and curved part of the work zone. At the time of camera installation, only white temporary striping was painted, which allowed AHMCT to record videos of this area until the orange temporary striping was installed.

Tables 2.3, 2.4, and 2.5 show the additional camera locations. The curves in the work zone (Table 2.2, at Las Flores Dr Overcrossing) and regular traffic zone (Table 2.5, at La Costa Overcrossing) curve in the same direction (right for the southbound traffic). The curve at La Costa Overcrossing was closer to the camera than the curve at Las Flores Overcrossing.

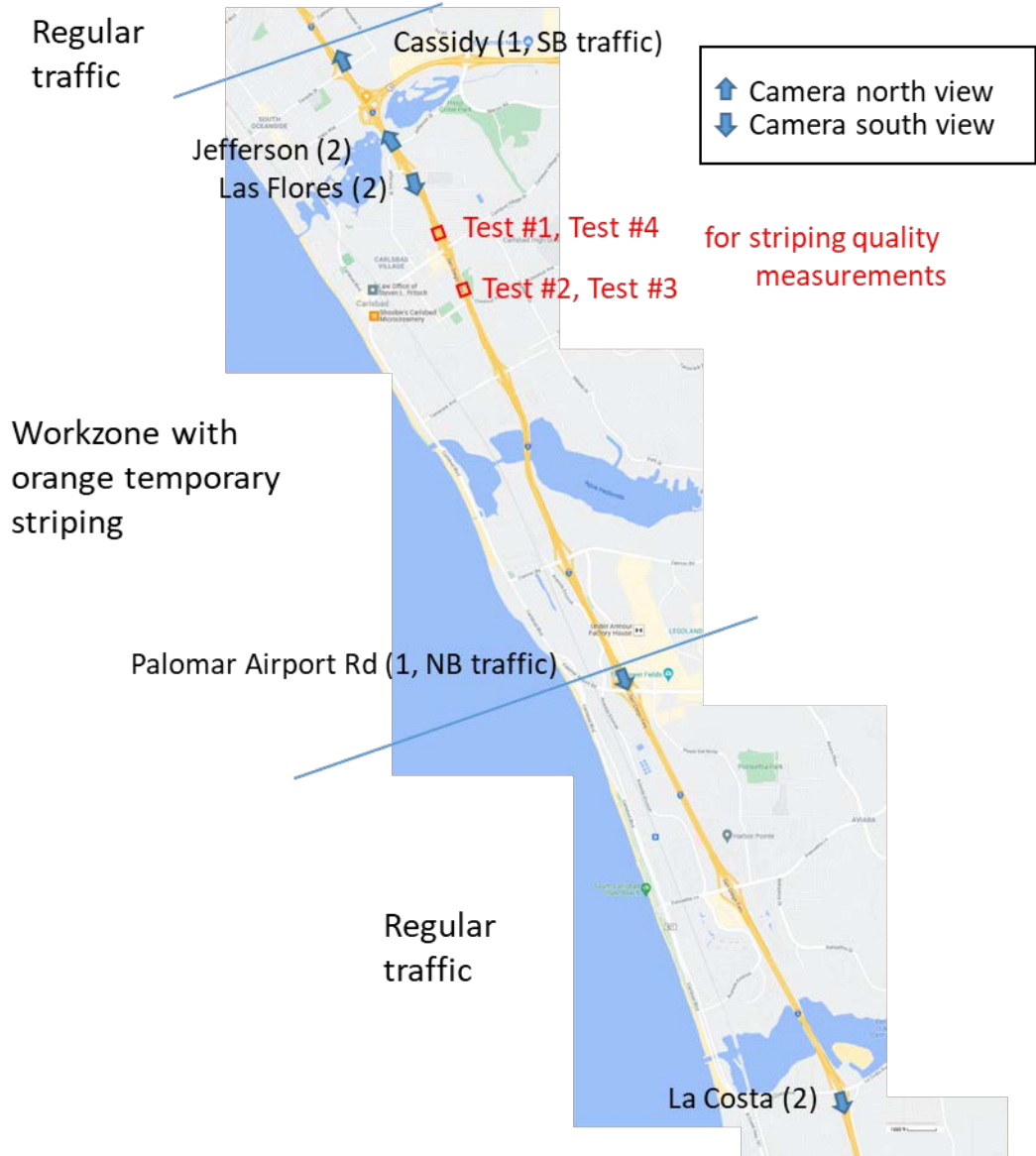







Figure 2.8: Camera locations on I-5 (map obtained from [www.google.com/maps](http://www.google.com/maps)).


**Table 2.1: Cameras at Jefferson Overcrossing (installed January 2022)**

Condition	Straight part in work zone with orange temporary striping and white temporary striping	
Location	Jefferson Overcrossing	
Camera screen shot	Overcrossing W end, view N, SB traffic 	Overcrossing E end, view N, NB traffic 


**Table 2.2: Cameras at Las Flores Overcrossing (installed January 2022)**

Condition	Curve in work zone with orange temporary striping and white temporary striping (southbound traffic curves to the right)	
Location	Las Flores Dr Overcrossing	
Curve overview (Google earth)	 <p>about 380 ft to curve</p>	
Camera screen shot	Overcrossing E end, view S, NB traffic 	Overcrossing W end, view S, SB traffic 




**Table 2.3: Camera at Cassidy Overcrossing (installed June 2022)**

Condition	Taper shift between regular traffic zone and work zone with orange temporary striping
Location	Cassidy St Overcrossing
Camera screen shot	Overcrossing W end, view N, SB traffic 

**Table 2.4: Camera at Palomar Airport Rd Overcrossing (installed June 2022)**

Condition	Taper shift between work zone with orange temporary striping and regular traffic zone
Location	Palomar Airport Rd Overcrossing
Camera screen shot	Overcrossing E end, view S, NB traffic 

**Table 2.5: Cameras at La Costa Overcrossing (installed June 2022)**

Condition	Curve in regular traffic zone (southbound traffic curves to the right)	
Location	La Costa Overcrossing	
Curve overview (Google earth)	 <p style="text-align: right;">about 280 ft to curve</p>	
Camera screen shot	<p>overcrossing E end, view S, NB traffic</p> 	<p>overcrossing W end, view S, SB traffic</p> 

## Road markings to support video analysis

Since the video was subject to perspective distortion, AHMCT added physical road markings to provide reference points (Figure 2.9 left). The AHMCT researchers painted five road markings each for the initial four cameras. The markings built a rectangle with the white stripes between lanes 3 and 4 (Figure 2.9, right). Figures 2.10 and 2.11 show installation and positioning. The marking closest to the overcrossing (0 ft) was followed by a second marking with  $y_i = 48$  ft. The next three markings were  $y_i = 3 \times 48$  ft = 192 ft apart so that five markings of up to 480 ft distance were visible from each camera. For the following camera installations, fewer road markings were installed closer together and by

Caltrans personnel. The first marking was at 0 ft, the next at 48 ft, and the third at 96 ft.

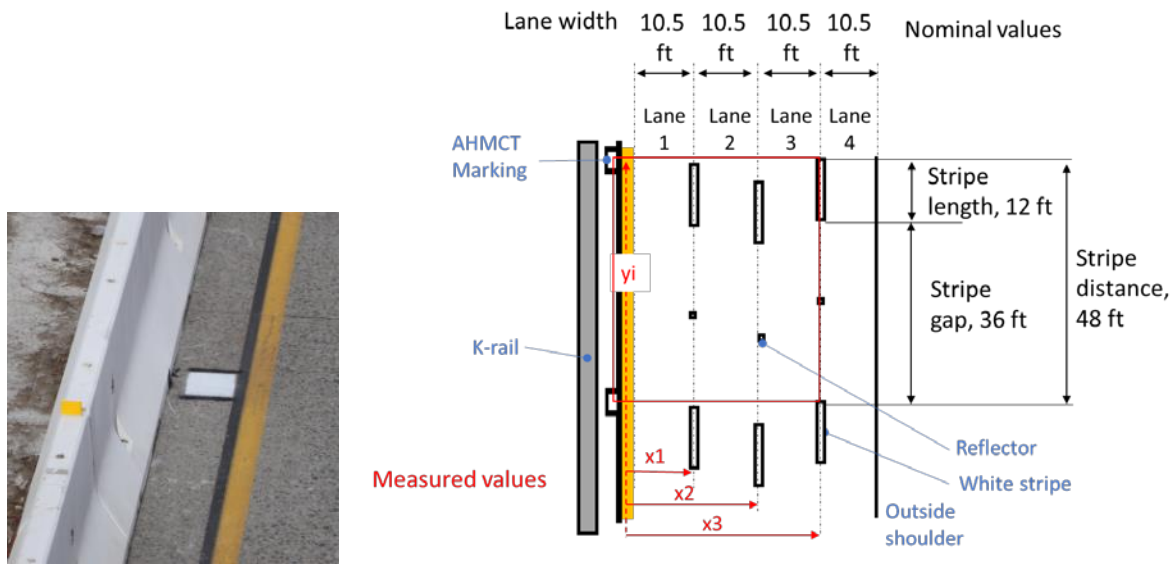
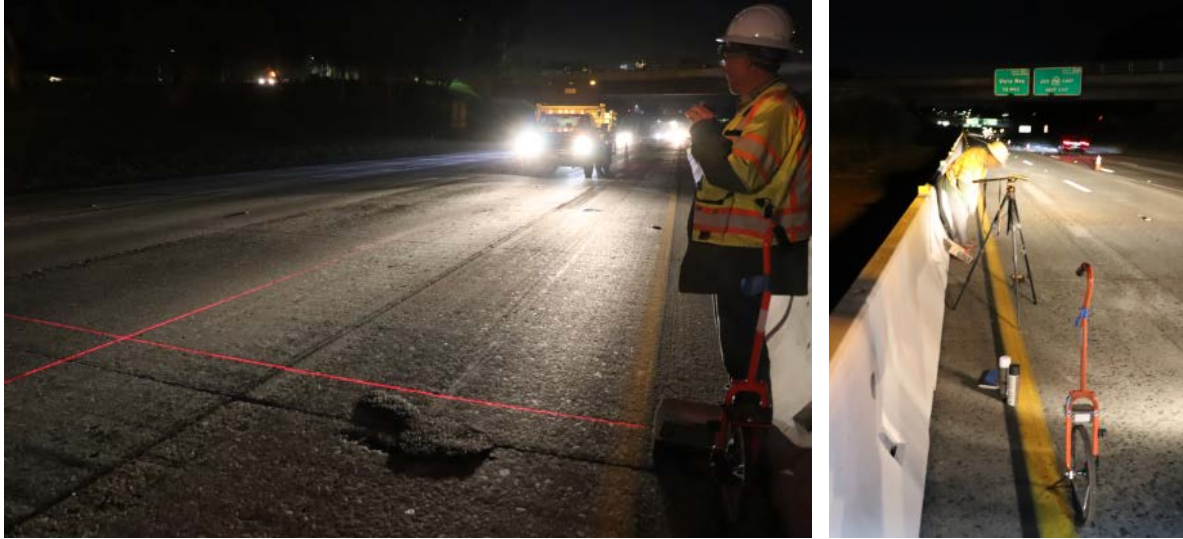


Figure 2.9: Road marking; Left: photo; Right: diagram of freeway and road markings with nominal values (black) and measured values (red)



Figure 2.10: Road marking application with spray paint





**Figure 2.11: Positioning of road markings; left: with laser perpendicular to road ( $x_1, x_2, x_3$ ); right: with wheel along the road ( $y_i$ )**

## Video analysis

### Metrics

The analysis of driver behavior included lane keeping behavior and vehicle speeds, which will be discussed later in Chapter 5. The literature defines lane keeping by *mean of vehicle distance from lane center (MLP)* and *standard deviation of lateral position (SDLP)* (Verster & Roth, 2011). MLP shows how well a vehicle stays in the lane center and is measured by the vehicle lateral center position from the lane center (Figure 2.12). SDLP shows how much a vehicle weaves back and forth. A large value means that the vehicle has large lateral positions from the lane center.

Since only road stretches of 48 ft or 96 ft were evaluated due to sufficient resolution, only the center lane deviation MLP was evaluated. We define the position to the left from the driver's perspective with a negative lateral position and position right with a positive value. A negative MLP will therefore indicate a left bias, zero is a centered position, and a positive MLP signifies a right bias (see Figure 2.19).

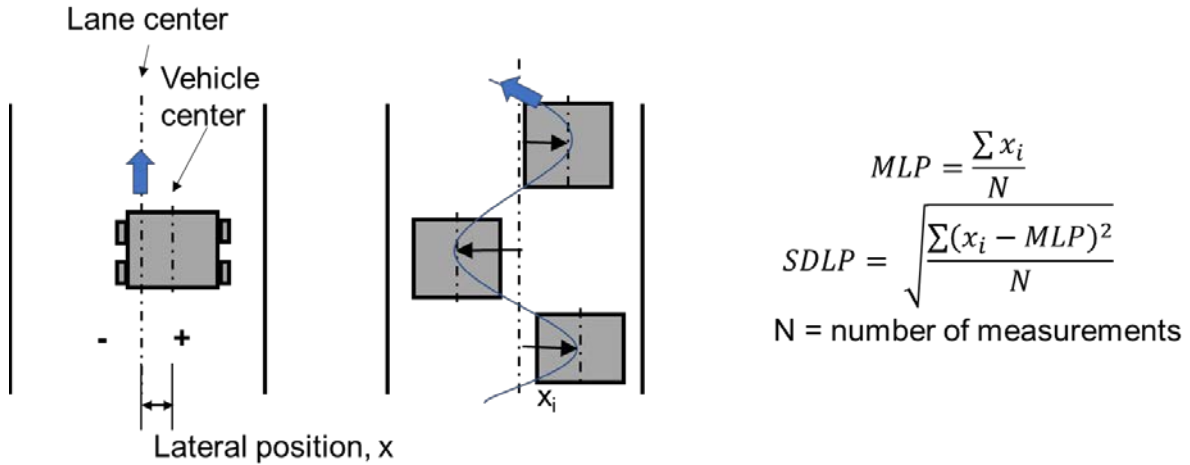


**Figure 2.12: Definition of Mean of vehicle distance from lane center (MLP) and Standard deviation of lateral position (SDLP)**

## Influence of recording conditions

Camera recordings were collected at different times of the day and at different time intervals. The accuracy of the measurements was strongly dependent on camera resolution, line of sight, and light conditions. The pan, tilt, and zoom options allowed for changing the camera view to see lane keeping behavior close-up or observe driver behavior and speeds over a longer stretch (Figure 2.13).



**Figure 2.13: Video screenshots with different views, from Las Flores Overcrossing, south view, SB traffic; left: close view; middle: intermediate view; right: far view**

The night videos were well lit when multiple vehicles were on the road, but quite dark when there were single vehicles on the road (Figure 2.14). The camera automatically switched from color to black and white mode when there was not much light (Figure 2.15).



**Figure 2.14: Video screenshots at night with different numbers of cars, left: from Jefferson Overcrossing, north view, NB traffic, night time; right: from Las Flores Overcrossing, S view, SB traffic**



**Figure 2.15: Video screenshots at night from Jefferson Overcrossing, north view, NB traffic; left: color video; right black & white video**

## **Preliminary analysis with Kinovea**

Initial analyses were performed with Kinovea,<sup>1</sup> a free and open-source software with a focus on technical analysis in sports. The following analysis tried to understand video resolution. The line measurement tool was first used to measure the lane pixel, which can be seen in Figure 2.16 (left). The resolution of the video was obtained by dividing the lane width in feet (12 ft in the example video) by the number of pixels across the lane. From Figure 2.16 (left) the resolution of the lane closest to the camera is  $12 \text{ ft} / 330.94 \text{ pixel}$  or approximately  $0.04 \text{ ft/pixel}$ .

---

<sup>1</sup> <https://www.kinovea.org/>

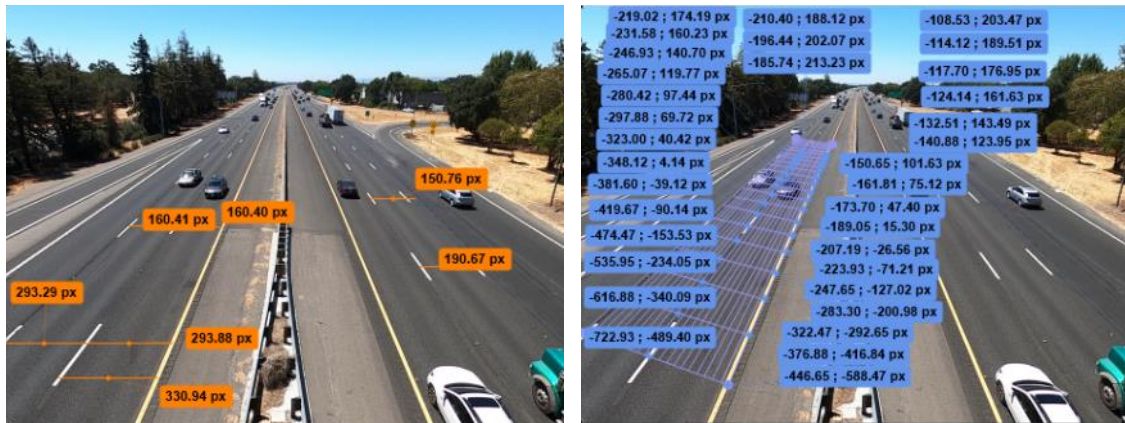


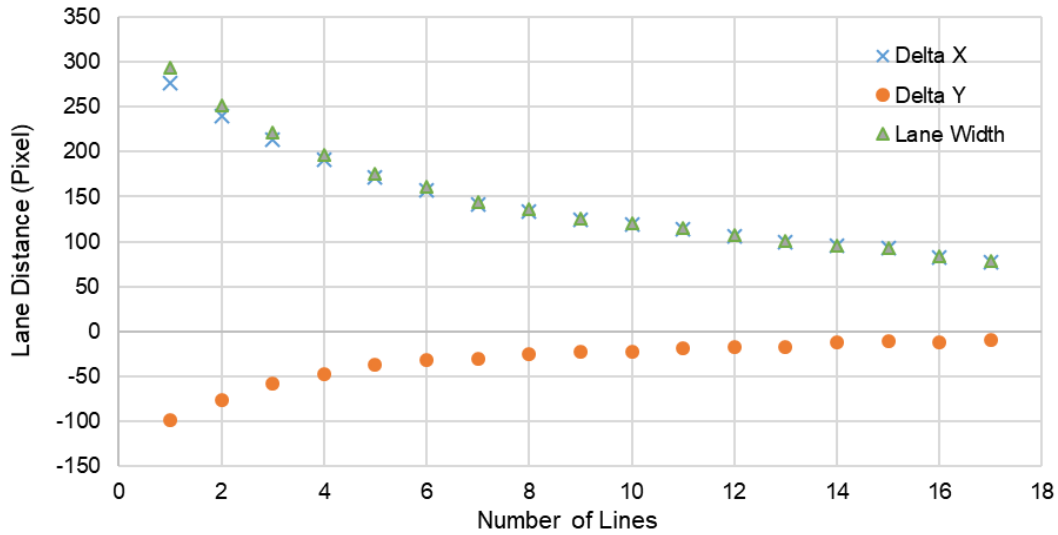
**Figure 2.16: Lane distance measurement (example video from Richards Blvd Overcrossing over I-80, Davis, CA), left: line tool, right: marker tool**

To explore the perspective distortion, the marker measurement tool and the built-in grid system in Kinovea were used to place the marker on each point across the lane in the horizontal direction, which is shown in Figure 2.16 (right). The marker tool gives the x- and y-coordinates as well as measures the distance in both the horizontal (x) and vertical (y) direction. The grid dimension of approximately 20 x 20 px was used to create each horizontal division. The data obtained with the marker tool were exported as a Windows Excel file and analyzed further (Figure 2.17). Delta X represents the horizontal difference of the line over one lane in the picture, delta Y represents the vertical difference, and lane width represents the hypotenuse, which is the lane width.

From Figure 2.17 (a), the delta X lane distance was approximately 279.28 px at line 1 and 77.21 px at line 17. Line 1 represents the line closest to the camera, and line 17 represents the line farthest away from the camera. With the assumed lane width of 12 ft, Figure 2.17 (b) shows the resolution in pixel per feet across each lane width. The resolution ranges from approximately 0.04 ft/pixel to 0.155 ft/pixel. The almost linear progression of resolution over the evenly spaced horizontal lines (= number of measurement) shows a normal perspective decrease in pixel number and no distortion error. The Kinovea software automatically spaced the horizontal grid lines evenly with regard to the theoretical perspective.

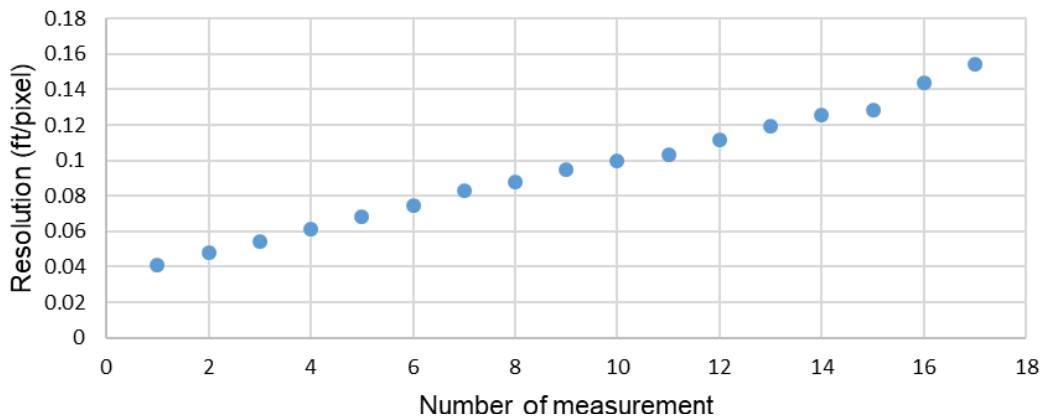
Based on the lane distance and resolution measurements, the vehicle to be analyzed should be close to the camera for better results because it provides better resolution. From these findings, it was decided to only analyze a road stretch close to the camera.

Lane Distance Measurement (DayB-Median GH010230)



(a)

Resolution Measurement (DayB-Median GH010230)



(b)

**Figure 2.17: Analysis of Figure 2.16 left measurements: (a) lane distance measurement in pixel and (b) resolution measurement for a lane width of 12 ft**

## Python based video analysis

The video recordings were analyzed with analysis routines programmed in Python and automated vehicle detection through YOLOv5. YOLO is the abbreviation of "You Only Look Once" and is a popular open-source video processing algorithm. In the original CCTV video, YOLOv5 detected vehicles either as cars, trucks, and possibly busses. Busses were not found in this study. We also decided to ignore motor bikes. Each vehicle received a number and an estimated center point. From the camera input image, the region of interest was marked, which was then cut out and transformed into a bird's eye-view (Figure 2.18). With the transformed image, vehicles were counted per lane, speed was analyzed, and vehicle center distance from the respective lane center was calculated.

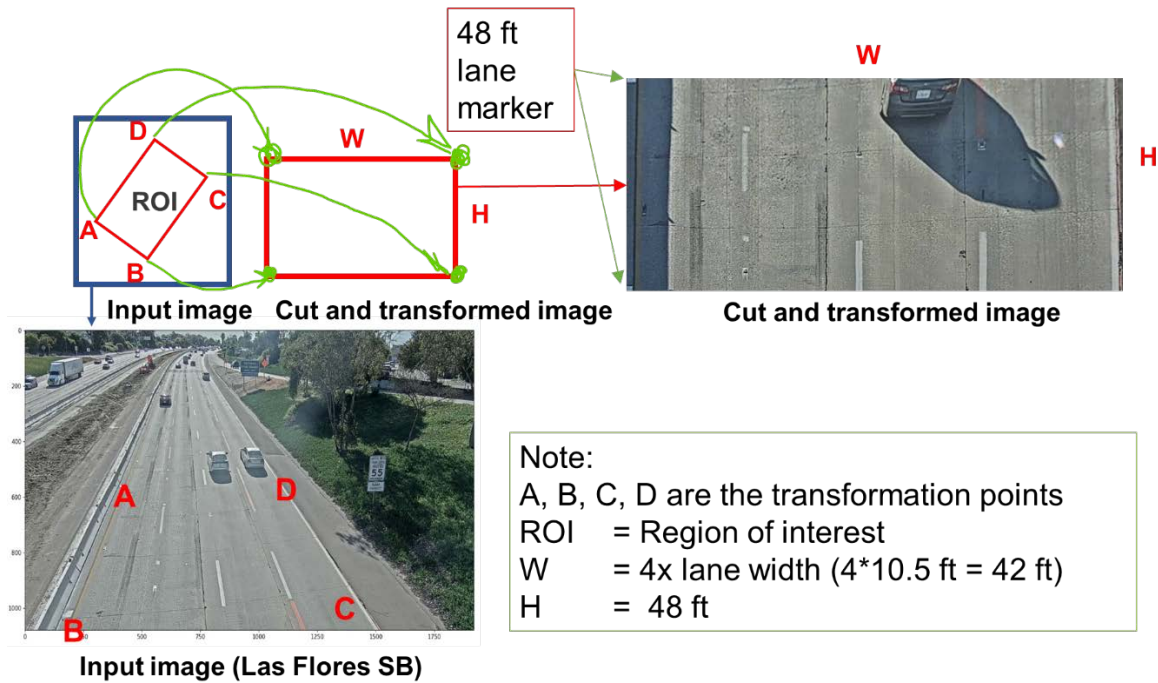


**Figure 2.18: Transformation of region of interest**

Figure 2.19 shows the definition of the Yolo MLP or vehicle center to lane center distance. The lane width in the work zone was 10.5 ft. As described above, a negative MLP means the vehicle is left of the lane center, towards the inner K-rail (left bias), whereas a positive MLP means the vehicle is right of the lane center towards the outer lanes (right bias).

## Errors from camera position

To evaluate the quality of the automatic Yolo MLP detection, the center positions of vehicles were manually obtained from processed video recordings. Figure 2.20 shows how the manual vehicle center to lane stripe measurement was derived from the left and right bumper distances to the lane stripes. As trucks were observed to have a higher MLP error, the manual evaluation intentionally considered a majority of cars instead of trucks and semi-trucks. This manual vehicle center to lane stripe distance was compared to the distance between lane stripe and the red marked vehicle center as determined by the Yolo vehicle center analysis routine on the same frame of the processed video.

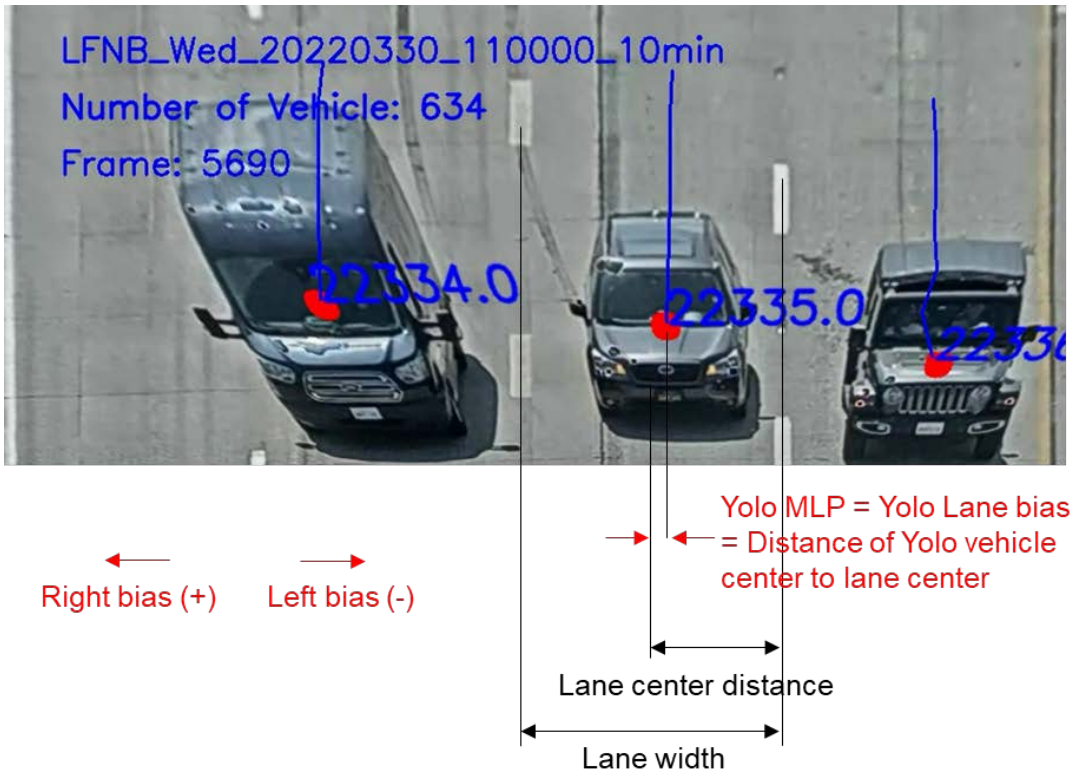
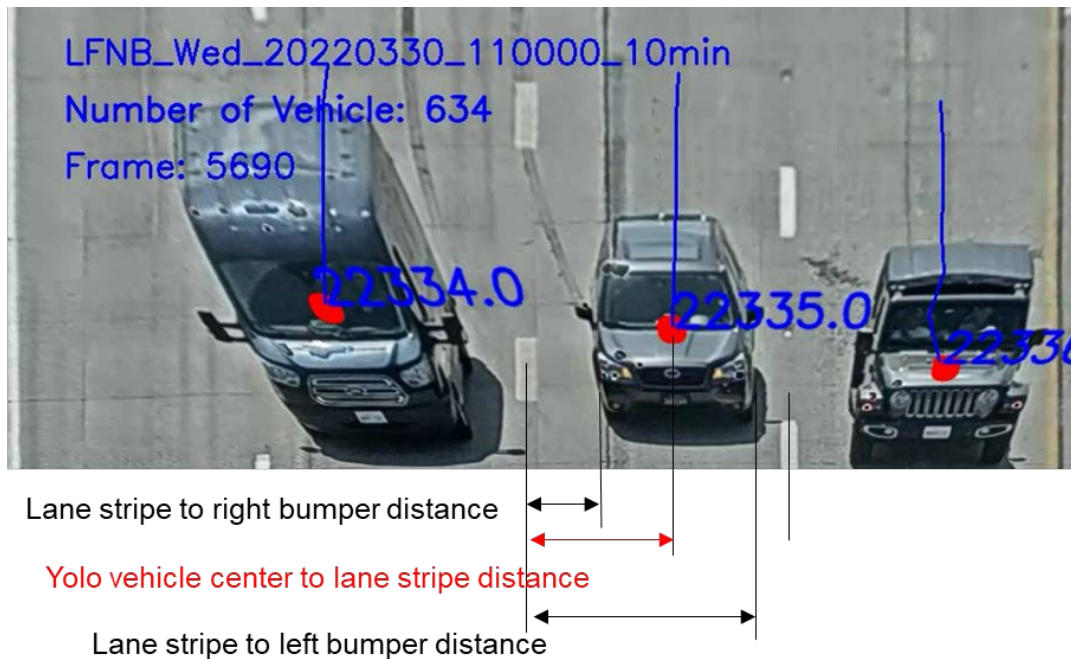


Figure 2.19: Automated Yolo vehicle center analysis



Manual vehicle center to lane stripe distance =  
 $0.5 * (\text{Lane stripe to left bumper distance} + \text{Lane stripe to right bumper distance})$

Figure 2.20: Manual vehicle center measurement

Figure 2.21 shows the difference between the manual vehicle center to lane stripe distance and the Yolo vehicle center to lane stripe distance for 10 cars per video for four different videos. This difference can be seen as error of the automated video processing from both perspective distortion and Yolo video processing. For Las Flores, the error on lane 1 was slightly negative, for lane 2 scattered around 0 ft and for lanes 3 and 4 increasingly positive. The night measurements had higher scatter. For Las Flores NB measurements, there was no clear trend over the four lanes.

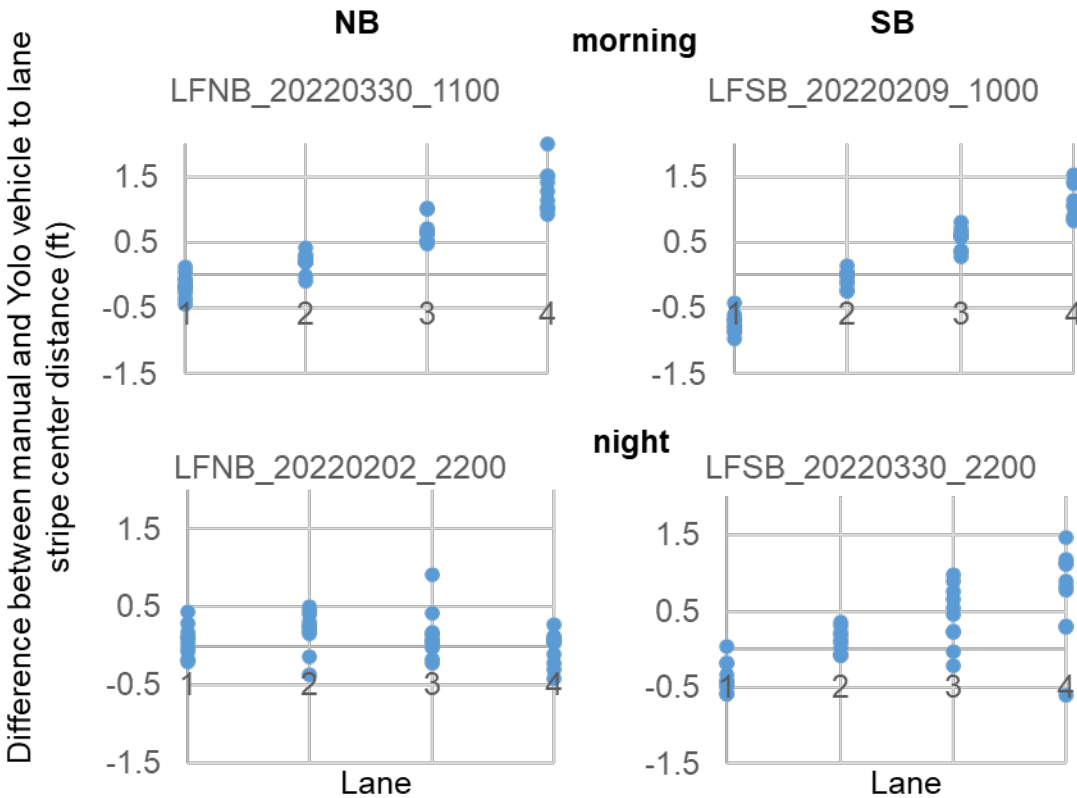


**Figure 2.21: Trendline of errors at Las Flores, NB and SB direction; in the morning (11 am and 10 am) and night (10 pm) for 10 cars each**

To increase the number of vehicles observed, six to nine videos for different day and night times and for 10 vehicles per video were evaluated. The averaged errors per CCTV camera and lane are shown in Figure 2.22. The CCTV cameras at Las Flores had the highest errors of up to 1.69 ft right bias for lane 4. The errors at Las Flores SB range from -0.18 ft to 1.34 ft in NB direction and -1.26 ft to 1.34 ft in SB direction. This high error might have resulted from the curved road and on-ramp merging behavior at Las Flores. The camera at Jefferson NB had errors between -0.84 ft to 0.24 ft, Jefferson SB between -0.14 ft to 0.47 ft, Cassidy between -0.17 ft to 0.56 ft, and Palomar Airport Rd between -0.23 ft to 0.44 ft.



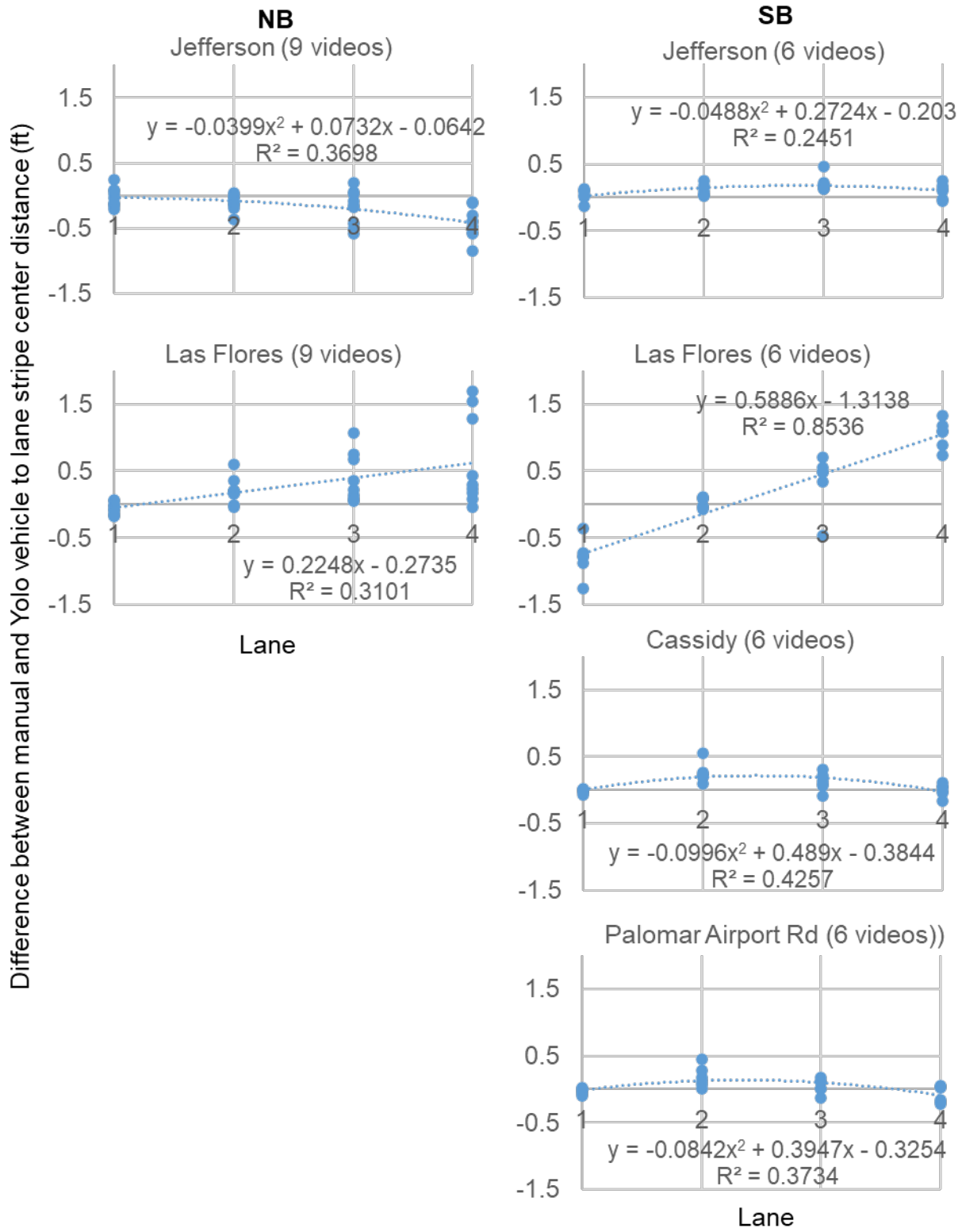
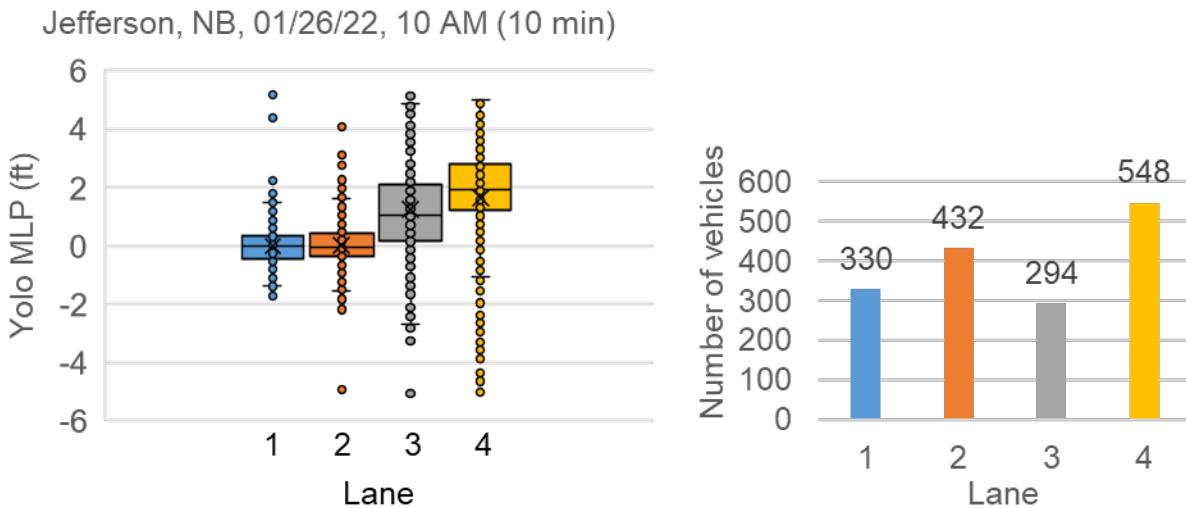


Figure 2.22: Trendlines of errors per CCTV camera (10 cars per video)

## Findings on lane keeping behavior

Video analysis focused on Wednesdays and Saturdays from 10 am to 12 pm (noon) and 10 pm to 12 am (midnight) to maximize video storage capacities and evaluate relevant days and traffic times. Figure 2.23 shows the analysis results for a single 10 min video. The 294 to 548 vehicles per lane had individual Yolo MLP values that spread from -5.1 ft to 5.3 ft. However, most of the large values were considered outliers in the histogram (Figure 2.23, left) and the average Yolo MLP ranged from -0.02 ft to 1.64 ft with increasing value from lane 1 to 4.



Lane	1	2	3	4
Average Yolo MLP (ft)	-0.02	0.02	1.23	1.64
Standard deviation of Yolo MLP (ft)	0.72	0.79	1.65	1.95

**Figure 2.23: Automated Yolo vehicle center analysis for 1,604 vehicles on 1/26/22 (Wednesday) at 10 am, 10-min video, Jefferson Overcrossing, NB traffic**

To compare the lane keeping behavior for W, with white temporary striping and WZ with orange temporary striping, the average MLP for five Wednesdays and one Thursday (2/3/2022) were compared (Figure 2.24). In the NB direction, vehicles had varying left and right bias for the six observed dates. In the NB direction, vehicles had just passed an on-ramp to the auxiliary lane 5 (Table 2.1). Also, there is a stronger error from camera distortion on the lanes 3 and 4 (Figure 2.22). The average speeds were obtained from Here Technologies data (the method is described Chapter 5). For the NB direction, all average speeds were between 67.71 mph and 70.13 mph.

In SB direction, there was a much lower range of average MLP, but a constant low right bias over all four lanes. In the SB direction, vehicles had just passed an off-ramp and the exit lane 5 started to merge into lane 4 (Table 2.1). The SB traffic was slightly slower than the NB traffic at the Las Flores and Jefferson Overcrossings, with speeds ranging between 44.15 mph and 67.28 mph.

The SB striping was white preceding orange whereas the NB striping was orange along white on both sides, but it cannot be said for sure that these different striping patterns affected the driver lane keeping behavior because of the different ramp, lane 5, and average speed conditions. In addition, the standard deviations of average Yolo MLP ranged between 0.72 ft to 2.03 ft as shown in Figure 2.24. With this large standard deviation and data scatter in the vehicle center position, there was high data uncertainty.

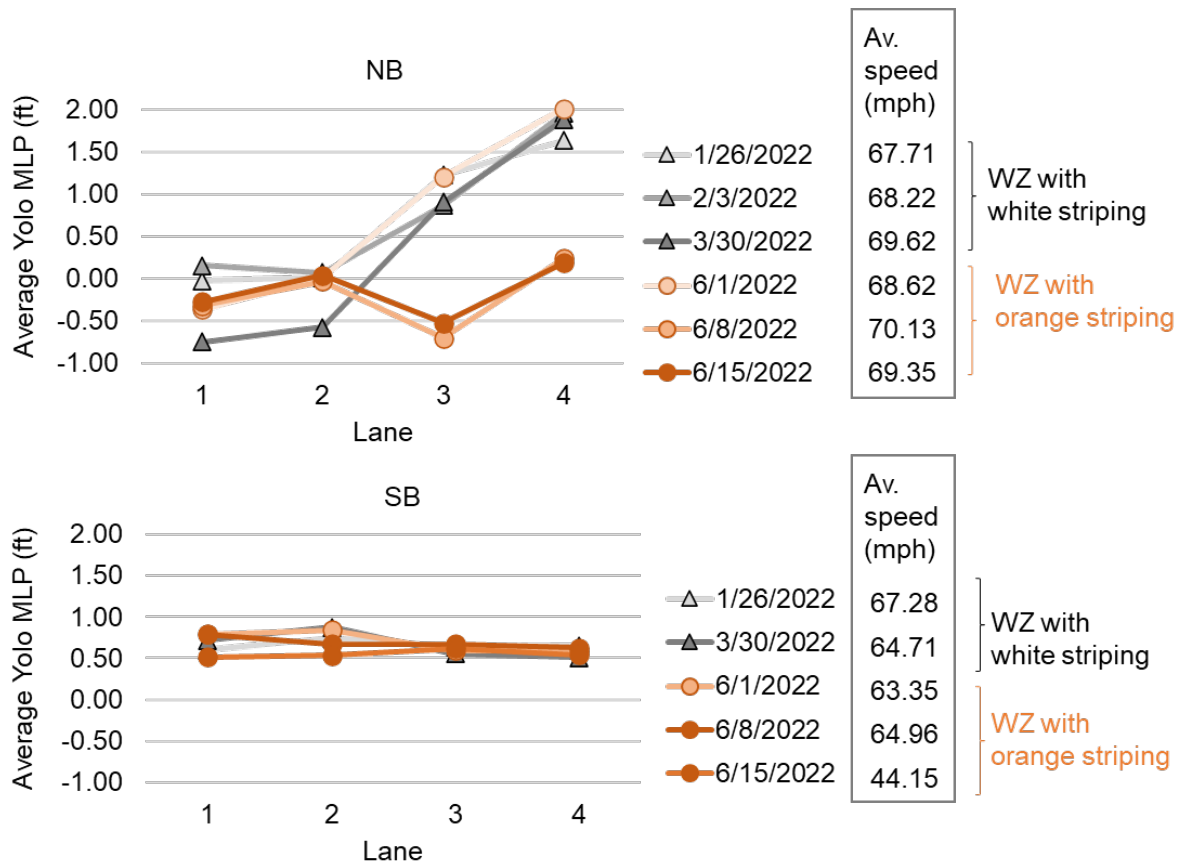


**Figure 2.24: Lane keeping behavior for lanes 1 to 4 from automated Yolo vehicle center analysis, Jefferson Overcrossing, selected weekdays at 10 am, 10-min videos; average speed from HERE Technologies data for 1 h at Las Flores Dr/Exit 51A (closest location to Jefferson Overcrossing)**

Lane keeping behavior was also evaluated at Las Flores (Figure 2.25). Since the Yolo MLP had large errors at Las Flores Overcrossing over most lanes (Figure

2.22), only lane 2 was compared for WZ with white and orange striping for three Wednesdays in each direction. Vehicles in the NB direction in lane 2 had a small right bias, which got stronger for the dates during WZ with orange striping compared to WZ with white striping. Vehicles in the SB direction in lane 2 had a small left bias, which also got slightly more pronounced during WZ with orange compared to white striping. The standard deviation ranged from 0.74 ft to 1.15 ft for the average Yolo MLP, which was in the range of the average Yolo MLP values; therefore, the data have a lot of uncertainty. The average speeds were comparable except for a slowdown on 6/15/2022 in the SB direction.

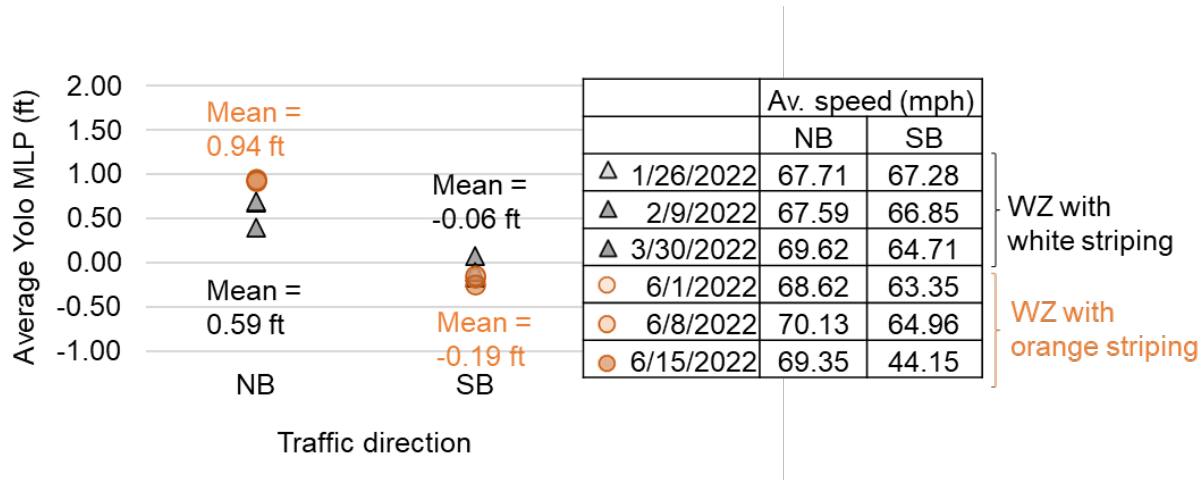


**Figure 2.25: Lane keeping behavior for lane 2 from automated Yolo vehicle center analysis, Las Flores Overcrossing, selected Wednesdays at 10 am, 10-min videos (Mean is not weighted by car count); average speed from HERE Technologies data for 1 h at Las Flores Dr/Exit 51A**

Figure 2.26 shows lane keeping behavior for Cassidy Overcrossing, which was on the north end of the work zone with the taper shift from regular traffic into the work zone. It shows data for three Wednesdays when the orange temporary striping was installed. Note the larger y-axis. There was a slight left bias towards the K-rail for lane 1 (average Yolo MLP had a mean of -0.4 ft) and stronger right bias for lane 3 (mean of 1.6 ft) and lane 4 (mean of 2.1 ft). The date with the highest absolute average Yolo MLP values per lane, 8/17/2022, was also the date with the significant lowest average speed of 36.05 mph compared to 64.51 mph and 64.75 mph on the other two days.

Vehicles approaching the camera at Cassidy Overcrossing going SB had passed an off-ramp and were at the beginning of the taper shift into the work zone (Table 2.3). The taper shift might explain the strong right bias on lanes 3 and 4.

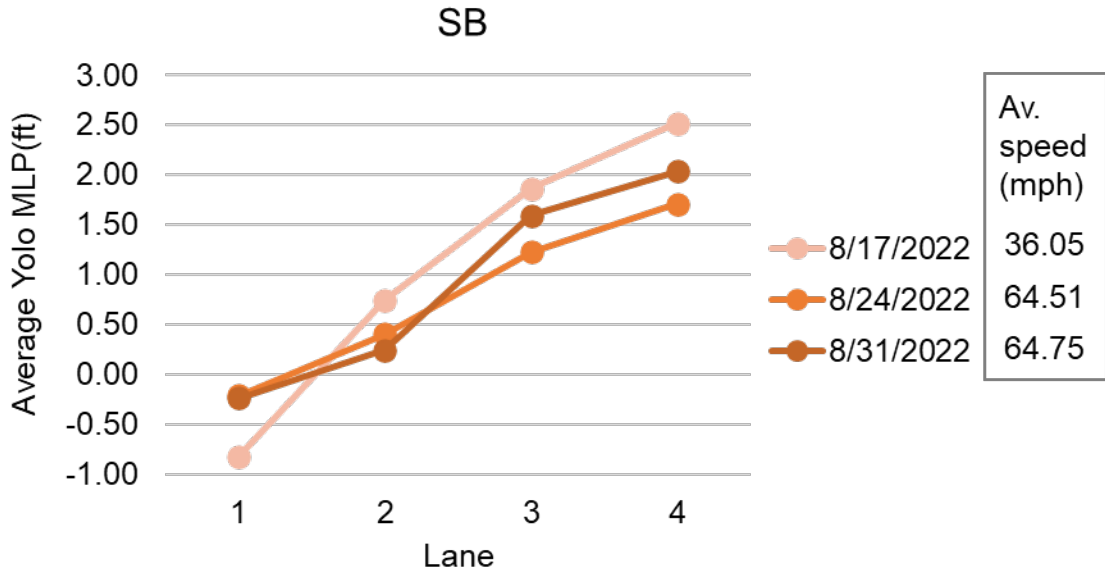


**Figure 2.26: Lane keeping behavior from automated Yolo vehicle center analysis, Cassidy Overcrossing, SB direction, selected Wednesdays at 10 am, 10-min videos; average speed from HERE Technologies data for 1 h at Cassidy St/Exit 51C**

Figure 2.27 shows the lane keeping behavior at Palomar Airport Rd Overcrossing, which was at the south end of the work zone, for the same three Wednesdays as Figure 2.26. Again, vehicles on lane 1 had a left bias (average Yolo MLP was a mean of -0.9 ft). Lanes 2 to 4 had a right bias with mean average Yolo MLP of 0.3, 1.1 and 1.4 ft respectively. Vehicles at this location had passed an off-ramp and were heading from the regular traffic zone into the work zone. Vehicles did not see the orange temporary striping at this location but at about 500 ft further north of the camera. The average speeds from 50.95 mph to 66.89 mph did not seem to influence the lane keeping behavior.

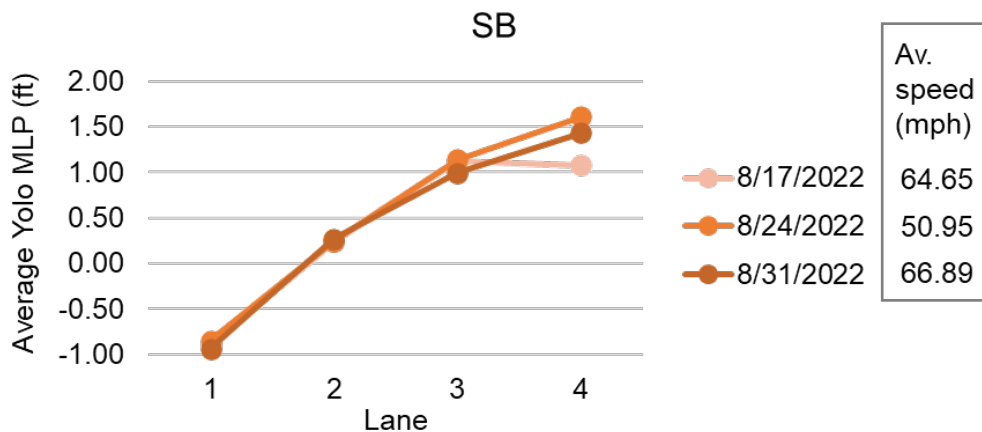


**Figure 2.27: Lane keeping behavior from automated Yolo vehicle center analysis, Palomar Airport Rd Overcrossing, SB direction, selected Wednesdays**

**at 10 AM, 10 min videos; average speed from HERE Technologies data for 1 h at Palomar Airport Rd/Exit 47**

## **Interim conclusion**

- Manual live lane keeping analysis is based on quick and ternary decisions. To increase data quality and reduce subjectiveness, CCTV camera recordings were analyzed.
- Visual observations highlighted that pavement joints, road defects, slabs, and curves also influence driver behavior in addition to lane striping.
- Vehicle lane keeping is best observed from a position directly above the lane. The CCTV cameras were installed above lane 2. However, any video recordings from a fixed camera position will result in distortions for positions farther away from the camera.
- Comparison of automated vehicle center position detection and manual detection in the video recordings showed that most results have comparatively small errors between -0.17 ft to 0.56 ft. However, processing of videos at Las Flores Overcrossing had significant errors for lanes 3 and 4 in the NB and SB direction up to 1.69 ft and lane 1 in the SB direction up to -1.26 ft.
- Automated video analysis was very time consuming but produced many data points. Ten-minute videos during day time often counted over 1,200 vehicles each with their respective speeds and lane position, whereas 10-min night videos counted up to 500 vehicles.
- The comparison of lane keeping behavior during work zone with white and with orange temporary striping was inconclusive on the influence of the presence of orange striping or striping type due to high data uncertainty over few data points.

# Chapter 3: Assessment of driver perception

The project panel and AHMCT personnel developed a survey to assess driver perception on work zone awareness, visibility of pavement delineation, and preference of white vs. orange contrasted white. AHMCT and Caltrans worked with the Public Information Offices (PIOs) of San Diego Association of Governments (SANDAG) and Caltrans, who hosted the survey on a website. Several questions were based on the survey in the *PROGRESS REPORT: Orange Work Zone Pavement Markings, February 3, 2020* by Melissa Finley (2020), Texas A&M Transportation Institute (Finley, 2020).

The survey was published in English and Spanish by Southwest Strategies, LLC with a “soft launch” on May 18, 2022, on the I-5 NCC project website. By June 5, 2023 a total of 1,185 responses were recorded for the English survey, and it was closed. Appendix C shows the survey questions, and asterisks mark mandatory questions. For the Spanish survey, only five responses were received by June 5, 2023 and were omitted due to the small sample size.

## Survey results

The population of the 1,185 survey respondents consisted mainly of frequent drivers with 57.0 % driving the I-5 between Lomas Santa Fe Drive and SR-78 at least once a week followed by 24.3 % driving at least once a month (Appendix C, Q1). The remaining 18.7% of respondents drove the respective road stretch less than once a month. A significant majority of 1,136 respondents (93.9%) lived in San Diego County, 2.4% lived in Orange County, 1.1% lived in Los Angeles County, 2.3% in “other regions”, and 0.4% lived in Baja California, Mexico (Appendix C, Q12). More than half (56.4 %) of 1,136 respondents drove a passenger car/sedan most commonly in the respective area followed by SUVs (33.1%), pick-up trucks (7.1%), vans (2.1%), commercial vehicles (0.7%), and motorcycles (0.5%) (Appendix C, Q13). The age of the respondents was almost normally distributed with the majority (27.6%) of 1,136 respondents in the 40- to 54-year-old category (Appendix C, Q11). About half of the 1,132 respondents identified as male (54.7%), 38.7% as female, 0.5% as other, and 6.1% preferred not to say (Appendix C, Q14).

Of the 1,185 survey respondents, 93.7% noticed the orange contrasted striping in the construction zone between Palomar Airport Road and SR-78 (Appendix C, Q2). This high number is not surprising since the survey specifically addressed the orange contrasted striping.

One thousand ninety-three people answered Q3, which asked if the orange contrasted striping increased their awareness of being in a road construction work zone. Of these, 80.4% reported an increased awareness (Appendix C, Q3), which is a strong indicator that the orange contrasted striping was effective.

Of 1,087 people, 43.2% noticed a difference in the NB and SB orange contrasted lane line striping, but the majority (56.9%) did not (Appendix C, Q4). Only the respondents who noticed the difference were asked Q5 concerning which orange contrasted lane line striping they preferred. In addition, a picture with both striping patterns was shown (Figure 3.1). Of the 465 respondents, the majority (60.4%) preferred the orange along both sides of the white lane line in the NB direction, 22.8% preferred the orange preceding the white lane line in the SB direction, and 16.8% reported no preference (Appendix C, Q5).



**Figure 3.1: Visual for question Q5 on pattern preference.**

A total of 1,078 and 1,076 people, respectively, scored two statements on the perceived influence of the orange contrasted striping on driving speed and lane keeping. They used a Likert-scale of “strongly agree” (5), “agree” (4), “neither agree or disagree” (3), “disagree” (2), and “strongly disagree” (1). Of 1,078 respondents, 19.7% strongly agreed and 38.1% agreed that the orange contrasted striping caused them to drive at a more reasonable or safe speed in the work zone. Twenty-six percent neither agreed nor disagreed, 9.0% disagreed, and 7.2% strongly disagreed (Appendix C, Q6). There was an average Likert scale value of 3.5 out of 5, which is a positive result.

For the statement that the orange contrasted striping makes it easier than traditional white lane line striping to stay in their lane, the majority of 1,076 respondents (32.8%) strongly agreed, followed by agreed (27.0%), neither agreed nor disagreed (23.6%), disagreed (9.6%), and strongly disagreed (7.0%)



(Appendix C, Q6). The result is an average score of 3.7 out of 5 on the Likert scale, which shows a stronger agreement with this statement regarding lane keeping than with the previous statement regarding driving at a safe speed.

One thousand sixty-seven people answered Q7, and the majority (72.1%) did not have prior knowledge of the orange contrasted striping before entering the work zone (Appendix C, Q7). Only 27.9% of respondents had prior knowledge.

Out of 1,142 people, an overwhelming majority (84.3%) would like to see orange contrasted striping used in more road construction zones, whereas the remaining 15.7% would not (Appendix C, Q8). More than half of 1,142 respondents (53.6%) answered with "yes" if they had driven through the work zone between Palomar Airport Road and SR-78 at night, whereas the other half (46.4 %) answered "no" (Appendix C, Q9).

The next question on respondents' opinion of the orange contrasted striping at night was answered by 608 people. A clear majority (62.3%) preferred the orange contrasted laneline striping at night (Appendix C, Q10), while 24.5% had no preference, and 13.2 % preferred the traditional white laneline striping.

## **Time progression of responses**

A hypothesis is that driver awareness changes over the time of installation of orange contrasted striping as drivers become familiar with it. Between the first set of survey responses collected through May 25, 2022, and those collected through June 14, 2022, there was a decrease in driver awareness of the work zone from 82.7% to 79.1% (Figure 3.2). However, during the following months, as more responses were recorded, there was only a minor reduction to 78.9% in the January 12, 2023, set of survey results, which increased again to 80.4% by the end of the survey in June 5, 2023.

Similarly, there was not a strong change in the proportion of respondents who would like to see orange contrasted striping used in more road construction zones (Figure 3.3). By May 25, 2022, 86.6% of respondents wanted to see more orange contrasted striping. By January 12, 2023, this percentage had dropped only slightly to 83.3%, but increased again to 84.3% by June 5, 2023.

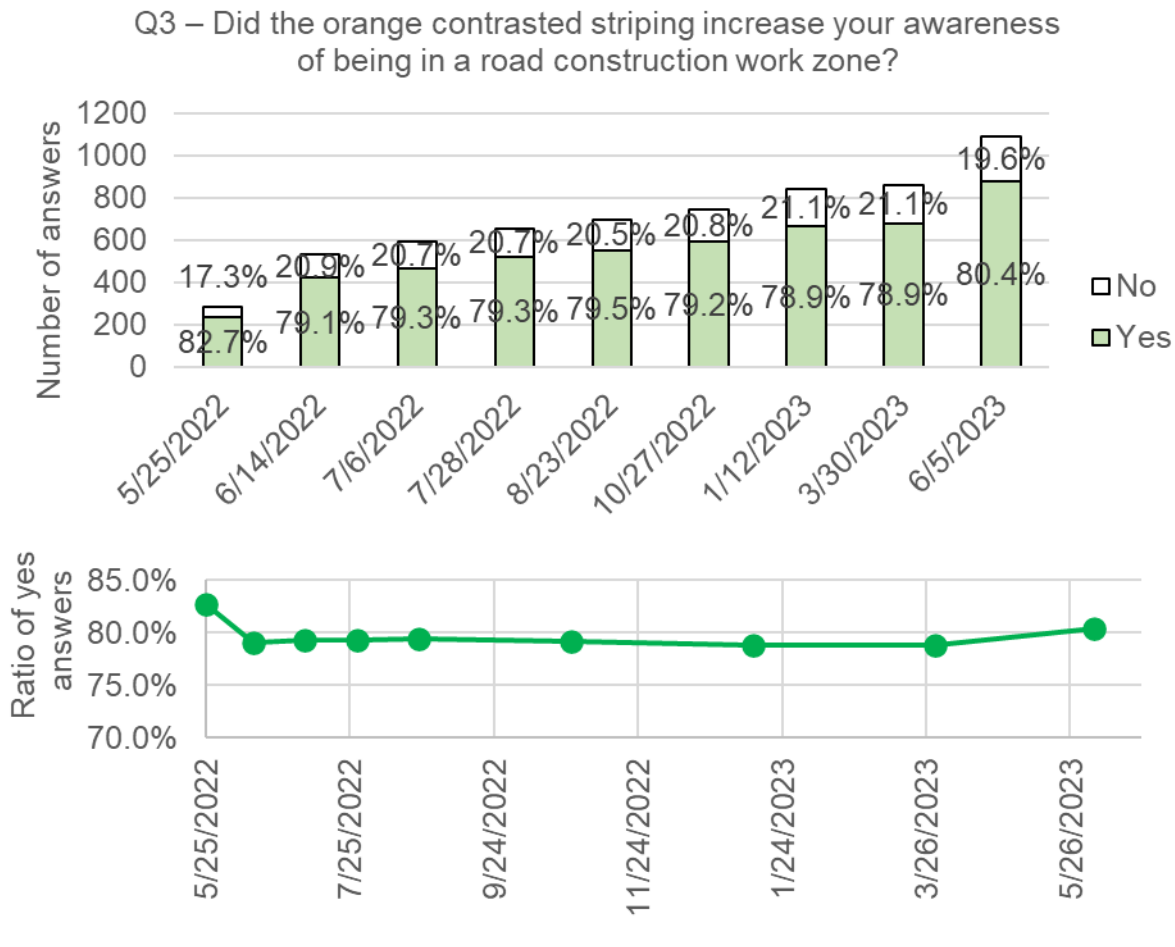


Figure 3.2: Change of responses and ratio of yes to no answers to question Q3

## Additional participant comments

Of the 1,185 respondents, 532 used the text box to leave comments. Of these:

- 95 entered “no”, “none”, “n/a”, or similar.
- At least 42 people mentioned that they found the color contrasted striping a distraction, distracting, or confusing.
- Forty-six people specifically mentioned that the public should be better informed about the purpose of the orange contrasted striping.
- About 26 people mentioned the tape striping getting loose and peeling off the road, especially when it rained. Some found the loose tapes hazardous or littering the area. Some of the tape stripe in the NB direction peeled off during rain events in December 2022 and was replaced with paint stripes.
- At least 70 comments were positive and mentioned “great work”, “excellent”, “good idea”, and similar. Some respondents commented

on the importance of keeping workers safe, while others would like to see permanent orange striping.

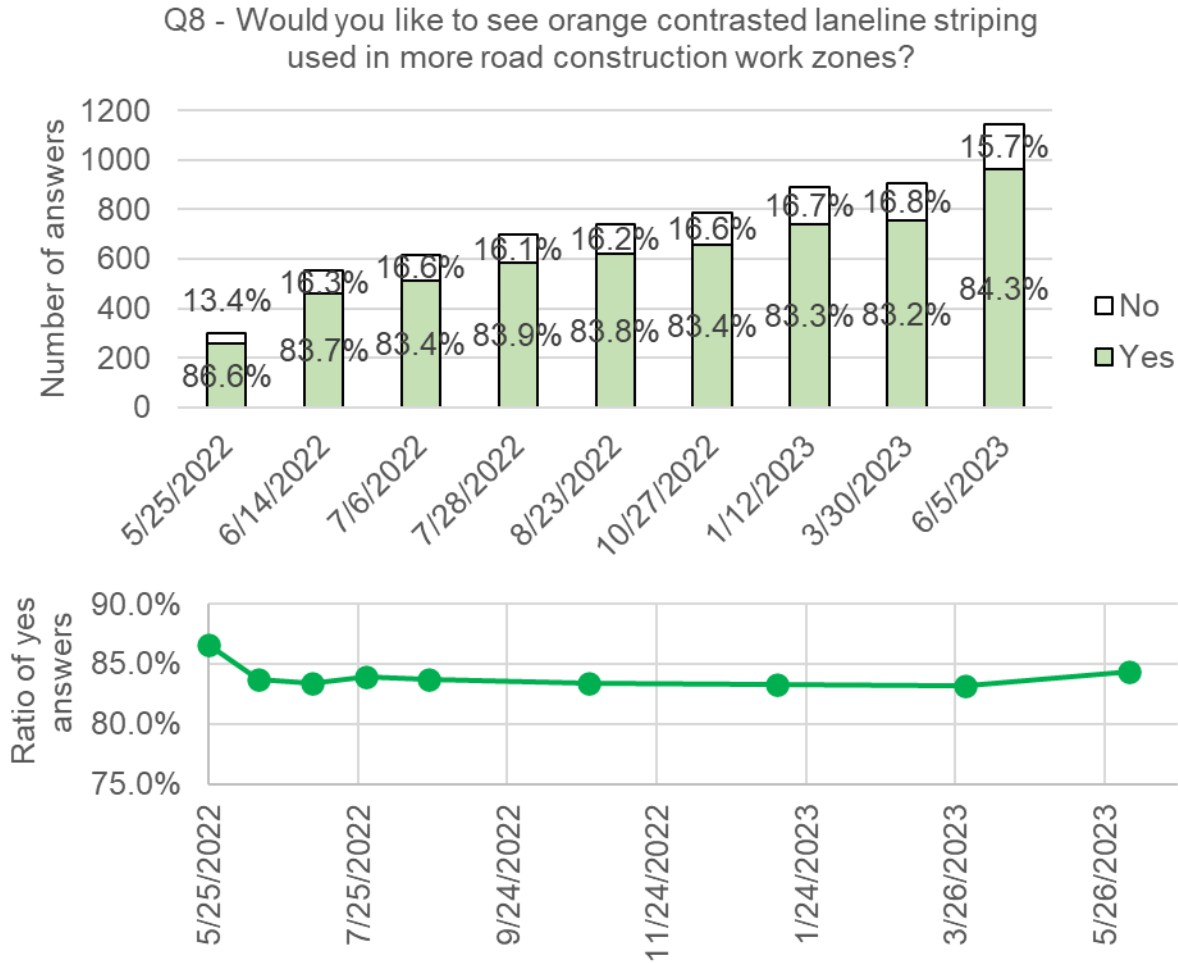


Figure 3.3: Change of responses and ratio of yes to no answers to question Q8

## Interim conclusion

- A total of 80.4% of 1,093 respondents found that the orange contrasted striping increased their awareness of being in a work zone. This finding shows effectiveness of the orange contrasted striping.
- Only about half of the survey respondents had driven through the construction zone between Palomar Airport Road and SR-78 at night. For those, a clear majority (62.3%) of 608 respondents preferred the orange contrasted laneline striping at night. The remaining 24.5% had no preference, and 13.2 % preferred the traditional white laneline striping.

- Respondents gave an average score of 3.5 of 5 to the statement, “The orange contrasted striping caused me to drive at a more reasonable or safe speed in the work zone”. An even higher average of 3.7 of 5 was given to the statement, “The orange contrasted lane line striping makes it easier than traditional white lane line striping to stay in my lane”.
- The overwhelming majority (84.3%) of 1,142 respondents would like to see orange contrasted striping used in more road construction zones.
- The majority respondents did not have prior knowledge of the orange contrasted striping before entering the work zone, which was commented about in the open feedback part of the survey. This finding shows that public communication could make the orange contrasted striping even more effective.

# Chapter 4: Evaluation of visibility of orange temporary striping

The visibility of orange contrast delineation was quantified through direct measurements of retroreflectivity and color on the striping and through dashboard camera videos. Figure 4.2 shows the device to measure retroreflectivity and nighttime color. The spectrophotometer for daytime color measurements can be seen in Figure 4.8 (top right). Additional trials to assess striping quality were performed with a portable Universal Serial Bus (USB) light microscope. Findings about temporary tape striping are reported in this chapter.

## State of the art

Smadi et al. (2008) showed that there is a statistically significant relationship between low pavement marking retroreflectivity levels and road safety measured in crash probability (Smadi et al., 2008). The visibility of striping is defined through retroreflectivity, or “the phenomenon of light rays striking a surface and being redirected directly back to the source of light” (McGee & Mace, 1978; Migletz et al., 1994). Retroreflectivity is measured as the coefficient of retroreflected luminance (RL) following ASTM standard E17102, which is the ratio of the luminance of a surface to the normal illuminance on the surface, with luminance being the luminous flux of a light ray on a surface per unit of projected area of that surface, per unit of solid angle (Migletz et al., 1994).

The retroreflectivity of pavement markings is ensured through glass beads and small glass spheres that are dropped on or mixed into pavement marking materials (Migletz et al., 1994). Index of refraction, bead shape, size, surface characteristics, and the number of beads affects the light that is then retroreflected (Migletz et al., 1994). There is an optimum immersion depth of the glass bead in the paint for maximum normalized intensity of about 60% of the bead diameter (Grosjes, 2008).

Pavement marking retroreflectivity is affected by age, traffic volume, road class, season in which the marking was applied, and paint color (MacEacheron, 2016). Pavement marking service life can be estimated with average daily traffic or number of wheels crossing a point on the road (Migletz et al., 1994). Tires passing over pavement markings lift, scatter, and abrade the

---

<sup>2</sup> E1710 – 18 Standard Test Method for Measurement of Retroreflective Pavement Marking Materials with CEN-Prescribed Geometry Using a Portable Retroreflectometer, ASTM International, West Conshohocken, PA

glass beads, which is increased by heavier vehicles (MacEacheron, 2016; Migletz et al., 1994). Temporary degradation of retroreflectivity might be caused by accumulated dirt and tire tread marks (Thanasupsin & Sukniam, 2021). Prior studies established that RL values of 100 to 160 mcd/m<sup>2</sup>/lx are considered satisfactory for night visibility (Burghardt et al., 2021; ERF, 2015; Gibbons et al., 2012; Lee & Oh, 2005).

## **Measurement of retroreflectivity**

### *Methodology*

Measurements were performed with a stationary reflectometer LTL3000 (Delta Instruments), which collects the coefficient of retroreflected luminance, RL, and nighttime chromaticity (Figure 4.2, right). At the same time, a spectrophotometer Spectro2guide, 45/0 (BYK-Gardner) collected daytime chromaticity values. The measurements were made within seconds, but the devices needed to be placed on top of the stripe. Due to safety concerns, measurements were only taken during lane closures, which occurred at night. Both devices had their own light sources for nighttime measurements and high consistency. The measurements were made shortly after the installation of the work zone (0 months) and six months after the installations by Caltrans and AHMCT. Further measurements were performed roughly every two months by Caltrans personnel.

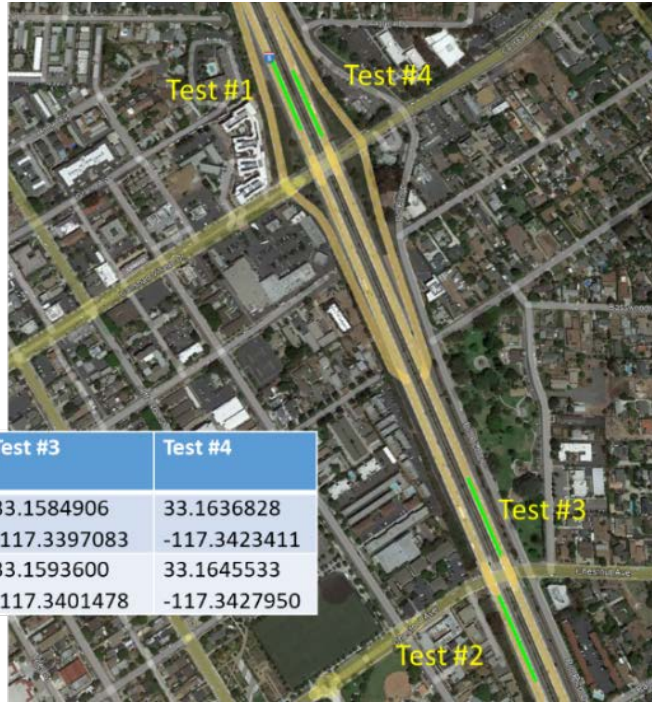
Based on ASTM standard D7585/D7585M,<sup>3</sup> retroreflectivity and colors were measured on two 400 ft segments for each striping pattern (Figure 4.1). For safety reasons, data points were collected at night on the stripes between lanes 1 and 2 during freeway lane closures (Figure 4.2, left). The measurement routine per stripe pattern is shown in Figure 4.3. There were three measurements per stripe and color.

---

<sup>3</sup> D7585/D7585M - Standard Practice for Evaluating Retroreflective Pavement Markings Using Portable Hand-Operated Instruments, ASTM International, West Conshohocken, PA

Southbound - Test #1, Test #2  
 Northbound - Test #3, Test #4

At Carlsbad Village Dr and  
 at Chestnut Ave



Measurement Sections	Test #1	Test #2	Test #3	Test #4
Start GPS Coordinates	33.1646742 -117.3431142	33.1579839 -117.3397278	33.1584906 -117.3397083	33.1636828 -117.3423411
End GPS Coordinates	33.1637767 -117.3426589	33.1570900 -117.3392611	33.1593600 -117.3401478	33.1645533 -117.3427950

Figure 4.1: Test locations



Figure 4.2: Left: Striping quality measurements performed by AHMCT researcher and Caltrans staff days after orange striping installation; Right: Retroreflectivity and nighttime color measurements on tape striping on I-5, northbound traffic, south of Las Flores Overcrossing

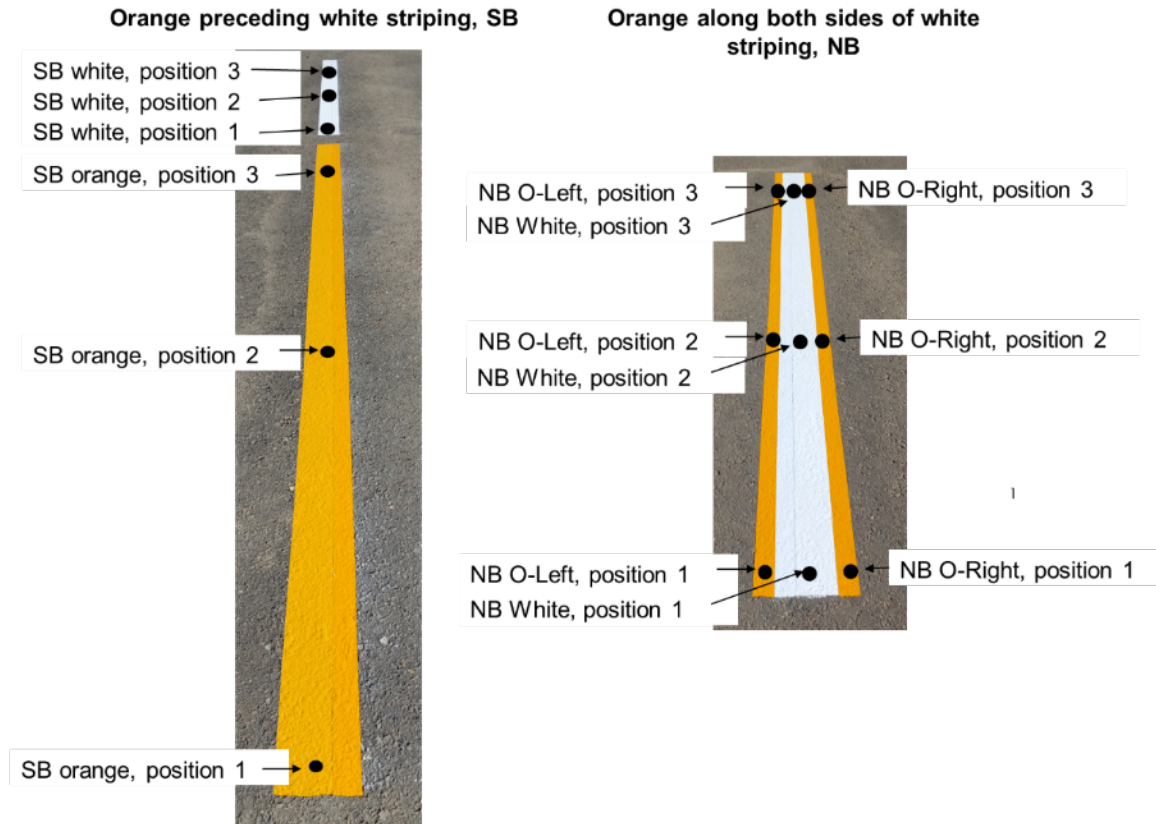


**Figure 4.3: Measurement routine per stripe pattern**

## *Results for orange temporary striping in the work zone*

In the beginning, the left and right orange sides of the orange along both sides of white paint stripes were evaluated separately. At 0 months, the retroreflectivity for the NB orange paint stripes was slightly higher for the left orange stripes (average of 112 mcd/m<sup>2</sup>/lx) than the right orange stripes (average of 104 mcd/m<sup>2</sup>/lx) and with less deviation (Figure 4.4, left). The white stripe in the middle of the NB stripe was freshly coated in April 2022 and had an average retroreflectivity of 226 mcd/m<sup>2</sup>/lx. For the SB stripe pattern, the orange preceding white stripe had an average retroreflectivity of 128 mcd/m<sup>2</sup>/lx (Figure 4.4 right), which was slightly higher than the NB orange stripes. The white stripes in SB direction had not been refreshed and showed an average retroreflectivity of 109 mcd/m<sup>2</sup>/lx.



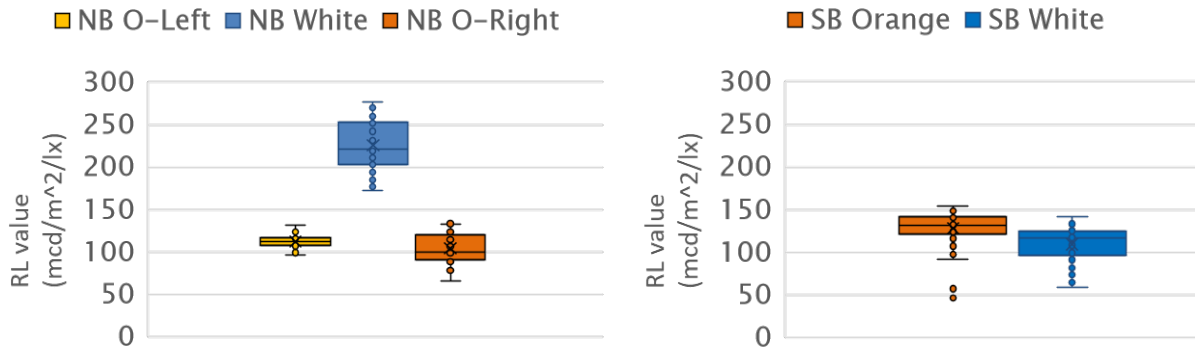


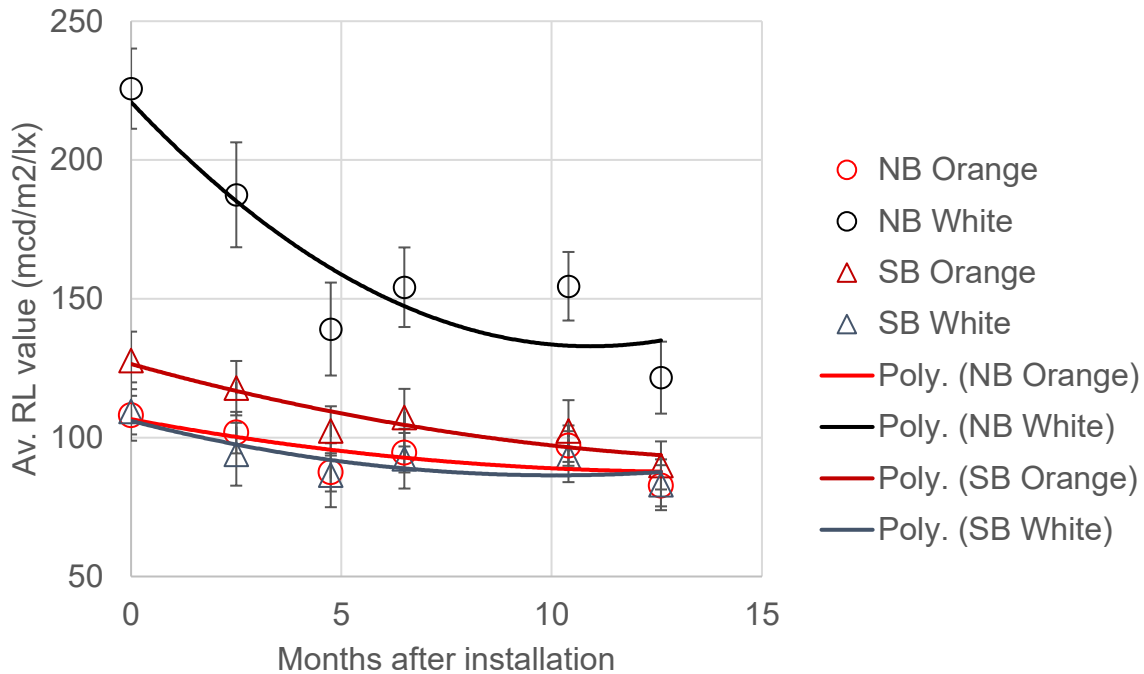
**Figure 4.4: Retroreflectivity measurements at 0 months after orange striping installation; Left: on northbound stripe (Orange left, white middle, orange right stripes); Right: on southbound orange preceding stripe (Orange and white stripes); n = 48 measurements per bar**

The following charts show the striping quality at specific dates:

- Directly after installation, denoted as 0 months, measured between May 3 to 5, 2022,
- 2.5 months after installation, measured on July 18 and 19, 2022,
- 4.75 months after installation, measured on September 28 and 29, 2022,
- 6.5 months after installation, measured on November 14 and 15, 2022,
- 10.4 months after installation, measured on March 16 and 17, 2023, and
- 12.6 months after installation, measured on May 23 and 24, 2023.

Figure 4.5 shows the left and right sides of the orange along both sides of white striping combined. The average retroreflectivity (Av. RL) values for all stripes declined over time. The white stripe (NB White) in the middle of the NB stripe was freshly coated in April 2022 and had the absolute highest average RL values (225.7 to 121.6 mcd/m<sup>2</sup>/lx). This value was 2.1 times of the value of NB orange paint stripes (NB Orange) and SB white and 1.7 times of the value of SB intermittent orange stripes (SB Orange). The white stripes in the SB direction (SB White) had not been refreshed after installation in November 2021 and showed the absolute lowest average RL values (109.4 to 83.0 mcd/m<sup>2</sup>/lx).

SB Orange had higher average RL values than NB Orange. The standard deviation  $\sigma_{RL}$  was highest for the NB white stripes (24.7 to 38.2 mcd/m<sup>2</sup>/lx) and lowest for the NB orange along both sides of white stripes (13 to 15 mcd/m<sup>2</sup>/lx) (Figure 4.5).



Months	NB Orange		NB White		SB Orange		SB White	
	Av. RL	$\sigma$ RL	Av. RL	$\sigma$ RL	Av. RL	$\sigma$ RL	Av. RL	$\sigma$ RL
0	108.13	13.91	225.71	28.89	127.83	20.73	109.42	21.01
2.5	101.82	14.95	187.48	37.79	117.83	19.60	94.04	22.65
4.75	87.51	13.78	139.13	33.48	102.44	17.75	86.48	23.03
6.5	94.58	14.21	154.19	28.66	107.21	20.75	92.44	21.52
10.4	97.14	14.53	154.54	24.70	102.40	22.24	93.17	18.35
12.6	82.68	14.83	121.63	25.92	90.00	17.31	83.04	18.30
Ratio of 12.6 mo to 0 mo	76.5%		53.9%		70.4%		75.9%	

all Av. RL and  $\sigma$ RL values in (mcd/m<sup>2</sup>/lx)

**Figure 4.5: Average retroreflectivity values Av. RL over time after orange striping installation; error bars show standard deviation  $\sigma$ RL (n = 48 measurements for NB White, SB Orange, and SB White; n = 96 measurements for NB Orange)**

The larger average RL values for the 4.75 months measurement in November and 6.5 months measurement in March were potentially higher due to these being the fall/winter months with higher humidity (fog or rain). A study in Thailand reported that rain fall can wash off accumulated dirt and tire tread marks from road striping (Thanasupsin & Sukniam, 2021).

For NB Orange, SB Orange, and SB White, the average RL value at 12.6 months after installation was reduced to 76.5%, 70.4%, and 75.9%,

respectively, of the initial values at 0 months. At 12.6 months, the average RL value of the NB White stripe, which had been renewed, dropped even more drastically to 53.9% of the value at 0 months.

Compared with the threshold of  $RL = 100 \text{ mcd/m}^2/\text{lx}$  for satisfactory visibility, SB White had lower RL values at 2.5 months, NB Orange at 4.75 months, and SB Orange at 12.6 months. NB White always exceeded the threshold.

A simple portable USB microscope was used to examine the glass bead embedding. Figure 4.6 shows orange and white temporary striping about 6.5 months after installation. The pavement grooves were visible. These microscope pictures were strongly influenced by lighting conditions so that a standardized and robust recording setup should be proposed for future measurements.

Figure 4.7 shows the NB orange stripes considered separately for the left and right stripes straddling the middle white stripe. The left stripes NB O-Left had constantly higher average RL values than the right stripes NB O-Right, which might be due to differences in the initial bead application process.

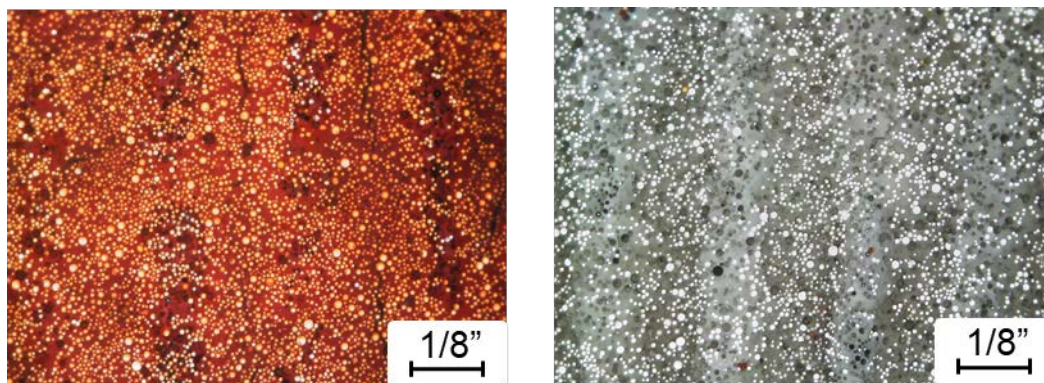
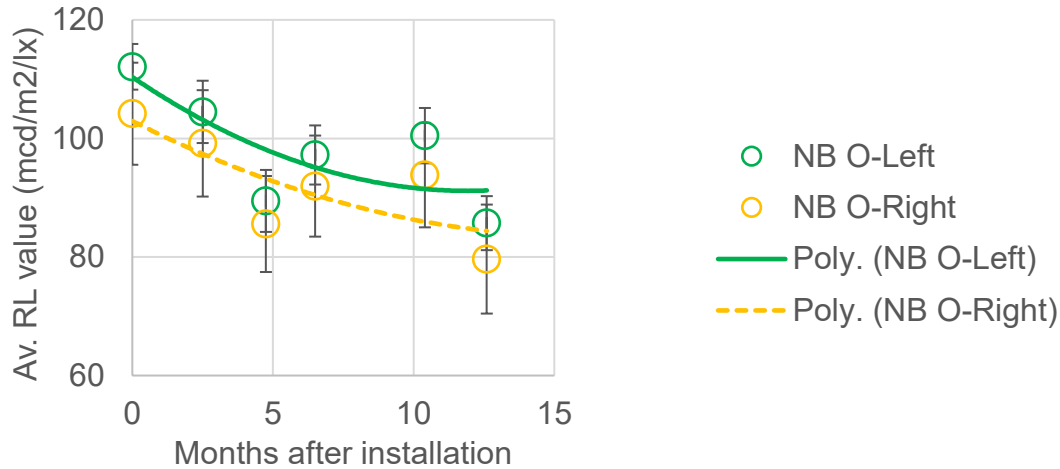


**Figure 4.6: Microscope pictures from orange (left) and white (right) temporary striping on Nov. 14, 2022**



Months	NB O-Left		NB O-Right	
	Av. RL	$\sigma$ RL	Av. RL	$\sigma$ RL
0	112.08	7.71	104.17	17.22
2.5	104.48	10.51	99.17	17.95
4.75	89.46	10.46	85.56	16.20
6.5	97.21	9.97	91.96	17.05
10.4	100.47	9.34	93.81	17.63
12.6	85.71	9.12	79.65	18.39

**Figure 4.7: Average retroreflectivity values Av. RL over time after orange striping installation for NB orange left and right stripes separately; error bars show standard deviation  $\sigma$ RL (n = 48 measurements for NB O-Left and NB-O-Right each)**

## Measurement of striping color

The color of pavement marking material was measured through daytime (x, y) chromaticity coordinates in accordance with test method ASTM E1349,<sup>4</sup> and nighttime (x, y) chromaticity coordinates in accordance with test method ASTM E811.<sup>5</sup> ASTM Standard D6628 *Standard Specification for Color of Pavement Marking Materials*<sup>6</sup> only defines daytime chromaticity for white, yellow, red, blue, and purple, and nighttime chromaticity for white, yellow, and purple. But the measurement devices gave the x- and y-coordinates, and they can be compared over time and with the painting manufacturer values or with values

<sup>4</sup> E1349 – 06 (Reapproved 2018) Standard Test Method for Reflectance Factor and Color by Spectrophotometry Using Bidirectional (45°:0° or 0°:45°) Geometry, ASTM International, West Conshohocken, PA

<sup>5</sup> E811 – 09 (Reapproved 2020) Standard Practice for Measuring Colorimetric Characteristics of Retroreflectors Under Nighttime Conditions, ASTM International, West Conshohocken, PA

<sup>6</sup> D6628 – 16 Standard Specification for Color of Pavement Marking Materials, ASTM International, West Conshohocken, PA

published by other researchers. Since the color measurements were done at the same time as the retroreflectivity measurements, the methodology is the same as described above.

## Test measurements

To compare different pavement markings, daytime and nighttime chromaticity coordinates were recorded and are displayed in relation to standard ASTM Standard D6628<sup>7</sup> (Figure 4.8). The daytime color coordinates for black contrast stripe, white temporary lane stripe, and freeway concrete all fell into the white material range in Figure 4.8. Brightness is not displayed in this standard. The yellow fog line shows color coordinates on the boundary of the yellow range in ASTM D6628. There is no color range established for orange. The nighttime color values show similar behavior with the concrete color coordinates varying more outside of the white color range (Figure 4.9).

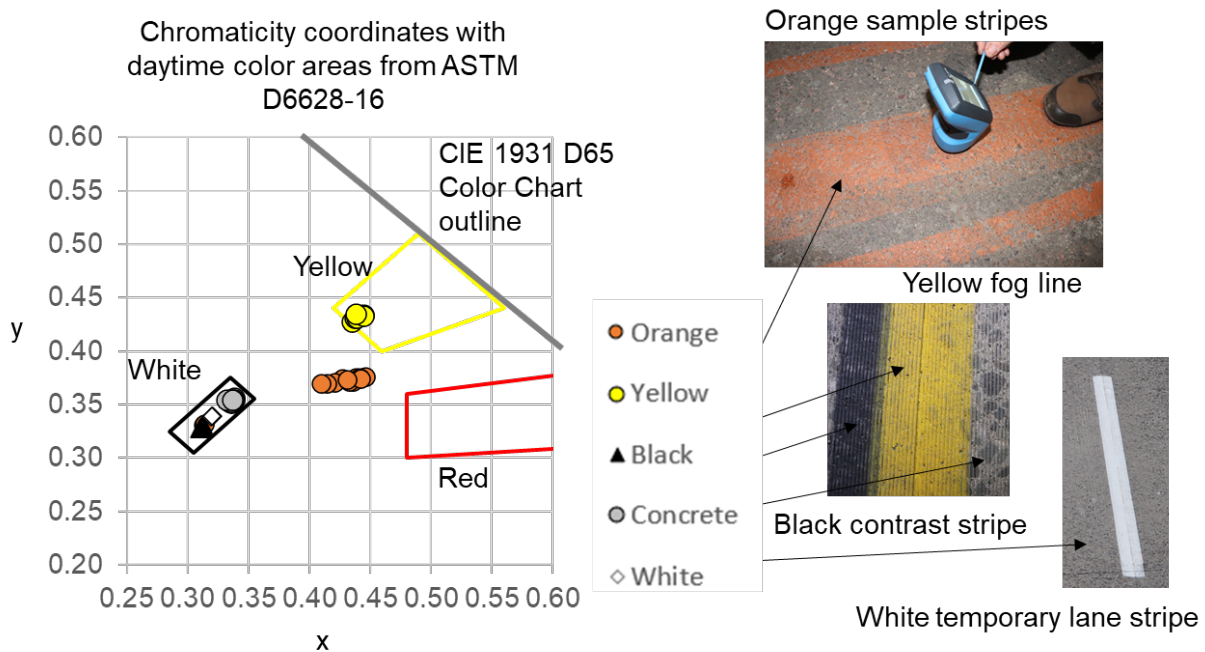


**Figure 4.8: Test daytime color measurements, n =5 to 13 measurements per sample type**

<sup>7</sup> D6628 – 16 Standard Specification for Color of Pavement Marking Materials, ASTM International, West Conshohocken, PA

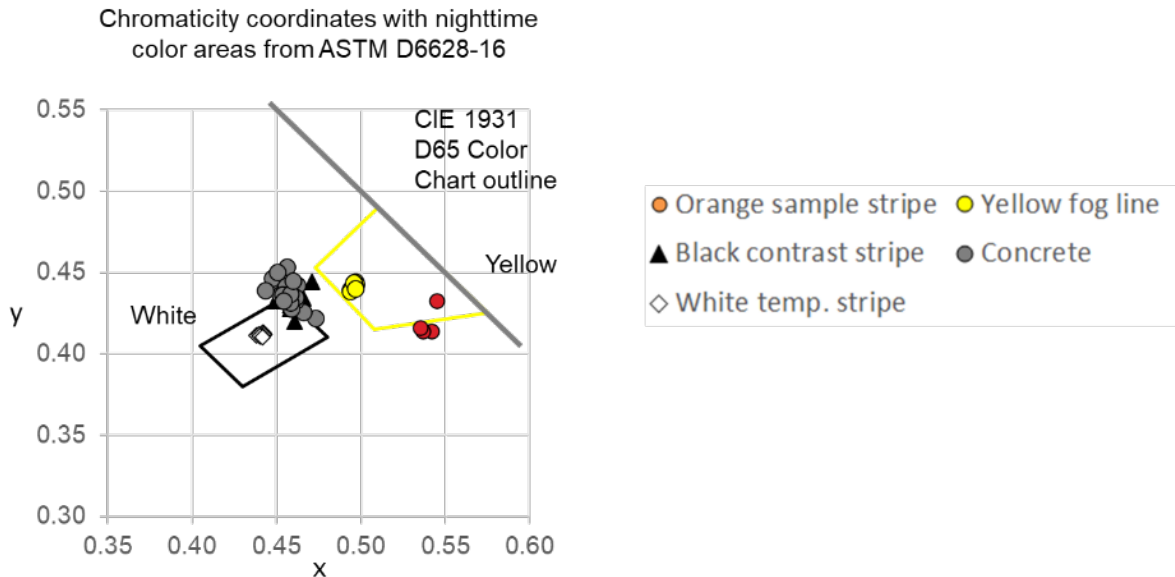


**Figure 4.9: Test nighttime color measurements, n= 6 to 20 measurements per sample type**

## Results for orange temporary striping in the work zone

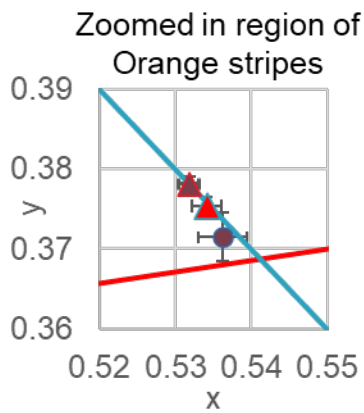
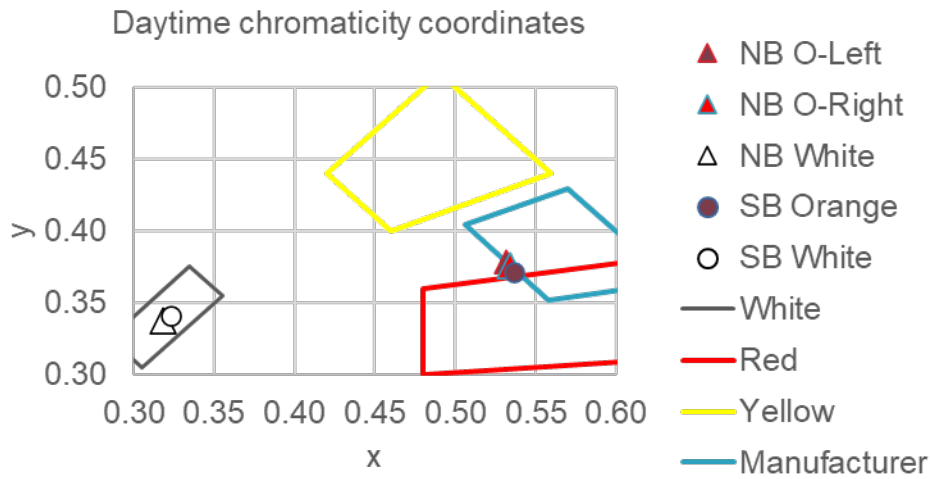
In the following, daytime and nighttime chromaticity coordinates are displayed in relation to colors defined in standard ASTM Standard D6628<sup>8</sup>. At 0 months, the NB and SB white stripes were in the white color region for daytime chromaticity coordinates (Figure 4.10). The daytime colors for the NB and SB orange stripes had color coordinates outside of the red color region in close proximity to each other. The SB orange chromaticity values had the largest deviation from 0.6 – 0.81% in both coordinate values.

Table 4.1 specifies the color coordinate range by the manufacturer. The daytime orange striping color values were all close to the manufacturer's color line (Figure 4.10).

For the nighttime chromaticity coordinates at 0 months, the NB and SB white stripes were again in the white color region (Figure 4.11). The nighttime colors however presented themselves within the yellow color region (Figure 4.11), which matched subjective human perception during nighttime driving (see dashboard camera photo in Figure 4.16). The right orange stripe of the orange along both sides of white pattern in NB direction (NB O-Right), SB intermittent

<sup>8</sup> D6628 – 16 Standard Specification for Color of Pavement Marking Materials, ASTM International, West Conshohocken, PA

orange stripes and SB white stripes had larger deviations within the x- and y-color coordinates (up to 0.80 % for x and up to 0.49% for y).

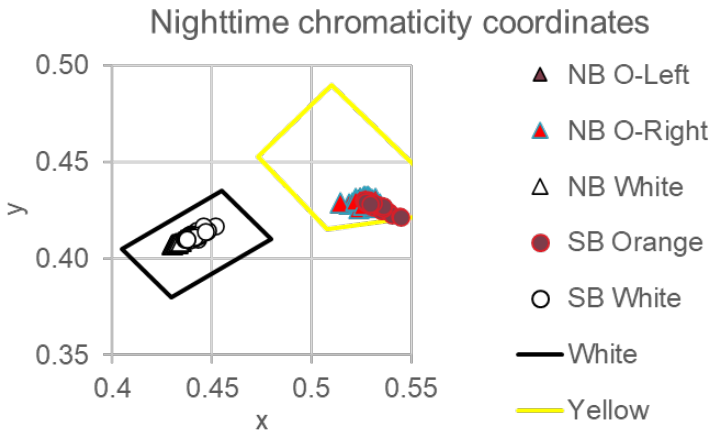


	average x-coordinate	average y-coordinate	standard deviation of x-coordinate		standard deviation of y-coordinate	
<b>NB O-Left</b>	0.5318	0.3781	0.00135	0.25%	0.00102	0.27%
<b>NB O-Right</b>	0.5342	0.3754	0.00198	0.37%	0.00113	0.30%
<b>NB White</b>	0.3186	0.3370	0.00092	0.29%	0.00075	0.22%
<b>SB Orange</b>	0.5362	0.3715	0.00322	0.60%	0.00301	0.81%
<b>SB White</b>	0.3228	0.3408	0.00116	0.36%	0.00106	0.31%

**Figure 4.10: Daytime color measurements on measurements at 0 months after orange striping installation, compared with ASTM Standard D6628 (n =48 measurements per stripe type)**

**Table 4.1: Manufacturer orange color coordinates (X,Y) for WZ Orange Fast Dry Waterborne (TT-P-1952F Type I & II), by 2020 Ennis-Flint, Inc, 2020**

RANGE COORDINATES (X,Y)	
X	Y
0.5580	0.3520
0.6360	0.3640
0.5700	0.4290
0.5060	0.4040



	average x-coordinate	average y-coordinate	standard deviation of x-coordinate		standard deviation of y-coordinate	
<b>NB O-Left</b>	0.5265	0.4310	0.00139	0.26%	0.00079	0.18%
<b>NB O-Right</b>	0.5276	0.4297	0.00379	0.72%	0.00135	0.31%
<b>NB White</b>	0.4324	0.4079	0.00158	0.36%	0.00077	0.19%
<b>SB Orange</b>	0.5313	0.4279	0.00423	0.80%	0.00209	0.49%
<b>SB White</b>	0.4407	0.4118	0.00347	0.79%	0.00168	0.41%

**Figure 4.11: Nighttime color measurements on measurements at 0 months after orange striping installation, compared with ASTM Standard D6628 (48 measurements per stripe type)**

The following charts show the striping quality over six measurements over 12.6 months. The NB and SB white stripes stayed in the white color region for daytime and nighttime chromaticity coordinates (NB White and SB White in Figures 4.12 and 4.13). The daytime color coordinates for the NB and SB orange stripes lay between the red and yellow color regions of daytime chromaticity (Figure 4.12), whereas the nighttime color coordinates were within the yellow region of nighttime chromaticity (Figure 4.13) as expected from the measurements at 0 months.



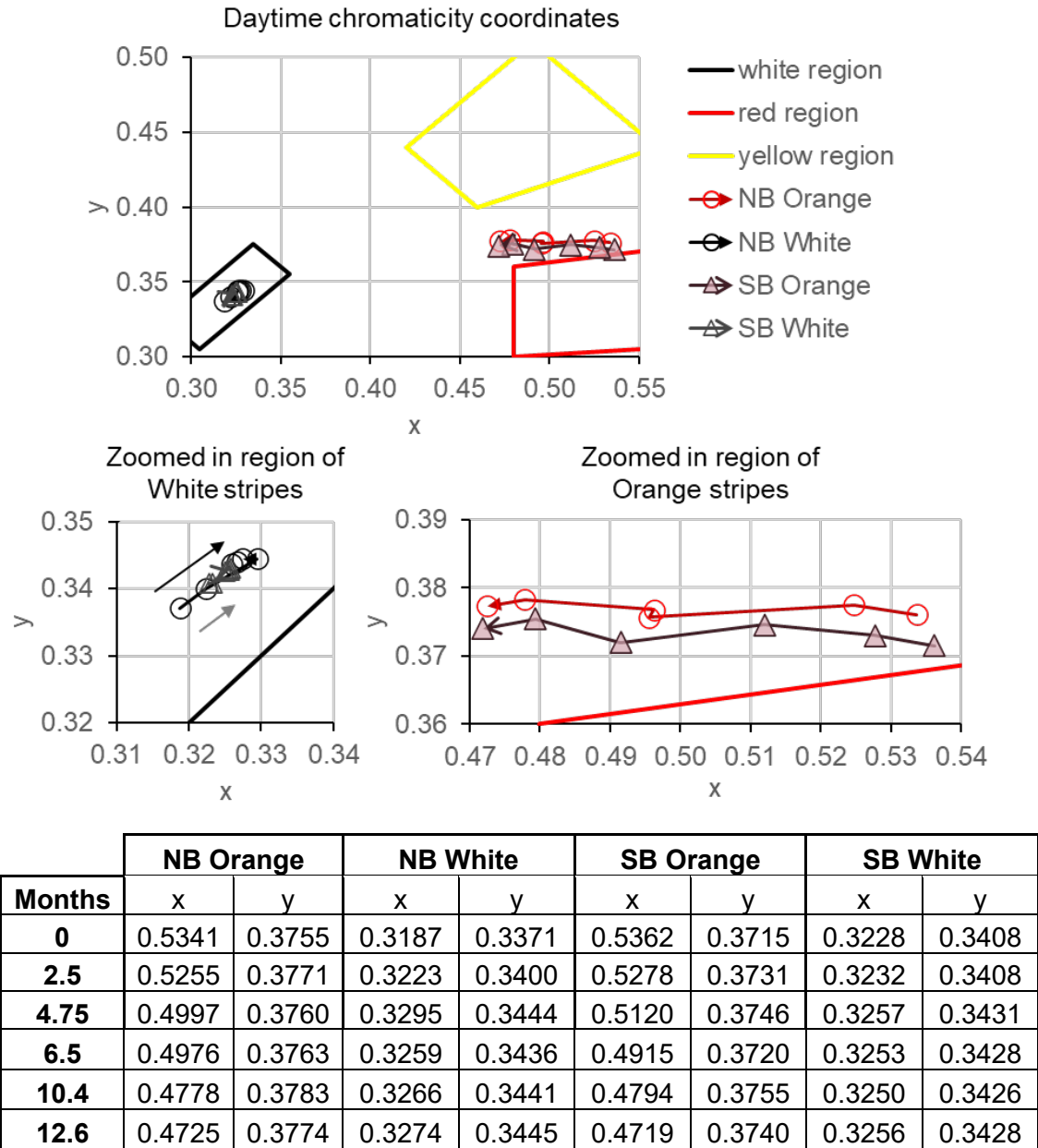
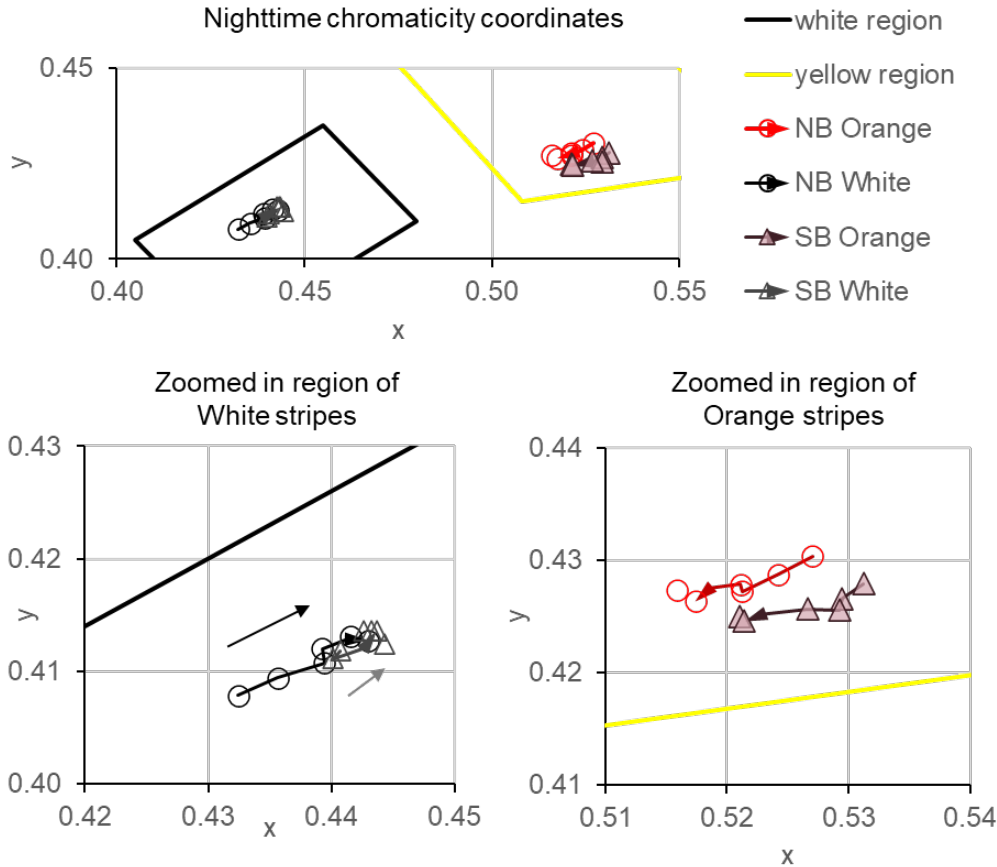


**Figure 4.12: Average daytime color coordinates over time after orange striping installation, compared with regions in ASTM Standard D6628 (n = 48 measurements for NB White, SB Orange, SB White (except for 12.6 months,  $n_{SB\ Orange} = 27$  and  $n_{SB\ White} = 24$ ); n = 96 measurements for NB Orange); arrows indicate increasing number of months**



Months	NB Orange		NB White		SB Orange		SB White	
	x	y	x	y	x	y	x	y
0	0.5270	0.4303	0.4324	0.4079	0.5313	0.4279	0.4407	0.4118
2.5	0.5242	0.4287	0.4356	0.4094	0.5295	0.4266	0.4402	0.4111
4.75	0.5212	0.4272	0.4394	0.4108	0.5293	0.4256	0.4443	0.4124
6.5	0.5211	0.4278	0.4392	0.4120	0.5266	0.4257	0.4426	0.4136
10.4	0.4799	0.3783	0.4757	0.3783	0.3266	0.3441	0.4794	0.3755
12.6	0.4744	0.3775	0.4706	0.3773	0.3274	0.3445	0.4719	0.3740

**Figure 4.13: Average nighttime color coordinates over time after orange striping installation, compared with regions in ASTM Standard D6628 (n = 48 measurements for NB White, SB Orange, SB White; n = 96 measurements for NB Orange); arrows indicate increasing number of months**

The daytime color coordinates of NB Orange and SB Orange all moved towards lower x-values over the installation months, which may indicate some bleaching effect over the 12.6-month period (Figure 4.12). A similar trend is apparent for the nighttime color coordinates as the NB Orange and SB Orange

coordinates both moved towards lower x- and y-values over the installation months (Figure 4.13).

For the white striping, all color coordinates trended from bottom left to top right. Whereas the daytime color coordinates changed only very little over the 12.6 months, the nighttime color coordinates for white stripes changed a lot and almost as much as the orange striping colors.

## **Dashboard camera recordings**

To evaluate striping visibility from the driver's perspective, video recordings were taken from inside the car with a dashboard camera video GoPro8. AHMCT personnel drove a vehicle with a dashboard camera on two occasions (about 0 and 6 months after orange striping installation) through the work zone with orange temporary striping. The work zone was recorded in the SB and NB directions during the daytime and nighttime as shown in Figure 4.14.

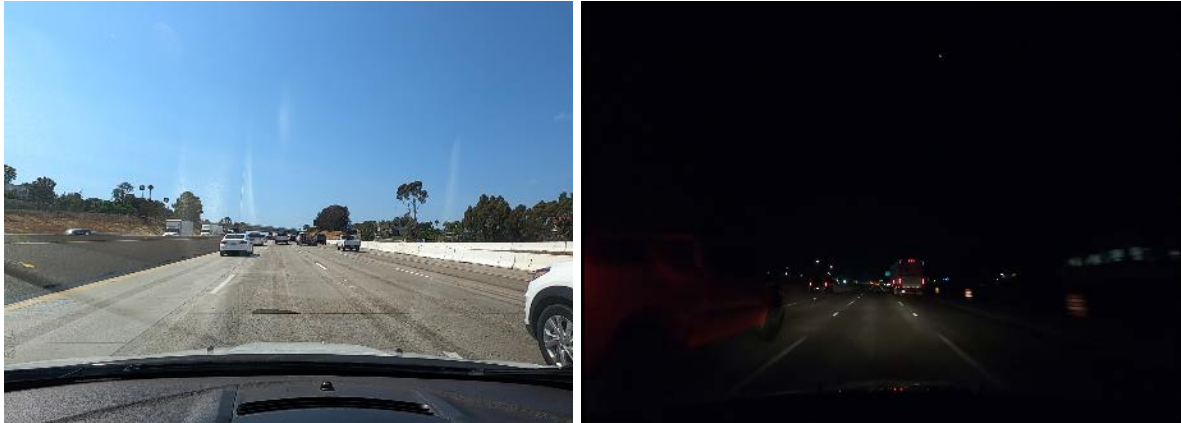


**Figure 4.14: Screenshots from dashboard camera videos from June 14 and 15, 2021 of work zones with temporary white striping; Left: I-5 northbound during the day; Right: I-5 southbound at night.**

Figure 4.15 shows the same location on the I-5 in the SB direction at Las Flores exit at daytime versus nighttime. The orange appeared less intense at night and more yellow than orange. Figure 4.16 shows orange along both sides of white striping in northbound direction. The yellow appearance at night aligned with the quantitative measurements (Figure 4.14). However, the automatic camera white balancing and the car head lights contributed to the color appearance on the pictures. In addition, there was a difference in head light quality and color for different vehicles used to drive through the work zone.



**Figure 4.15: Screenshots from dashboard camera videos in southbound direction, at Las Flores exit, daytime versus nighttime, lane 3, May 2022**

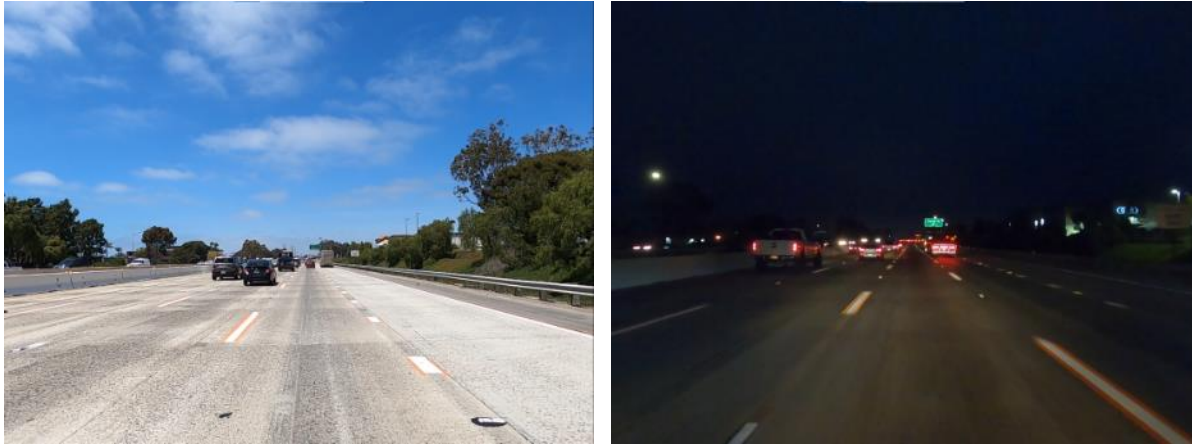


**Figure 4.16: Screenshots from dashboard camera videos in northbound direction, at Cannon Rd exit, daytime versus nighttime, lanes 3 and 4, May 2022**

The dashboard camera video proved to be less sharp than cell phone camera photos from inside the vehicle. Therefore, no further analysis was performed with the dashboard camera videos.

## **Striping quality evaluation for orange tape striping**

Orange along both sides of white tape stripes were installed in November 2021 on the north half of NB I-5, but they did not adhere well to the freeway surface after rain events. This may be related to the fact that no primer was used on the pavement, which also had visible grinding grooves (Figure 4.17 left). The tape stripes were removed from I-5 on April 12 and 13, 2022. The orange contrast with the tape stripe had noticeable discoloration just five months after installation (Figure 4.17, right).



**Figure 4.17: Tape on freeway concrete surface with grinding grooves (left); Orange tape striping worn (at 5 months) and new**

For the orange tape, the daytime color clearly changed from x- and y-coordinates in the red chromaticity area to smaller x-coordinates for the new tape after 5 months (Figure 4.18). The nighttime color (Figure 4.19, left) was also significantly different from the orange sample paint stripe in Figure 6.1 (left). The retroreflectivity values (Figure 4.19, right) reached high values with  $246 \text{ mcd/m}^2/\text{lx}$  for the orange parts left and right and  $357 \text{ mcd/m}^2/\text{lx}$  for the white middle part.

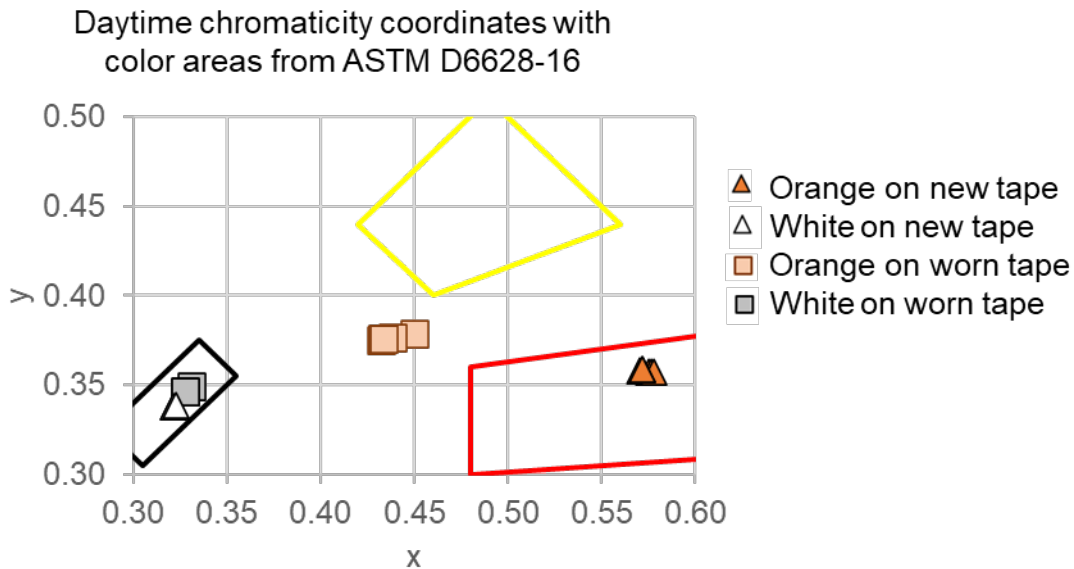


**Figure 4.18: Daytime color measurements on new and worn orange tape, 3 worn stripes after 5 months of installation, 1 new stripe**

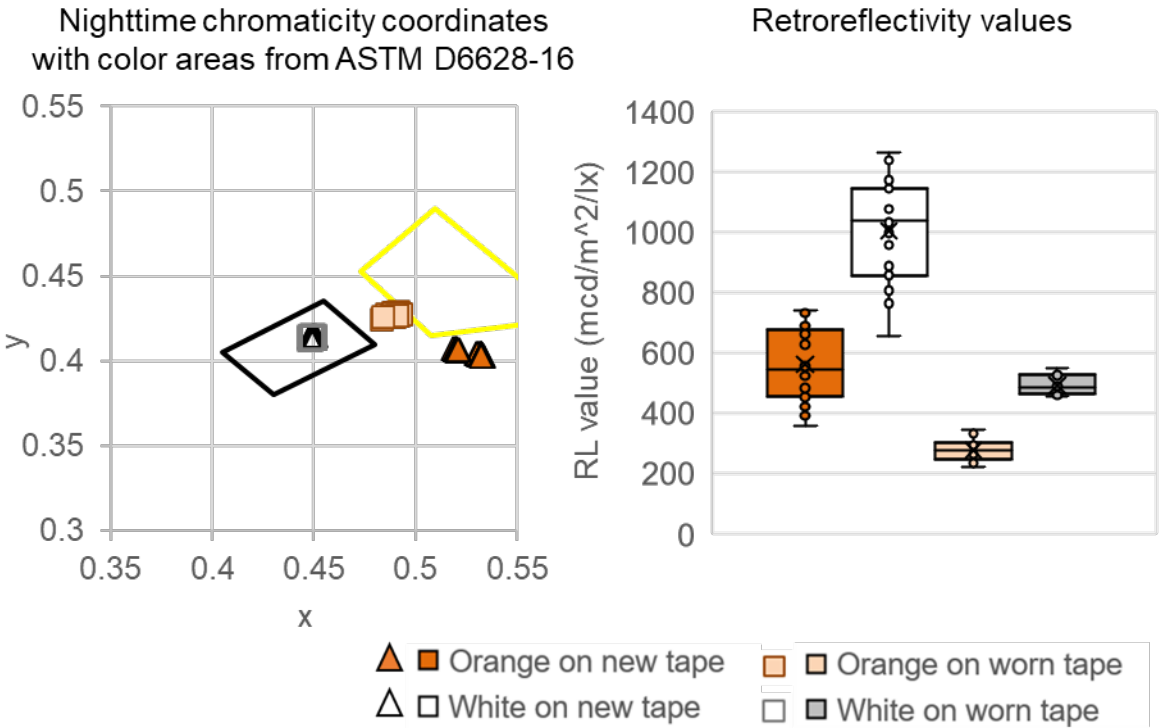


**Figure 4.19: Nighttime color and retroreflectivity measurements on new and worn orange tape, 3 worn stripes after 5 months of installation, 1 new stripe**

To study the color degradation in more detail, new orange tape stripes (Figure 4.20, left) were installed at AHMCT on asphalt in the sunshine on May 22, 2022. Measurements on May 25, June 3, and June 11, 2022 showed no significant changes in retroreflectivity (Figure 4.21). The orange stripes (left and right) have slightly lower retroreflectivity (average of 479 mcd/m<sup>2</sup>/lx for the left stripe and 496 mcd/m<sup>2</sup>/lx for the right stripe) than the white stripes (average of 599 mcd/m<sup>2</sup>/lx).

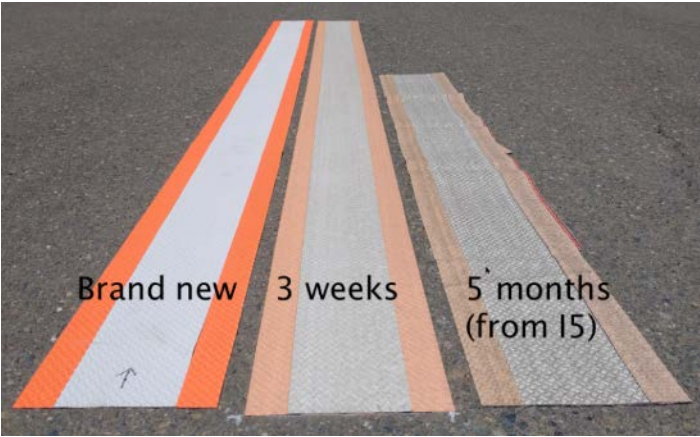


**Figure 4.20: Color degradation of orange along both sides of white tape after exposure to sunlight**

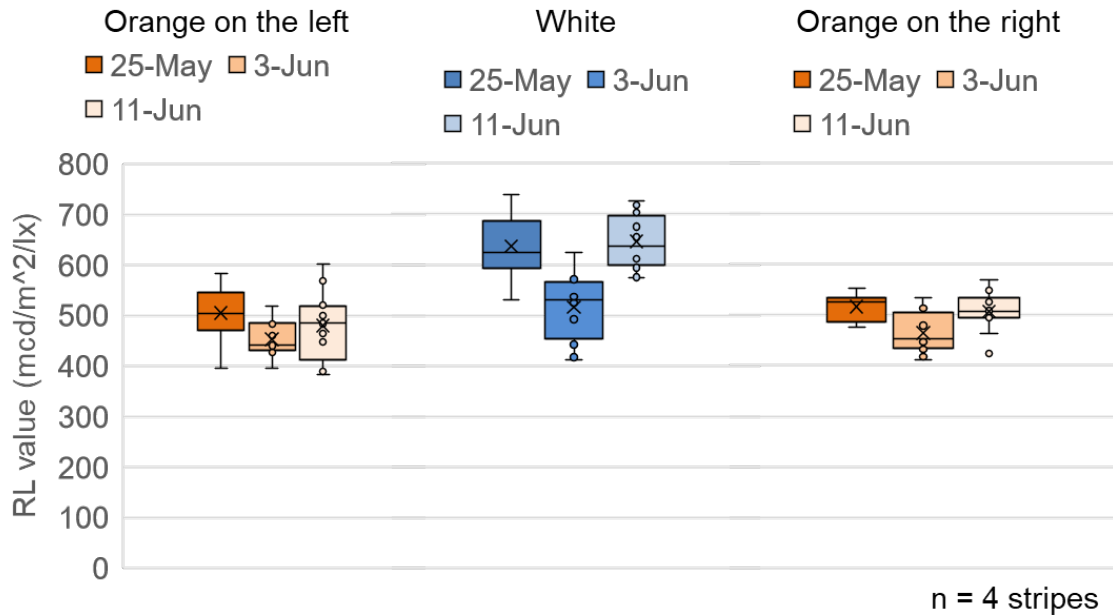


**Figure 4.21: Retroreflectivity measurements of orange tape, left in the sunshine after installation on May 22, 2022, 4 stripes, measured 3x each**

However, there were significant changes of chromaticity coordinates over the 12 days outside in the sun (Figure 4.22 and Figure 4.23). The daytime chromaticity values for the left and right orange parts of the tape stripe start with a mean of  $x = 0.50$  on May 25 and move towards  $x = 0.42$  on the 12<sup>th</sup> day after installation (June 11), which was a 16% change. The white color coordinates stay within the white color area as defined in ASTM standard D6628-16.

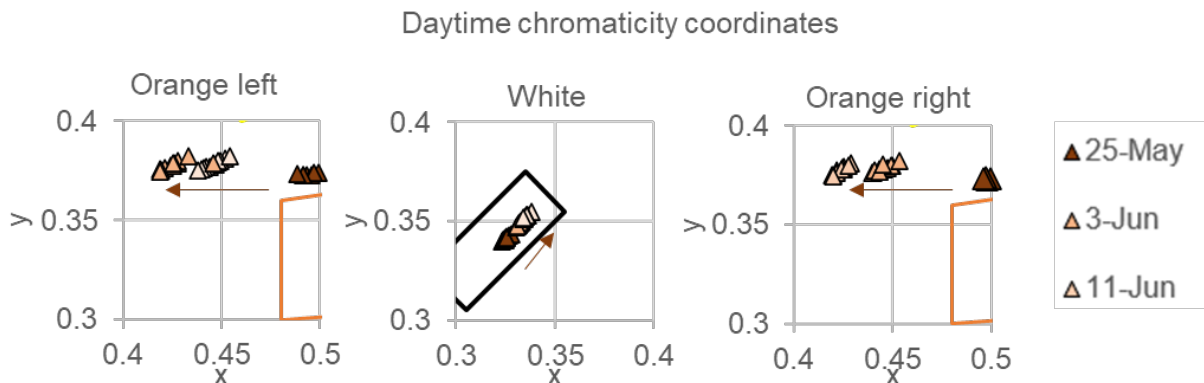


**Figure 4.22: Daytime color measurements of orange tape, left in the sunshine after installation on May 22, 2022; 4 stripes, measured 3x each; white, yellow and red color areas from ASTM D6628-16**

The nighttime color coordinates on May 25 were close to the yellow color area as defined in the ASTM standard D6628-16 (with an average of  $x = 0.50$ ).

They moved towards the white area (average of  $x = 0.46$  on June 11; 8% change) (Figure 4.23). The white stripe stayed within the white area.

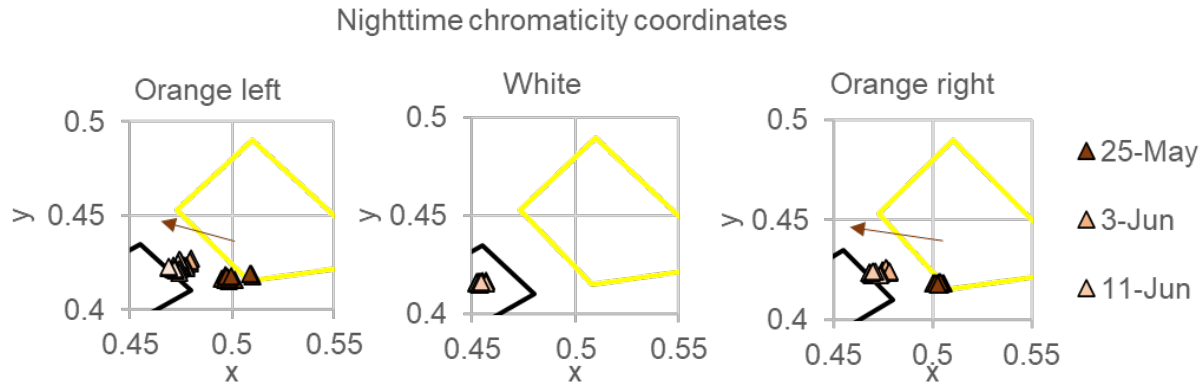


**Figure 4.23: Nighttime color measurements of orange tape, left in the sunshine after installation on May 22, 2022; 4 stripes, measured 3x each; white and yellow color areas from ASTM D6628-16,**

## Interim conclusion

- Retroreflectivity values RL of freshly painted white temporary striping was 2.1 times higher than freshly painted orange temporary striping.
- Retroreflectivity values RL of painted white and orange temporary striping decreased over 12.6 months between 53.9% to 76.5% of the initial value at installation (0 months).
- Compared with the threshold of  $RL = 100 \text{ mcd/m}^2/\text{lx}$  for satisfactory visibility, SB White striping had lower RL values at 2.5 months, NB Orange along both sides of white striping at 4.75 months, and SB Orange striping (white preceding orange) at 12.6 months. NB orange falls in between SB white and SB orange striping. NB White striping, which had been repainted when orange striping was applied, always exceeded the threshold.
- Both daytime and nighttime color coordinates for orange paint stripe showed a color change over the 12.6 months of installation.
- The nighttime colors of orange paint striping presented within the yellow color region, which matched subjective human perception during nighttime driving as seen in dashboard camera videos.
- Dashboard camera recordings gave an impression of driver perception of orange temporary striping. However, the automatic camera white balancing and the car head lights contributed to varying color appearance on the pictures. No quantitative analysis was performed on the dashboard camera videos.



- For tape stripes, the orange along both sides of white showed a significant bleaching effect already after 12 days of sun exposure.

# Chapter 5: Analysis of Influence on speed and accidents

The influence of orange striping on traffic incidents was analyzed with regard to collision occurrences and vehicle speeds in the work zone. The researchers aimed to compare traffic incidents and speeds for the work zone with orange temporary striping and with only standard temporary white pavement markings as well as periods before the work zone installation. It was hoped to gain qualitative insight into driver awareness or confusion.

## State of the Art

Many studies showed that work zones increase the likelihood of motor vehicle crashes (Rouphail et al., 1988). Speed is established as one of the major risk factors for crashes in work zones (Silverstein et al., 2016; Steinbakk et al., 2019).

Driving is a complex task with simultaneously occurring physical and physiological processes (Kummetha et al., 2020). Kummetha et al. (2020) analyzed the dynamics of work zone configurations from a behavioral perspective and found that the configurations play a critical role in a driver's mental workload (Kummetha et al., 2020).

In their analysis of work zone accidents, Harb et al. (2008) showed that driver inattentiveness and hostile driving are critical factors (Harb et al., 2008). Steinbakk et al. (2019) found that speed limit signs might not be enough to make drivers slow down in work zones and so suggested additional measures like road delineators (Steinbakk et al., 2019). Li and Bai (2009) found for accidents that occurred in Kansas work zones between 1992 and 2004 that head-on collisions were the dominant type of fatal crashes while rear-end collisions were the dominant type of crashes with an injury (Li & Bai, 2009). They also found that most fatal crashes involved trucks, while crashes with injury usually involved light-duty vehicles only (Li & Bai, 2009).

## Traffic incidents in the work zones

Data were collected from the Caltrans Performance Measurement System (PeMS), the Statewide Integrated Traffic Records System (SWITRS), and Transportation Injury Mapping System (TIMS). PeMS collects traffic data in real-time from over 39,000 individual detectors. SWITRS is a database collecting and processing data gathered from collision scenes. TIMS is a database where SWITRS data are corrected and upgraded.

The construction zone on I-5 reached roughly from Absolute Post mile (Abs PM) 46.9 (Palomar Airport Rd Overcrossing) in the south to Abs PM 51.4 (Cassidy Overcrossing) in the north. The following locations were defined as locations of interest, e.g. the northern and southern ends of the length of I-5 being analyzed (Table 5.1). Cross streets were used in the manual processing steps to select accidents.

**Table 5.1: Locations of interest**

Abs PM	CA PM (R)	Latitude	Longitude	Location of interest	Additional comments
54	54.122	33.207020	-117.384941	Corridor north end	S of boundary between San Diego and Oceanside county
52	52.122	33.187932	-117.360508	WZ north end at Abs PM 52	1045 ft S of Oceanside Blvd, 1445 ft N of California St
51	51.122	33.176118	-117.350443	WZ north end at Abs PM 51	On-/off-ramps to 78/Vista Way
47	47.122	33.123365	-117.322664	WZ south end at Abs PM 47	N of Palomar Airport Rd
46	46.122	33.110416	-117.31504	WZ south end at Abs PM 46	4790 ft S of Palomar Airport Rd, 2890 ft N of Poinsettia
26	26.122	32.8398310	-117.23546	Corridor south end	Intersection with SR52

For comparison of similar time periods, five-month periods were defined by removing the WZ installation in November 2021 and striping dates in April 2022 (Table 5.2).

**Table 5.2: Examined 5-month periods**

S18	W18/19	S19	W19/20	S20	W20/21	S21	W21/22	S22	W22/23
04/14/18 - 09/14/18	11/10/18 - 04/10/19	04/14/19 - 09/14/19	11/10/19 - 04/10/20	04/14/20 - 09/14/20	11/10/20 - 04/10/21	04/14/21 - 09/14/21	11/10/21 - 04/10/22	04/14/22 - 09/14/22	11/10/22 - 04/10/23
no WZ				no WZ, COVID19-pandemic shutdowns		no WZ	WZ w. white striping	WZ w. orange striping	

Between Abs PM 46 and 52, the Vehicle Miles Traveled (VMT) averaged 88 million miles ( $8.8 \times 10^7$  miles) for the five-month period before COVID-19 pandemic shutdowns started in March 2020 (S18, W18/19, S19; Figure 5.1).

Since April 2021 (periods S21, W21/22, S22, W22/23), the average VMT rose to an average of 84 million miles ( $8.4 \times 10^7$  miles) per period again. NB and SB traffic volumes in VMT were very similar, with up to 22% differences.

Figure 5.2 displays the VMT over the year 2022 in the SB and NB direction. March to August had a larger traffic volume than September to February. November and February had the lowest VMT for both directions.

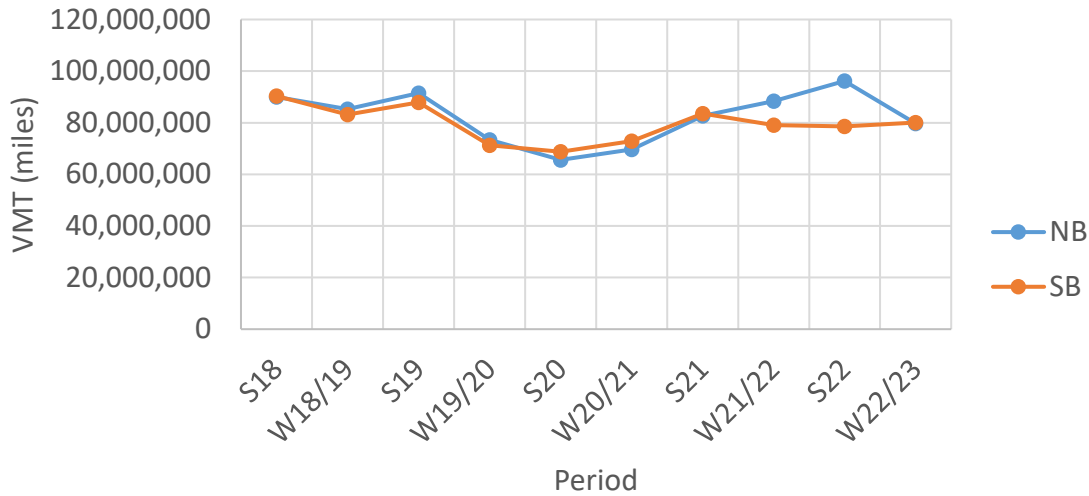


**Figure 5.1: Vehicle Miles Traveled for 5-month periods in NB and SB direction, Abs PM 46 – 52, from PeMS database**

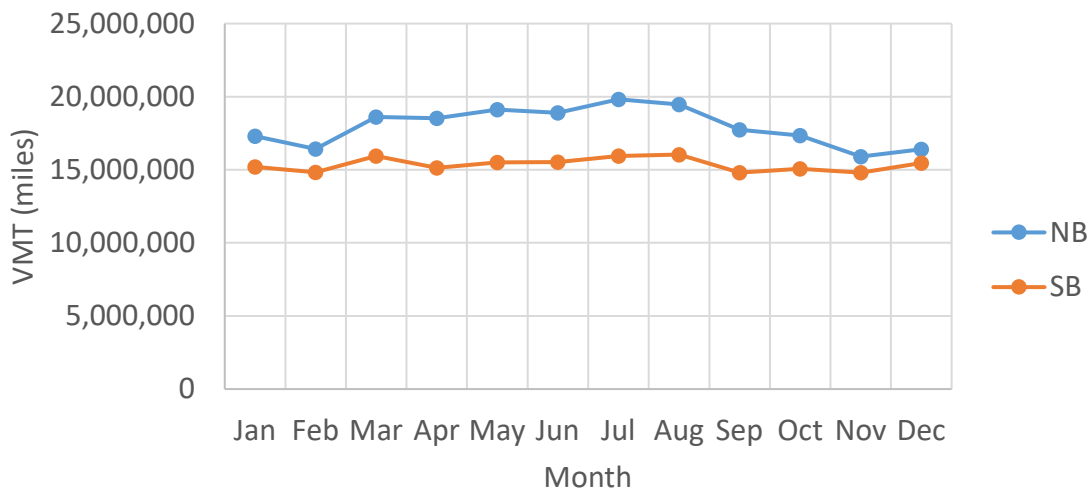


**Figure 5.2: Vehicle Miles Traveled per month for 2022 in NB and SB direction, Abs PM 46 - 52, from PeMS database**

## Comparison of data bases

SWITRS is a California Highway Patrol (CHP) service that collects and maintains all accident data. Reports and data are finalized two years after the year of the accident, but raw data are regularly uploaded and available through I-SWITRS. TIMS provides various reports and data mapping services. TIMS takes the SWITRS data and corrects and upgrades the latitude/longitude data fields of the SWITRS files. Various other entries are completed in this process as well. The TIMS raw data were considered provisional after 2020 and the last data set extended through the end of end of 2022. The TIMS raw data did not include accidents categorized as personal damage only (PDO), which was about two-thirds of the accidents.

In the analysis of accidents in the WZ, the SWITRS raw data file was processed with some Python coding but had to be manually processed using Excel. The geospatial latitude and longitude values were not reliable. Fields describing the accident were used inconsistently, and terminology varied and had to be interpreted on a case-by-case basis.

The total counts for the accidents found using the three databases is shown in Table 5.3. It does not include the last period W22/23 because it was not available in TIMS.

**Table 5.3: Total accident count (NB and SB) for the 9 first 5-months periods from 04/14/18 to 9/14/2022 (as defined in Table 5.2) for Abs PM 46 – 52; data downloaded in June and July 2023**

Data Source	Count	% of SWITRS count
PeMS	1761	155%
SWITRS	1137	100%
SWITRS w/o PDO	400	35%
TIMS	422	37%

The SWITRS data were cross checked against the available TIMS data on a case-by-case basis to understand the differences between the two sources. The PeMS accident count was much higher. It was conjectured that this difference was due to how accidents are grouped via searches of SWITRS that gather all the primary and secondary road references to I-5, and since the lat/long positions are imprecise, cross streets might have been included in the data base. This would be significant if incidents occur at intersections such as SR-78.

Figures 5.3 and 5.4 compare the data from PeMS and SWITRS and include a plot of only rear end accidents from SWITRS. The trend lines tracked each other well with general reduced accident rates during S20.

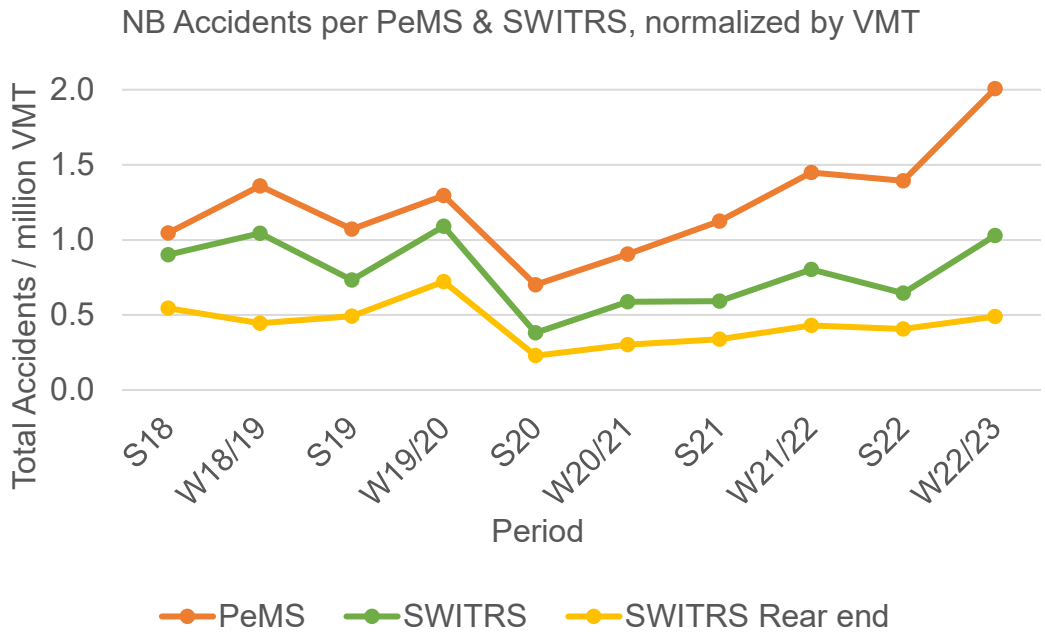


**Figure 5.3: PeMS and SWITRS NB accidents between Abs PM 46 – 52 in 5-month periods, normalized by VMT**

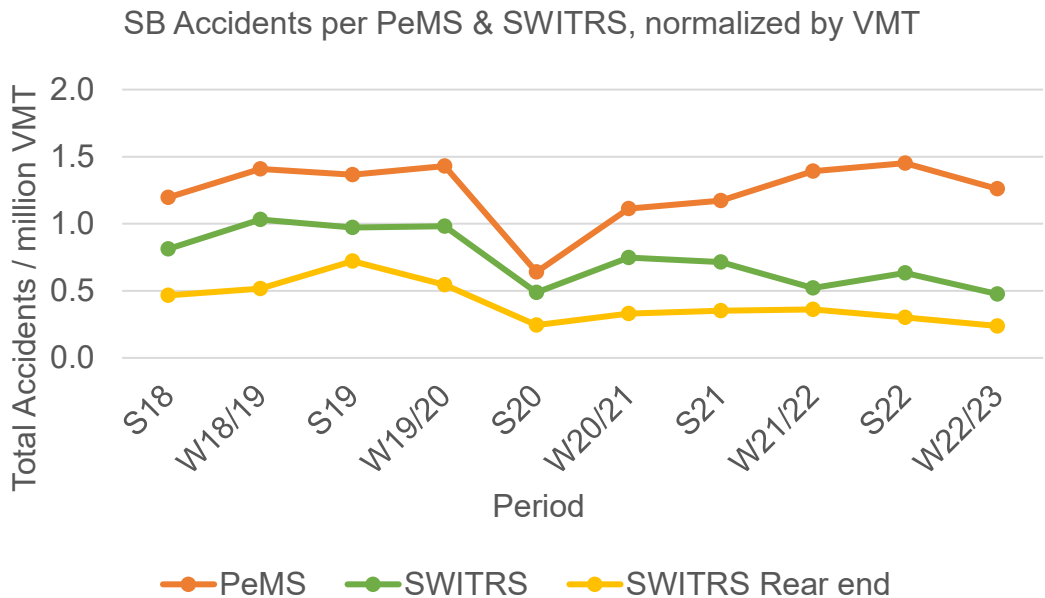


**Figure 5.4: PeMS and SWITRS SB accidents between Abs PM 46 – 52 in 5-month periods, normalized by VMT**

The plots suggest:

- NB WZ accidents dipped slightly but then increased.
- SB WZ accidents remained generally unchanged.

## *Localized PeMS accident data analysis*

Accident data from PeMS were further analyzed by looking at the weekly accident count for the WZ and comparing it to a longer length of I-5 in which the WZ is located. A corridor was defined from Abs PM 26 at the intersection with SR-52 to Abs PM 54 near the northern border of San Diego County to Oceanside (a total of 29 miles). This corridor was selected as it was similar to the freeway in the WZ and within city jurisdictions. It avoided the busier downtown area of San Diego and the less busy area near Camp Pendleton. A shorter WZ length of 5 miles between Abs PM 47 to Abs PM 51 was used to exclude the transition into and out of the WZ. The accident counts and trends were compared to the corridor from Abs PM 26 to Abs PM 54 excluding the WZ (24 miles). Weeks started on Sunday, and the periods were divided as follows:

- Before striping and WZ installation - Week 1 to 50 (11/29/2020 to 11/13/2021),
- WZ installed with white striping - Week 51 to 71 (11/14/2021 to 4/9/2022),
- WZ installed with orange striping - Week 72 to 122 (4/10/2022 to 4/1/2023).

Counts for the WZ area and for the corridor excluding the WZ were plotted with linear trendlines for absolute accident numbers in the NB direction in Figure 5.5 and in the SB direction in Figure 5.6. The trendlines show a generally slowly increasing trend for accidents over the whole 122 weeks observed, which can be explained by increasing traffic rates after the COVID-19 pandemic shutdowns. However, the data scatter was very large, and trendlines for the shorter time periods were not statistically significant. It does appear that there was generally an upward trend for all accidents which was expected as the traffic returned to normal after the reduction caused by the pandemic shutdowns. The SB WZ accident rate (Figure 5.6) does seem to be flat, whereas the NB WZ stretch tends to track the overall increase (Figure 5.5).

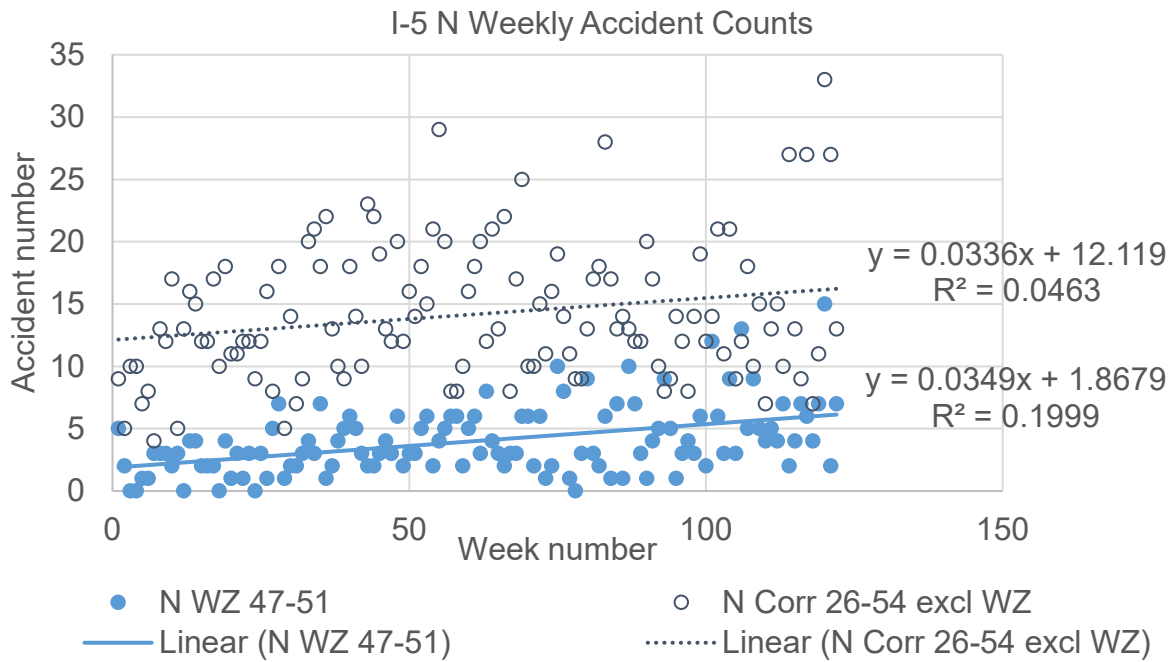


**Figure 5.5: Northbound accident counts with linear continuous trendlines in WZ and corridor excluding WZ, PeMS data**

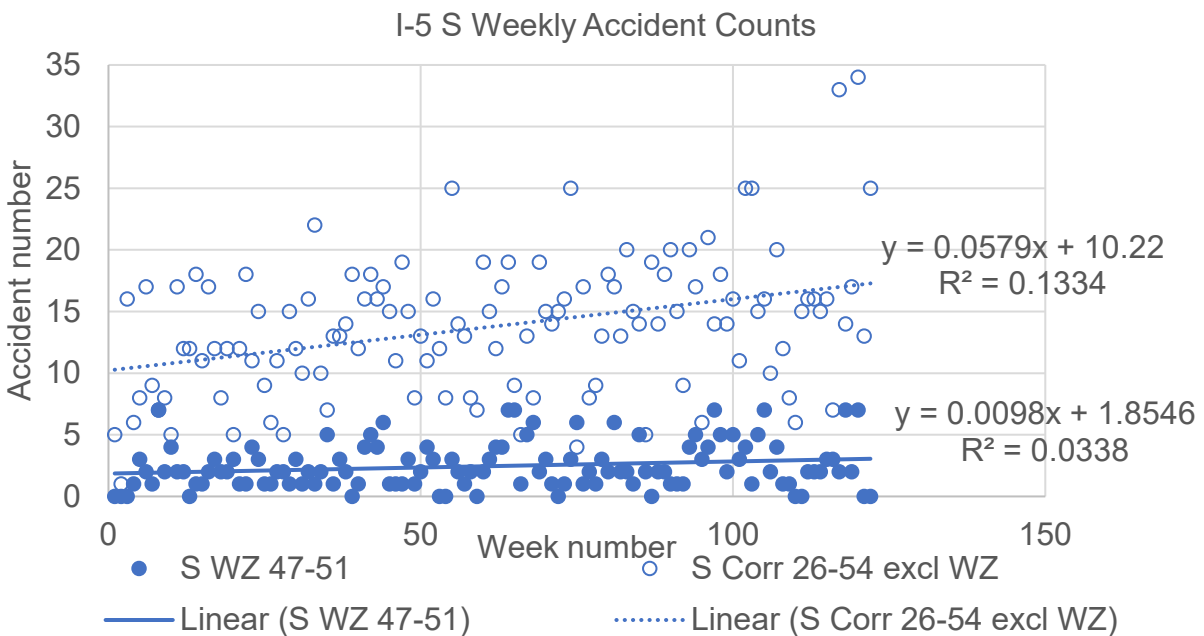


**Figure 5.6: Southbound accident counts with linear continuous trendlines in WZ and corridor excluding WZ, PeMS data**



Figure 5.7 shows the same traffic incidents for I-5 NB as Figure 5.5, but normalized by VMT and split into the time periods before WZ installation, WZ with temporary white striping, and WZ with orange temporary striping. Accident rates per VMT before WZ installation was similar for the WZ and corridor without WZ. There was a slightly decreasing trend for accidents per VMT during the WZ with only white temporary striping, but increase for WZ with orange temporary striping. The individual linear trendlines are described in Table 5.5. The coefficient of determination  $R^2$  was generally very low, which indicates a poor fit. This was due to the large scatter of values because there were relatively few accidents per week over the observed corridor (6 to 48 accidents per week in the NB direction). Comparisons between white and orange striping are not reliable because the  $R^2$  values are very low.

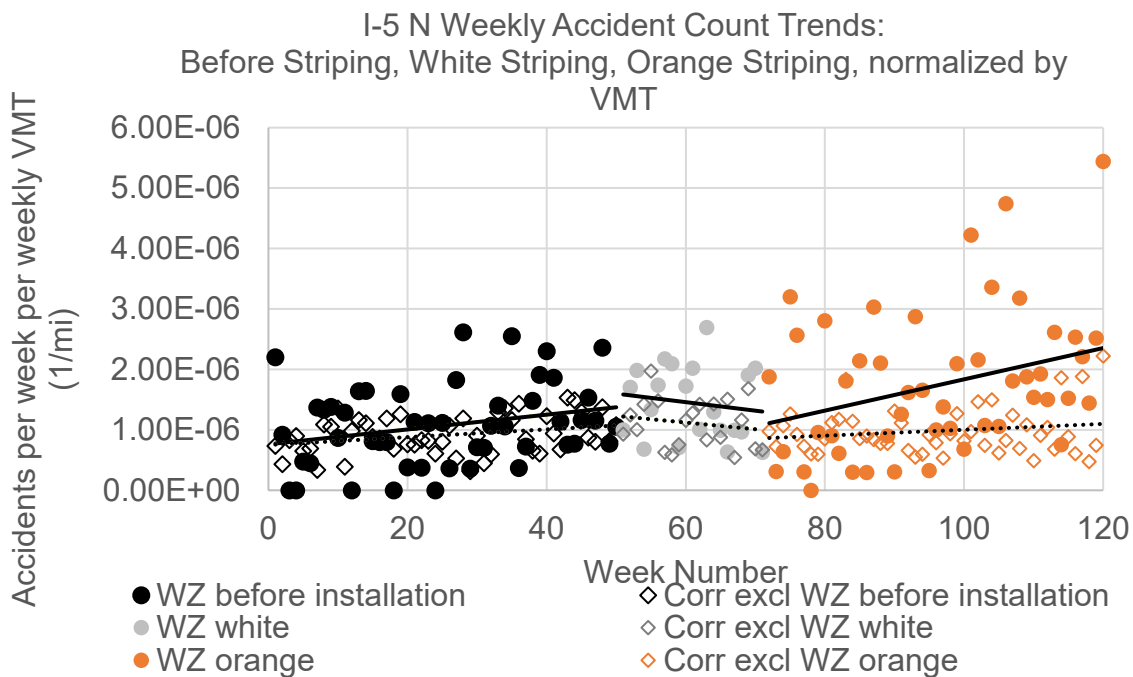


**Figure 5.7: Northbound weekly accidents normalized by the weekly VMT with linear trendlines (bold lines for WZ, dotted lines for corridor excluding WZ), divided into three time periods, PeMS data**

Southbound traffic also behaved similarly with a very slight increasing trend before WZ installation in both road stretches, in the WZ, and in the corridor excluding WZ (Figure 5.8 and Table 5.6). There were relatively few accidents per week over the observed corridor (1 to 41 accidents per week in SB direction), and large data scatter leading to low coefficients of determination  $R^2$  for the accident trend lines.

**Table 5.5: Northbound Trendline Equations and R<sup>2</sup> value**

Northbound Trendline Equations and R <sup>2</sup> value		
Corr excl WZ before inst.	Corr excl WZ white	Corr excl WZ orange
$y = 6.40E-09x + 7.51E-07$ $R^2 = 0.0887$	$y = -1.11E-08x + 1.79E-06$ $R^2 = 0.0294$	$y = 4.86E-09x + 5.15E-07$ $R^2 = 0.033$
WZ before installation	WZ white	WZ orange
$y = 1.22E-08x + 7.62E-07$ $R^2 = 0.1192$	$y = -1.41E-08x + 2.31E-06$ $R^2 = 0.0207$	$y = 2.59E-08x - 7.52E-07$ $R^2 = 0.1066$

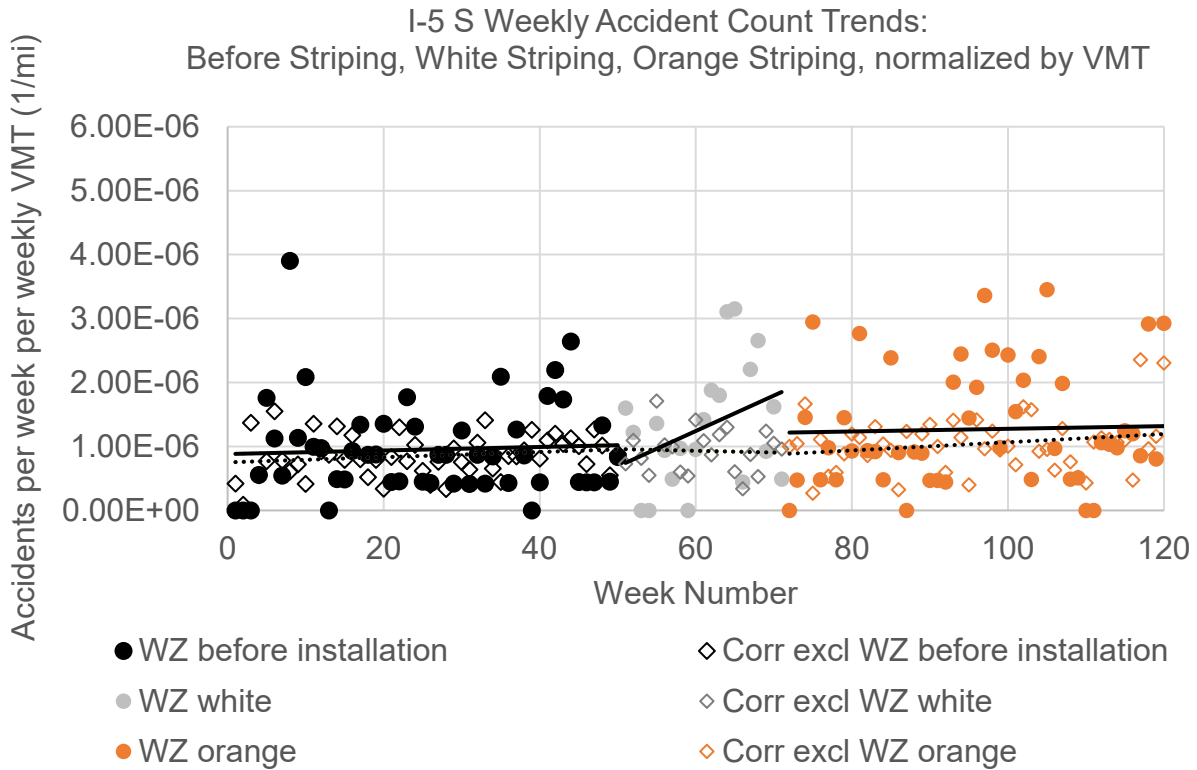


**Figure 5.8: Southbound weekly accidents normalized by the weekly VMT with linear trendlines (bold lines for WZ, dotted lines for corridor excluding WZ), divided into three time periods, PeMS data**

**Table 5.6: Southbound Trendline Equations and R<sup>2</sup> value**

Southbound Trendline Equations and R <sup>2</sup> value		
Corr excl WZ before inst.	Corr excl WZ white	Corr excl WZ orange
$y = 4.04E-09x + 7.52E-07$ $R^2 = 0.0335$	$y = -2.65E-09x + 1.09E-06$ $R^2 = 0.0023$	$y = 6.40E-09x + 4.26E-07$ $R^2 = 0.0502$
WZ before installation	WZ white	WZ orange
$y = 2.76E-09x + 8.82E-07$ $R^2 = 0.0028$	$y = 5.54E-08x - 2.08E-06$ $R^2 = 0.1332$	$y = 2.09E-09x + 1.07E-06$ $R^2 = 0.001$

# TIMS accident data analysis

The TIMS accident data were compared for Abs PM 46 to 51 for five months just before WZ installation (S21, 04/14/21 - 09/14/21), WZ with white temporary striping (W21/22, 11/10/21 - 04/10/22), and WZ with orange temporary striping (S22, 04/14/22 - 09/14/22). As described above, TIMS does not include PDO accidents but only accidents with injuries and fatalities. The total number of accidents during the three five-month periods was only 62 in both directions.

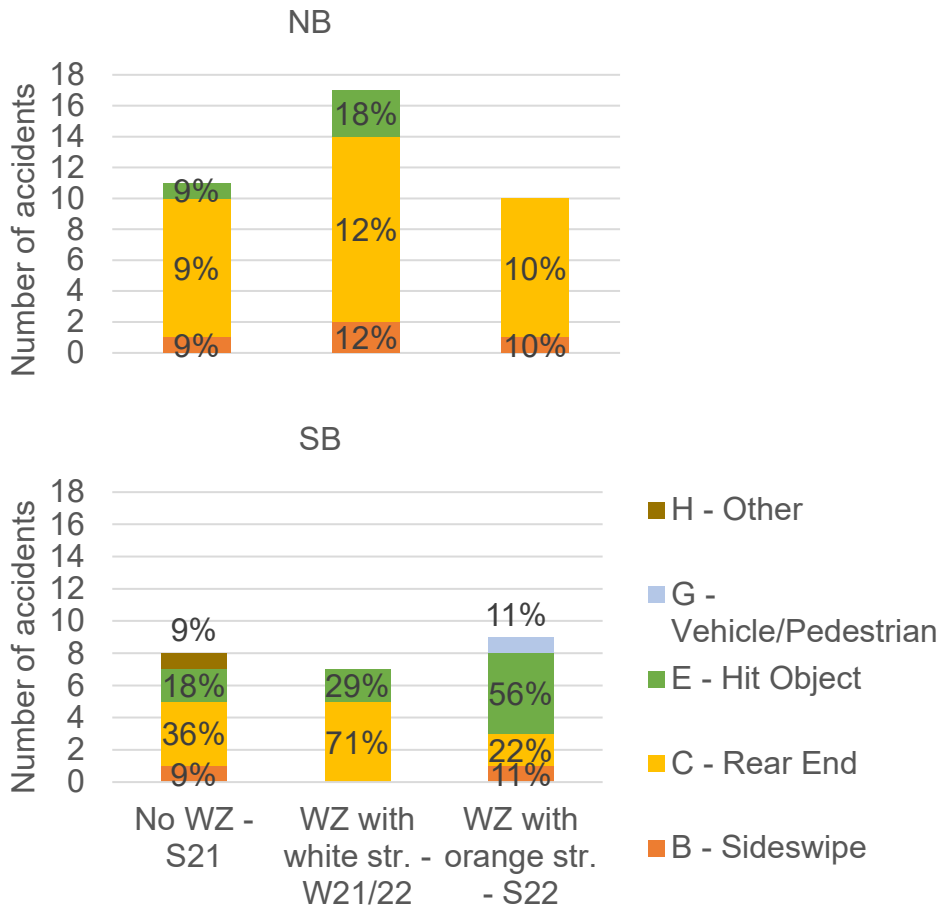


**Figure 5.9: TIMS accident type numbers and distribution for Abs PM 46 – 51 during selected 5-month periods (data downloaded on 7/31/23)**

Figure 5.9 shows that there were fewer accidents in the SB than NB direction. For all periods, except for the WZ with orange striping for SB direction, rear-end collisions were the main accident type. No significant trend could be found for the influence of work zone installation or temporary striping type because the number of accidents was too low for reliable statistics.

## Vehicle Speed in the Work zone

To assess vehicle speed in the work zone, data were collected from three sources: video recordings with CCTV cameras installed in the work zones, HERE technologies, and PeMS. HERE Technologies is a location data and technology company that provides speed data for given road segments on an hourly resolution. The three data sources are compared in Table 5.7. Data were obtained as follows:

- A) The speed from CCTV video recordings was collected from video processing as described in Chapter 2.
- B) From the PeMS database, data at Las Flores SB were at Abs PM 50.57 and from sensor VDS 1108463, whereas data at Las Flores NB were obtained at Abs PM 50.34 and from sensor VDS 1119941. The PeMS sensors at Las Flores were loop sensors, which are located underneath the pavement. Over the Abs PM 46 to 53 range, about half of the sensors were loop sensors, and the other half were MVDS (radar) sensors. PeMS receives data per lane. The aggregate flow is the sum of lane flows. The aggregate speed is the speed per lane weighted by the flow per lane. PeMS data were obtained as *Time series* or as *Time-of-day contours*.
- C) HERE Technologies data were provided as hourly speed data based on smartphone tracking data.

Challenges for the vehicle speed evaluation and comparison included:

- Different systems might use Abs PM or Realignment (R) post miles,
- Different systems have different sampling resolutions (e.g., hourly data, per vehicle data, or in 5-min increments),
- Different systems have different spatial resolution (per lane or aggregated over all lanes in one direction; vehicle passing over one sensor vs. vehicles in a stretch of 48 ft),
- Different systems used sensors at different locations (camera vs. VDS sensor locations).

PeMS data had uncertainty because the data quality varied between "100% observed" to "25% observed". According to the PeMS manual, this means that up to 75% of the data is estimated. PeMS data had generally lower speeds than the Yolo data from CCTV camera recordings and data from HERE Technologies. The CCTV video analysis overestimated speeds with uncertainty from video frame rate and short evaluation distance of 48 ft or 96 ft. Therefore, only HERE data will be shown in the following sections.

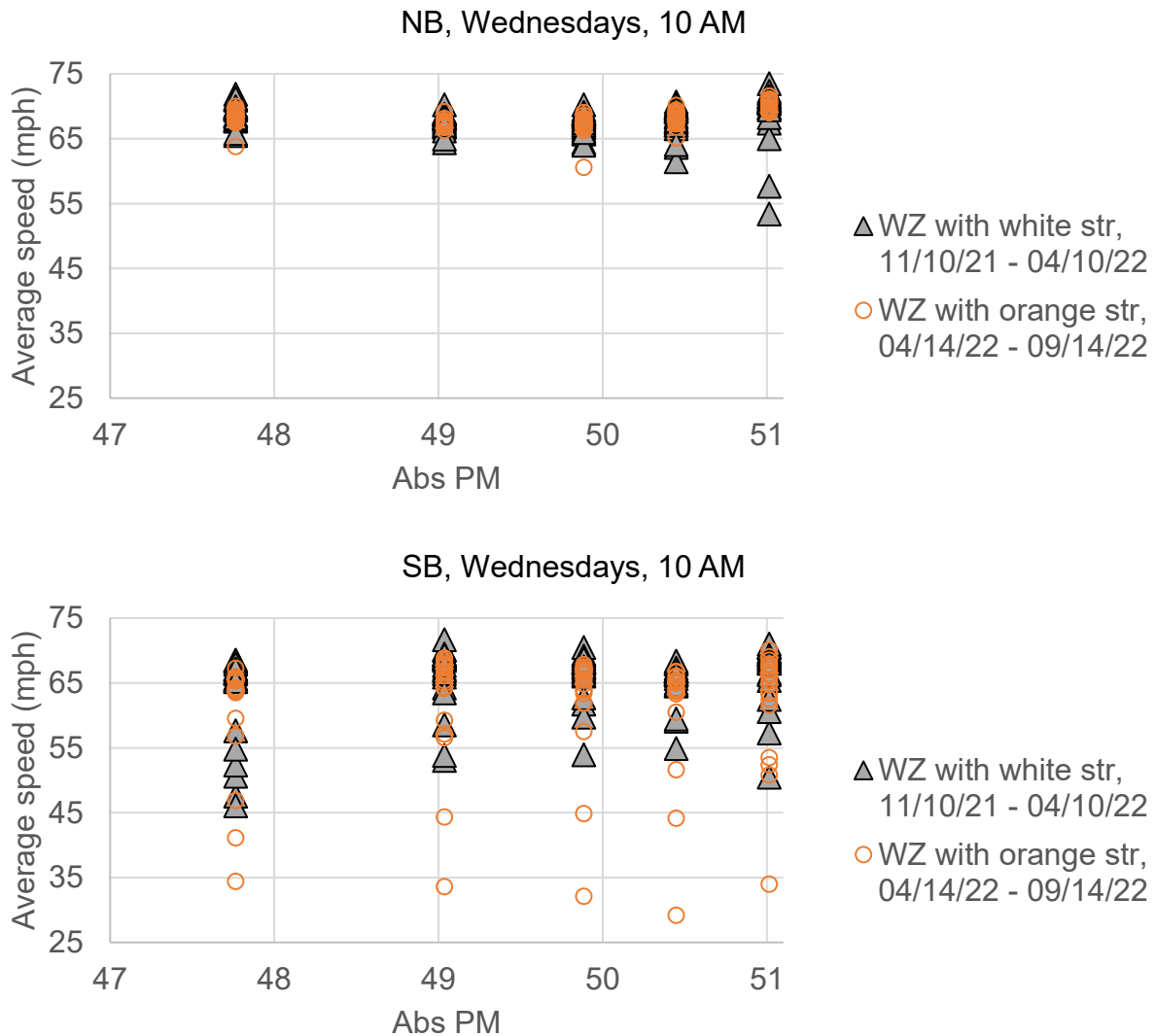
**Table 5.7: Comparison of data source quality for average vehicle speed**

	<b>CCTV video analysis</b>	<b>PeMS</b>	<b>HERE</b>
<b>Sampling rate</b>	Individual vehicle to 20 min	5 min, hourly, daily	hourly
<b>Spatial resolution</b>	Per lane	Per lane or all lanes	All lanes
<b>Data source</b>	Video recording over a road stretch of 48 or 96 ft	Per sensor (loop or radar)	Between on- and off-ramps
<b>Findings</b>	Depends on automatic vehicle detection and overestimated	Data quality is varying; sometimes data is not observed but estimated; lane shift might have affected data quality	Coarse resolution with only 1 h averages

Figure 5.10 shows HERE average speeds over the Abs PMs for the work zone for selected Wednesdays for 10:00 am to 10:59 am:

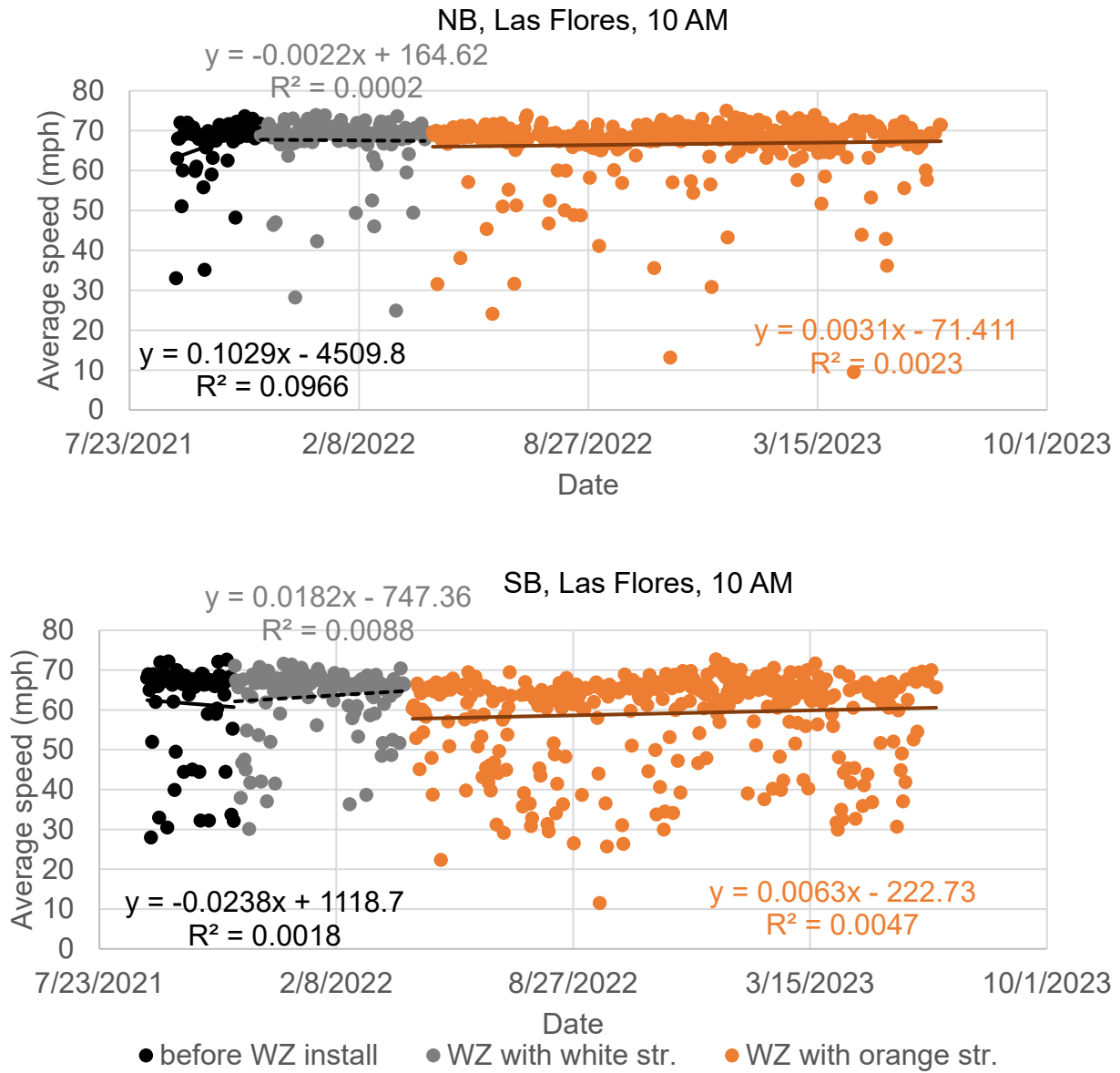
- WZ with white temporary striping: 11/10/21 to 04/10/22,
- WZ with orange temporary striping: 04/14/22 to 09/14/22.

The SB direction had more scatter with average speeds between 29.2 mph to 70.1 mph, whereas average speeds in NB direction were between 53.4 mph to 73.5 mph. Abs PM 51 usually had the highest speeds in NB direction, and Abs PM 49.035 had the highest speeds in the SB direction.



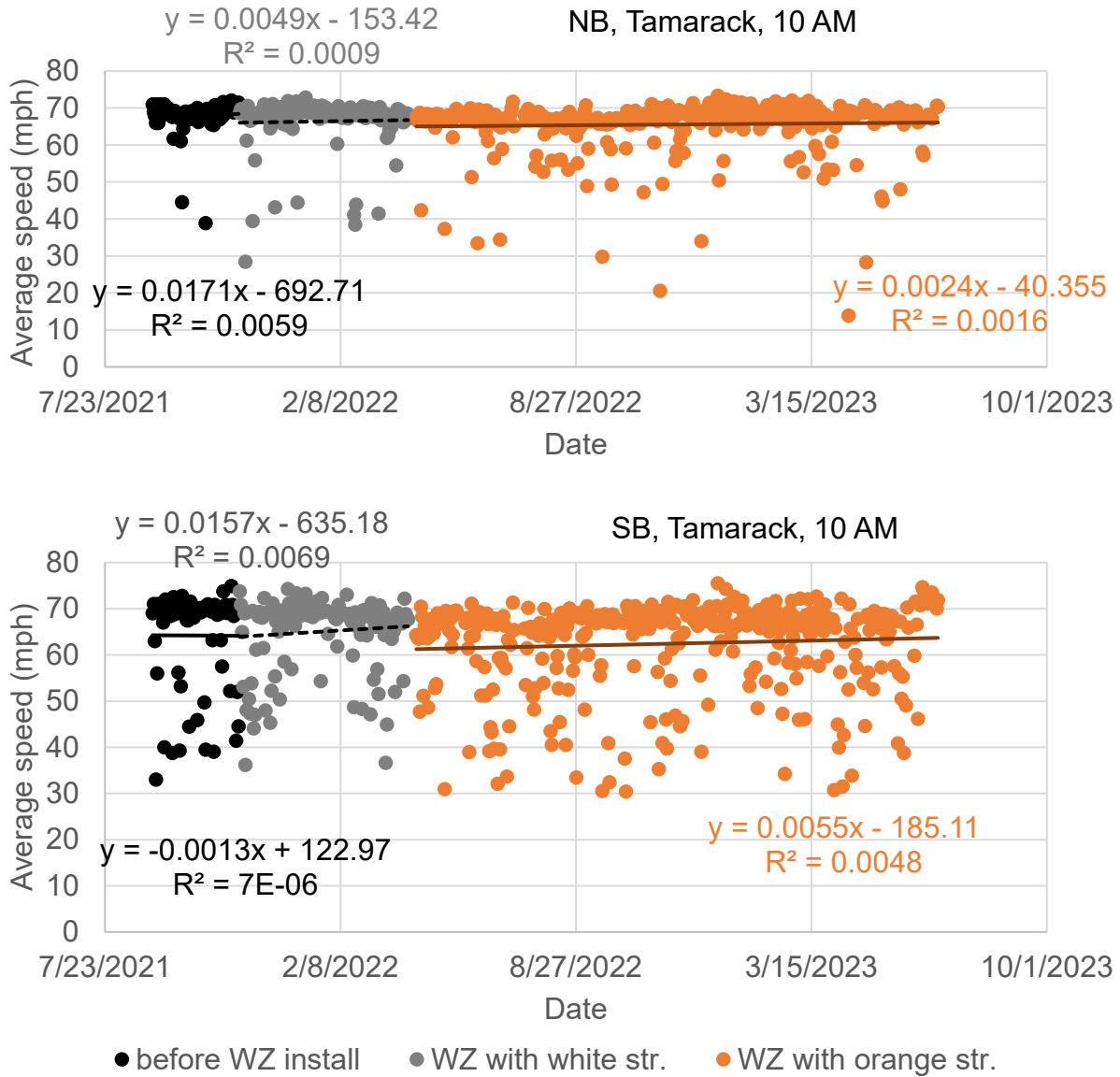
**Figure 5.10: HERE average speed data at 10:00 am to 10:59 am from Abs PM 47 to 51, only Wednesdays**

Figure 5.11 shows the average speeds at the Las Flores ramps (Abs PM 50.448). In general, the SB average speeds were lower and more scattered, which indicated more traffic slowdowns in the SB direction. The time before WZ installation (9/1/21 to 11/13/21) had an increasing average speed trend for the NB direction and a slightly declining trend for the SB direction. For the WZ with white temporary striping (11/14/21 to 4/9/22), the average speeds slightly increased and then decreased for the WZ with orange temporary striping (4/10/22 to 6/30/23).



**Figure 5.11: Average speed from HERE data, per day, at 10:00 am, Las Flores ramps, with linear trendlines**

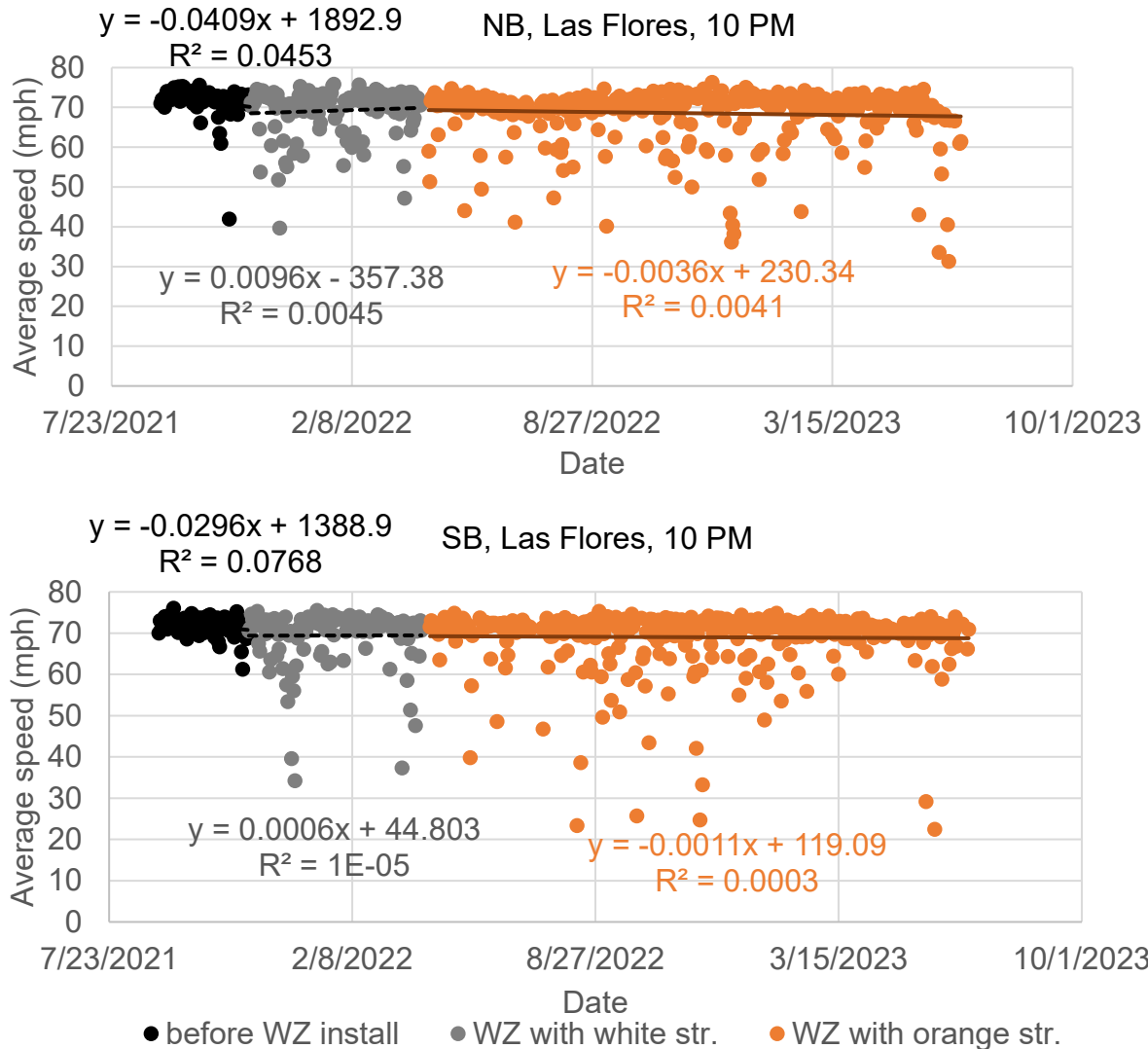
Figure 5.12 shows similar trends at the Tamarack ramps (Abs PM 49.035) with SB speeds generally lower and the average speed for WZ with orange striping lower than WZ with white striping.



**Figure 5.12: Average speed from HERE data, per day, at 10:00 AM, Tamarack ramps, with linear trendlines**

The average speeds at 10 pm were generally higher than the daytime speeds at 10 am (Figure 5.13) for the Las Flores location. The SB average speeds had less scatter at night than during the day (compare to Figure 5.11).





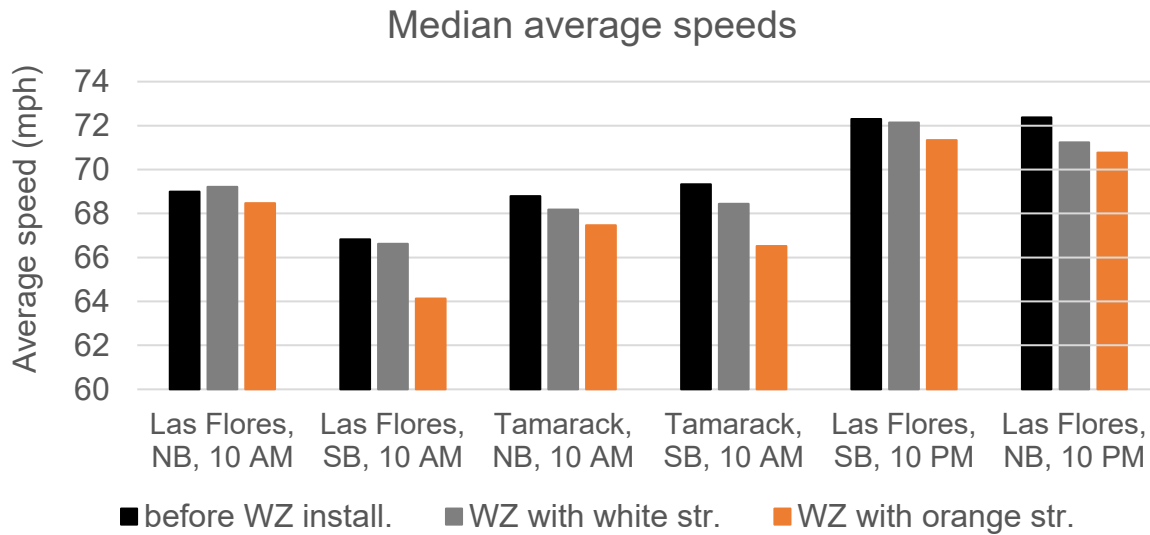
**Figure 5.13: Average speed from HERE data, per day, at 10:00 pm, Las Flores ramps, with linear trendlines**

Table 5.8 and Figure 5.14 show the median average speeds illustrated in Figures 5.11 to 5.13. The median average speeds were generally highest before WZ installation and lowest for WZ with orange striping. The average speeds in the work zone for orange temporary striping were between 0.47 mph to 2.49 mph lower than in the work zone with white temporary striping with differences.

The median average speeds for 10 am reduced more when orange striping was installed in the SB direction than in the NB direction, which can be an effect of the striping pattern (white preceding orange in the SB direction compared to orange along both sides of white in the NB direction). However, other effects, such as differences in traffic flow and VMT or general work zone design, can be alternative explanations.

**Table 5.8: Median average speeds (mph) from HERE data for different time periods and locations**

Location	Direction	Time	Median average speed (mph)		
			9/1/21 - 11/13/21	11/14/21 - 4/9/22	4/10/22 - 6/30/23
			before WZ install.	WZ with white str.	WZ with orange str.
Las Flores	NB	10 AM	69.00	69.21	68.47
Las Flores	SB	10 AM	66.83	66.63	64.13
Tamarack	NB	10 AM	68.80	68.18	67.47
Tamarack	SB	10 AM	69.32	68.44	66.52
Las Flores	NB	10 PM	72.38	71.24	70.77
Las Flores	SB	10 PM	72.30	72.14	71.35



**Figure 5.14: Median average speed from HERE data, per day, at 10:00 pm, Las Flores ramps, with linear trendlines**

## General findings and interim conclusions

- Communication with the local CHP found that no officers referred to the orange striping in their collision reports. Additionally, no CHP officer had taken any complaints regarding the orange striping. Collision speeds were not analyzed because there was no information available. Also, there was no specific insight from Caltrans construction personnel on collisions.

- Accident data from different sources showed a drop in accident rates during the time periods affected by the COVID-19 shutdowns. Accident rates continued to increase afterwards.
- The PeMS database reported about 50% more accidents than the SWITRS database. TIMS is the most reliable database where location data are confirmed, and missing information is added. However, PDO data are excluded, which account for two-thirds of the accidents, and data are only available after multiple months.
- In the WZ road stretch, NB accident rates from PeMS and SWITRS were generally slightly higher than in the SB direction.
- TIMS only reported on 27 accidents in the NB direction and 16 in the SB direction for two five-month periods of work zone installation. Therefore, no clear trend of striping color and pattern can be detected. Rear-end collisions were the main accident types as expected.
- Three different speed data sources were used but provided different average speeds. PeMS data had generally lower speeds than the Yolo data from CCTV camera recordings and data from HERE Technologies. HERE data were chosen for further analysis.
- Median average speeds in the work zone for orange temporary striping were slightly lower than in the work zone with white temporary striping with differences between 0.47 mph to 2.49 mph. This finding indicates a positive effect of orange temporary striping on average vehicle speeds.

# Chapter 6: Conclusions

The influence of orange pavement delineation was investigated in a work zone in Caltrans District 11 in the Interstate I-5 NCC Construction Project in San Diego County. The following findings were made:

- Visual observations of lane keeping are based on quick and ternary decisions. These observations highlighted that pavement joints, road defects, slabs, and curves influence driver behavior in addition to lane striping.
- To increase data quality and reduce subjectiveness, CCTV camera recordings were taken. CCTV cameras were selected for high video quality, remote accessibility, pan, tilt, and zoom functions. The systems were powered by a solar panel per two cameras and a battery. Data were transmitted over mobile phone networks and direct Ethernet connection. In total, eight cameras were mounted on six overcrossings with different road conditions (work zone with curved or straight part, taper shift in and out of work zone at the north and south end, and curve in regular traffic).
- A routine for automated video analysis was programmed in Python and with the YOLOv5 algorithm. Ten-minute videos for Wednesdays and Saturdays at day and at night produced many data points.
- Comparison of automated vehicle center position detection and manual detection in the video recordings showed that most results had comparatively small errors between -0.17 ft to 0.56 ft. However, processing of videos at Las Flores Overcrossing had significant errors for lanes 3 and 4 in the NB and SB direction and lane 1 in the SB direction. Speed analysis from the videos overestimated the vehicle speeds.
- The comparison of lane keeping behavior during work zone with white and with orange temporary striping was inconclusive on the influence of the presence of orange striping or the striping type. Reasons include high data uncertainty over few data points.
- A web-based survey assessed driver perception on work zone awareness and visibility of pavement delineation and preference regarding white vs. orange delineation for over one year (5/18/2022 to 6/5/2023). The overwhelming majority (84.3%) of 1,142 people would like to see orange contrasted striping used in more road construction zones. A large majority (80.4%) of 1,093 respondents found that the orange contrasted striping increased their awareness of being in a

work zone. Respondents stated benefits for reasonable, safe speeds and easier lane keeping from orange striping in work zones.

- Of 608 respondents who had driven through the work zone at night, a clear majority (62.3%) preferred the orange contrasted lane line striping at night over white temporary striping.
- Survey results recommend that public communication can make the orange contrasted striping even more effective.
- Striping visibility was evaluated with a stationary reflectometer, which collected the coefficient of retroreflected luminance, RL, and nighttime chromaticity, and a spectrophotometer for daytime chromaticity values. Due to safety concerns, measurements were only taken during road closures at night and on lane stripes between lane 1 and 2 when two or three of the inside lanes were closed. Both devices had their own light sources for nighttime measurements and high consistency.
- Retroreflectivity values RL of painted white and orange temporary striping decreased over 12.6 months to between 53.9% and 76.5% of the initial value at installation.
- Compared with the threshold of  $RL = 100 \text{ mcd/m}^2/\text{lx}$  for satisfactory visibility, SB White striping had lower RL values at 2.5 months, NB Orange along both sides of white striping had lower values at 4.75 months, and SB Orange striping (white preceding orange) at 12.6 months. NB orange fell in between SB white and SB orange striping. NB White striping, which had been repainted when orange striping was applied, always exceeded the threshold.
- Both daytime and nighttime color coordinates for orange paint stripe showed a color change ("bleaching") over the 12.6 months of installation. Nighttime colors of orange paint striping presented within the yellow color region, which matched subjective human perception during nighttime driving as seen in dashboard camera videos.
- The experimental tape striping with orange along both sides of white tape stripes did not adhere well to the freeway surface after rain events, which was noted by many survey participants. Also, the tape showed a significant bleaching effect five months after installation. Further measurements at UC Davis confirmed that 12 days of sun exposure led to significant bleaching of the orange color.
- No CHP officer referred to the orange temporary striping in their collision reports or received any complaints regarding the orange striping.

- Accident data from different various sources showed a drop in accident rates during the time periods affected by the COVID-19 shutdowns. Accident rates continued to increase afterwards. In the examined work zone area, NB accident rates were generally slightly higher than in the SB direction before and during work zone installation. Rear-end collisions were the main accident types for accidents with injuries or fatalities.
- Average vehicle speeds were evaluated from smartphone GPS data as provide by HERE Technologies. Median average speeds in the work zone for orange temporary striping were slightly lower than in the work zone with white temporary striping with differences between 0.71 mph to 2.49 mph, which seems to indicate a positive effect of orange temporary striping on average vehicle speeds.

In conclusion, the effectiveness of the orange contrasted striping to increase driver awareness of being in a work zone was strongly confirmed from a driver survey. Also, average speeds were lower during orange temporary striping compared with white striping. The influence of the orange striping pattern on lane keeping behavior and accidents was not provable due to data uncertainty and additional influencing parameters, such as delayed effects from COVID-19 shutdowns and busy junctions.

# References

- Burghardt, T. E., Maki, E., & Pashkevich, A. (2021). Yellow thermoplastic road markings with high retroreflectivity: Demonstration study in Texas. *Case Studies in Construction Materials*, 14, e00539. <https://doi.org/10.1016/j.cscm.2021.e00539>
- Chiu, H.-K., Li, J., Ambrus, R., & Bohg, J. (2021). Probabilistic 3D Multi-Modal, Multi-Object Tracking for Autonomous Driving. *2021 IEEE International Conference on Robotics and Automation (ICRA)*, 14227–14233. <https://doi.org/10.1109/ICRA48506.2021.9561754>
- ERF. (2015). *Marking a Road Toward a Safer Future. An ERF Position Paper on How Road Markings Can Make Our Road Safer.*
- Finley, M. (2020). *FHWA Progress report: Orange Work Zone Pavement Markings, July - December 2019.*
- Gibbons, R. B., Williams, B., & Cottrell, B. (2012). Refinement of Drivers' Visibility Needs during Wet Night Conditions. *Transportation Research Record: Journal of the Transportation Research Board*, 2272(1), 113–120. <https://doi.org/10.3141/2272-13>
- Grosjes, T. (2008). Retro-reflection of glass beads for traffic road stripe paints. *Optical Materials*, 30(10), 1549–1554. <https://doi.org/10.1016/j.optmat.2007.09.010>
- Harb, R., Radwan, E., Yan, X., Pande, A., & Abdel-Aty, M. (2008). Freeway Work-Zone Crash Analysis and Risk Identification Using Multiple and Conditional Logistic Regression. *Journal of Transportation Engineering*, 134(5), 203–214. [https://doi.org/10.1061/\(ASCE\)0733-947X\(2008\)134:5\(203\)](https://doi.org/10.1061/(ASCE)0733-947X(2008)134:5(203))
- Kummetha, V. C., Kondyli, A., Chrysikou, E. G., & Schrock, S. D. (2020). Safety analysis of work zone complexity with respect to driver characteristics — A simulator study employing performance and gaze measures. *Accident Analysis & Prevention*, 142, 105566. <https://doi.org/https://doi.org/10.1016/j.aap.2020.105566>
- Lammers-Staats, E., Staats, W., & Agent, K. (2021). *Evaluation of Orange Pavement Striping for Use in Work Zones.* <https://doi.org/https://doi.org/10.13023/ktc.rr.2021.03>
- Lee, H.-S., & Oh, H.-U. (2005). MINIMUM RETROREFLECTIVITY FOR PAVEMENT MARKINGS BY DRIVER'S STATIC TEST RESPONSE. *Journal of the Eastern Asia Society for Transportation Studies*, 6, 1089–1099. <https://doi.org/10.11175/easts.6.1089>
- Li, Y., Allu, K. R., Sun, Z., Tok, A. Y. C., Feng, G., & Ritchie, S. G. (2021). Truck body type classification using a deep representation learning ensemble on 3D point sets. *Transportation Research Part C: Emerging Technologies*, 133, 103461. <https://doi.org/10.1016/j.trc.2021.103461>

- Li, Y., & Bai, Y. (2009, January 13). Fatal and Injury Crash Characteristics in Highway Work Zones. *Transportation Research Board 87th Annual Meeting*.
- MacEacheron, C. (2016). *Deterioration of Pavement Marking Retroreflectivity in the Province of New Brunswick* [MS Thesis]. University of New Brunswick.
- McGee, H. W., & Mace, D. L. (1978). *Retroreflectivity of Roadway Signs for Adequate Visibility: A Guide, Report No. FHWA/DF-88/001*.
- Migletz, J., Fish, J. K., & Graham, J. L. (1994). *Roadway Delineation Practices Handbook, FHWA-SA-93-001*.
- n/a. (2023, June 6). *Washington State DOT Testing Orange Striping to Improve Work Zone Safety*. Roads & Bridges.  
<https://www.roadsbridges.com/safety/news/33006209/washington-state-dot-testing-orange-striping-to-improve-work-zone-safety>
- Ritchie, S. G., Tok, A., Li, Y., & Allu, K. R. (2022). *Investigation of LiDAR Sensing Technology to Improve Freeway Traffic Monitoring*.  
[https://www.metrans.org/assets/research/psr%2021-34\\_ritchie\\_final%20report.pdf](https://www.metrans.org/assets/research/psr%2021-34_ritchie_final%20report.pdf)
- Roughail, N. M., Yang, Z. S., & Frazio, J. (1988). *Comparative study of short-and long term urban freeway work zones*.
- Shaw, J. W., Chitturi, M. V., Santiago-Chaparro, K. R., Qin, L., Bill, A. R., & Noyce, D. A. (2018). *Orange Work Zone Pavement Marking Midwest Field Test*.
- Shaw, J. W., Chitturi, M. V., & Noyce, D. A. (2017). Special-Color Pavement Marking for Highway Work Zones: Literature Review of International Practices. *Transportation Research Record: Journal of the Transportation Research Board*, 2617(1), 78–86. <https://doi.org/10.3141/2617-10>
- Silverstein, C., Schorr, J., & Hamdar, S. H. (2016). Work zones versus nonwork zones: Risk factors leading to rear-end and sideswipe collisions. *Journal of Transportation Safety & Security*, 8(4), 310–326.  
<https://doi.org/10.1080/19439962.2015.1036332>
- Smadi, O., Souleyrette, R. R., Ormand, D. J., & Hawkins, N. (2008). Pavement Marking Retroreflectivity. *Transportation Research Record: Journal of the Transportation Research Board*, 2056(1), 17–24.  
<https://doi.org/10.3141/2056-03>
- Steinbakk, R. T., Ulleberg, P., Sagberg, F., & Fostervold, K. I. (2019). Effects of roadwork characteristics and drivers' individual differences on speed preferences in a rural work zone. *Accident Analysis & Prevention*, 132, 105263. <https://doi.org/https://doi.org/10.1016/j.aap.2019.105263>
- Thanasupsin, K., & Sukniam, S. (2021). Degradation of the retroreflectivity and diffuse illumination of thermoplastic pavement markings: a case study in Thailand. *IOP Conference Series: Materials Science and Engineering*, 1088(1), 012056. <https://doi.org/10.1088/1757-899X/1088/1/012056>
- Verster, J., & Roth, T. (2011). Standard operation procedures for conducting the on-the-road driving test, and measurement of the standard deviation of lateral position (SDLP). *International Journal of General Medicine*, 359.  
<https://doi.org/10.2147/IJGM.S19639>



- Williamson, M. R. (2023). 1353033 - Experimental Orange Pavement Markings in Work Zones Lessons Learned. In *ASCE International Conference on Transportation & Development*.
- Xia, Y., Sun, Z., Tok, A., & Ritchie, S. (2022). A dense background representation method for traffic surveillance based on roadside LiDAR. *Optics and Lasers in Engineering*, 152, 106982. <https://doi.org/10.1016/j.optlaseng.2022.106982>
- Zhang, J., Xiao, W., Coifman, B., & Mills, J. P. (2020). Vehicle Tracking and Speed Estimation From Roadside Lidar. *IEEE Journal of Selected Topics in Applied Earth Observations and Remote Sensing*, 13, 5597–5608. <https://doi.org/10.1109/JSTARS.2020.3024921>

# Appendix A – Details on camera system design and installation

## Power system including batteries and solar panel

Since the installation was only temporary and access to the electricity grid was limited for the specified highway locations, electricity generation from solar power and power storage by battery were selected for the cameras used in this research. The system power design considered the necessary power for the cameras, modem, LiDAR sensor, and other electrical components, the maximum and average input power from the solar panel, and the storage capacity of the battery. The system was sized for a maximum of 350 Wh of energy use per day.

Solar energy availability was evaluated, keeping in mind that electricity generation is region-specific. Solar panel tilt angle should be chosen so the sunlight will fall onto the panel as much and as perpendicular as possible. The solar panel tilt angle depends on the location and must account for the sun position in the different seasons. Overcast days were taken into account to calculate the maximum, average, and minimum power availability. We used the NREL PVWatts calculator (<http://pvwatts.nrel.gov/pvwatts.php>), which includes location and weather conditions.

The panels in the prior Wrong Way Driving project were placed in Sacramento and set at 60°, which was selected as optimal for winter (0° is horizontal). The chart in Figure A1.1 shows the effect of tilt on panels in Sacramento (Lat. 39°) and San Diego (Lat. 33°). Note that for convenience a 1,000 W panel is referenced. The Sacramento systems had a total output of 140 W per pair.

Based on the experience with the Sacramento panels, the energy is not sufficient to operate continually during December and January. Weather conditions in February 2021 also caused problems. The angle of 60° produces a dip in daily energy for San Diego.

Figure A1.2 studies the daily energy output in San Diego closer and includes 30° and 50° tilt settings. A 45° tilt angle is chosen for the design to be conservative.

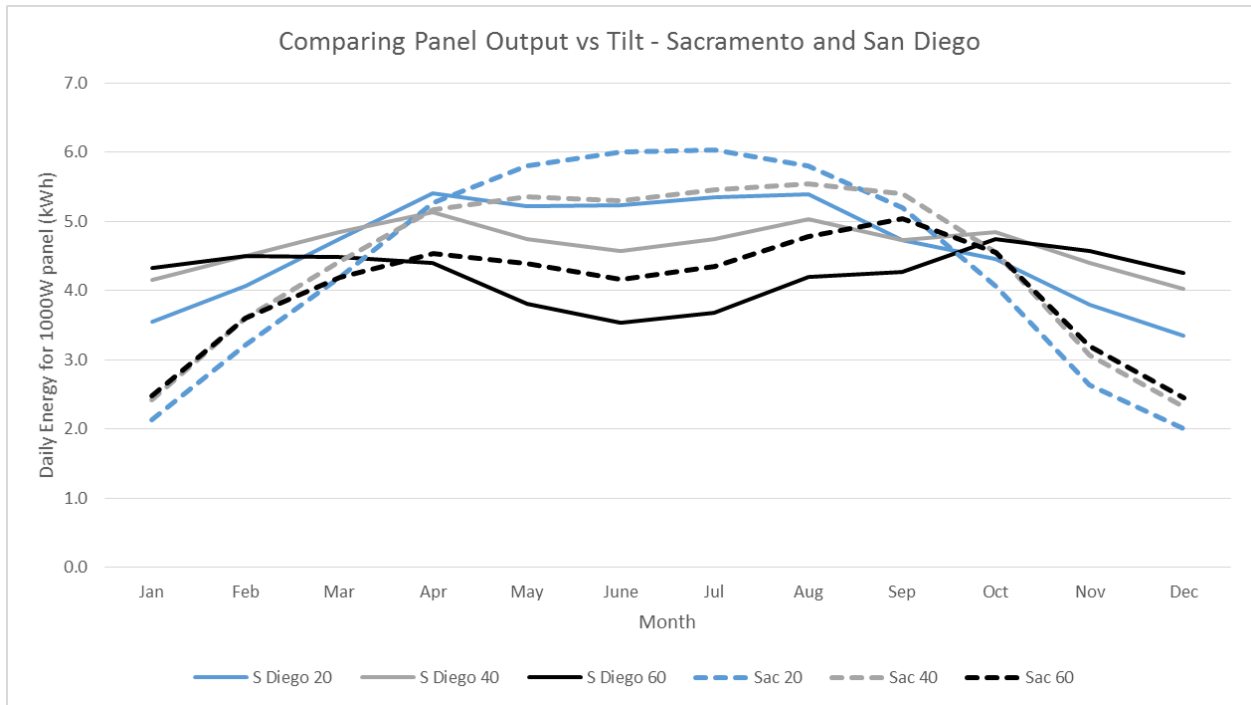


**Figure A1.1: Comparing the effect of panel tilt (20°, 40°, 60°) on energy output – San Diego and Sacramento**

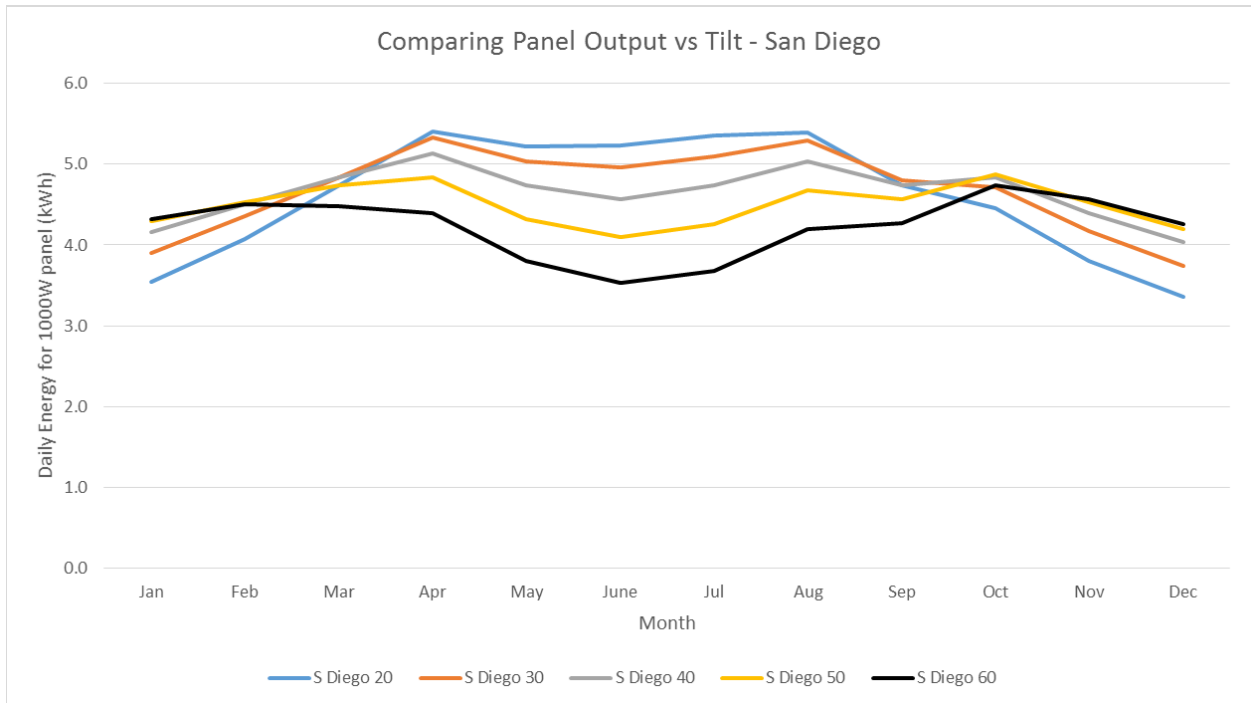


**Figure A1.2: Comparing the effect of panel tilt on energy output – San Diego**

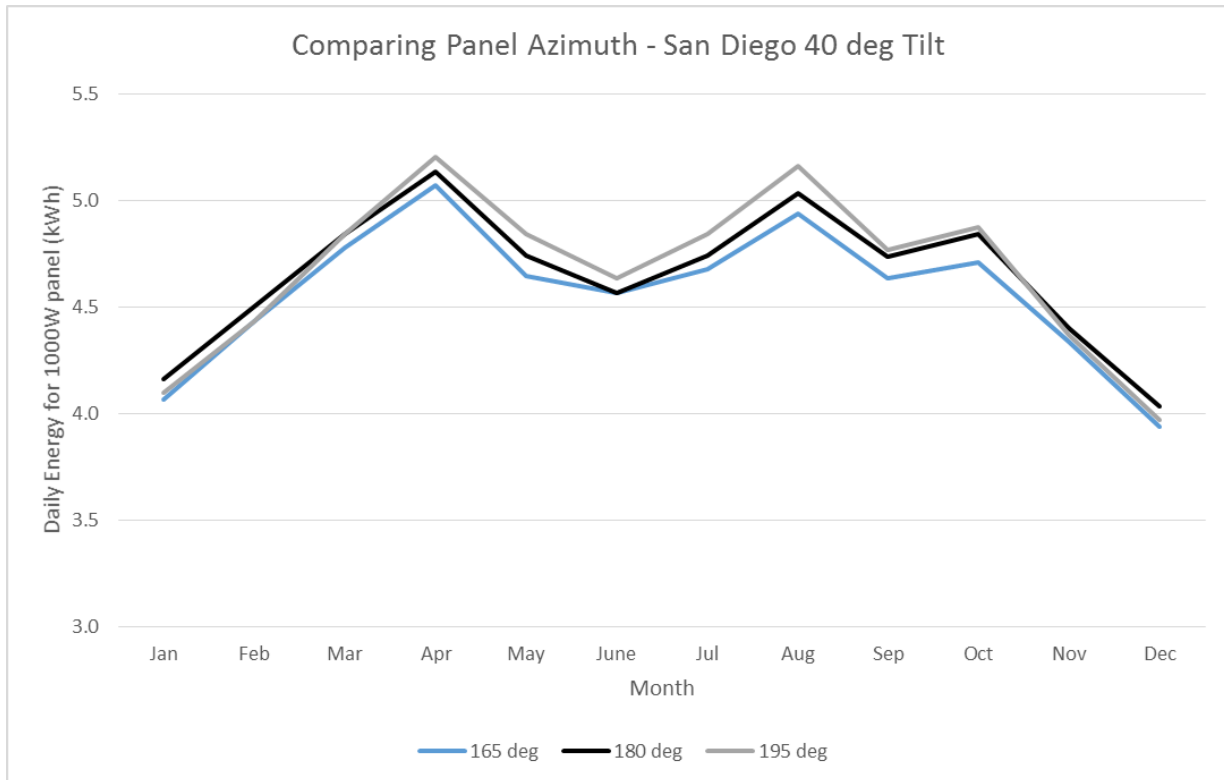


**Figure A1.3: Comparing the effect of azimuth angle (Vertical scale different than prior figures)**

Pointing the solar panel to the south (azimuth angle of  $180^\circ$ ) is normally optimal, but this can be affected by weather. Figure A1.3 shows variations in daily energy due to the azimuth angle in San Diego. It seems that the summer days in San Diego begin with overcast conditions; hence, there is a slightly higher output if pointed a few degrees to the east ( $195^\circ$ ). Since an orientation of  $180^\circ$  (straight towards south) is best for the winter and camera recordings started in the winter, the panel orientation was chosen to point straight to the south (Figure A1.4). Individual locations had to be examined closely as well. For example, an initially chosen camera location at La Costa Bridge needed to account for large trees at the west end of the overcrossing, which could have led to a significant shadow.

The battery size was based on camera and modem power draw (non-continuous), with and without LiDAR sensor. Important features included a low temperature charge cut off and high temperature cut off.



**Figure A1.4: Solar panel and electronics box installation**



**Figure A1.5: Pictures of electronics box and solar panel**

The cell phone modem allowed for remote camera access and data download. Initial calculations determined about 3.5 GB per hour of video. Therefore, a local storage of 256GB would hold more than 70 hours of video. A direct download of data from the electronics box in certain intervals was preferred because the transmission by modem incurs high costs for cell phone plans. Reasonable data plans range between 5 GB to 35 GB download data

per month. Figure A1.5 shows components inside the electronics box and its installation under the solar panel.

## Component Installation Details

There is a desired camera location from the video information standpoint, but this location might not be feasible for safety and access (ex., the median is not well accessible for the camera installation and may interfere with construction operations). After it was decided that box, solar panel, and cameras did not need to be on the same pole, there was increased flexibility for component placing. The cameras faced towards the freeway, which made them less invasive to people (Figure A1.6). They were mounted on poles strapped to poles on the overcrossings and the ethernet cables between cameras and electronics box run through a conduit (Figure A1.7).

Caltrans arranged for the temporary installation of the cameras onto the overcrossing structures. The cameras were strapped to 2.5-in metal conduit poles, which were then strapped to existing overcrossing fencing poles. The overcrossing fence pole nearest to the ideal location of the camera was selected. The large and heavy hardware, made up by electronics box and solar panel, was installed on a 3.5-inch metal conduit pole near the end of the overcrossing. The cameras were connected with CAT 6 shielded Ethernet cable carrying power and communications. This cable was run through the metal conduit along the bottom edge of the fencing and along the ground to the electronics box. The cable was buried a few inches deep where there was danger of people stepping on it.

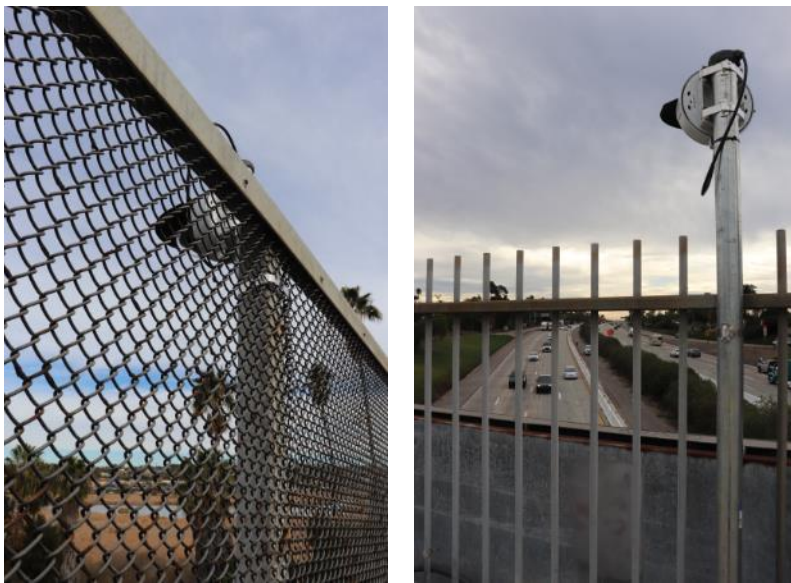


**Figure A1.6: Camera installation on Jefferson Overcrossing (left) and Las Flores Overcrossing (right)**

The AHMCT researchers brought partially assembled components by truck and designed the system for easy installation. The on-site contractor crew got familiar with the installation and installed four cameras in two nights (Figure A1.8). AHMCT researchers made sure that the cameras and modems worked. One camera at Jefferson Overcrossing had to be re-wired by the contractor.



**Figure A1.7: Details of camera mounting and cabling at Las Flores Overcrossing**

The electronics box needed to be reached by a 6 ft ladder but could not be lower to hinder tampering (Figure A1.9). The solar panel needed to be mounted as high as possible depending on pole length and cable length.



**Figure A1.8: Left: Installation of electronics box at Jefferson Overcrossing with a bucket truck; right: straps around the steel pole.**



**Figure A1.9: Access to electronics box: Left: at Jefferson Overcrossing, Right: at Las Flores Overcrossing.**



## **General findings for camera installation**

The component pricing had to be balanced against component reliability. For example, the high-quality solar controller from Victron excelled due to its high reliability and enabled the researchers to quantify electricity generation on-site. Selecting this panel also allowed for balancing electricity generated. A smaller battery size could be used very comfortably, which reduced the battery cost, box size, and mounting weight.

Some installation details were improved spontaneously on-site. For example, a higher installation of the box was used than planned at the shaded location on Jefferson Overcrossing to capture more sunlight.

# Appendix B – Feasibility study of use of Light Detection and Ranging sensors

## Introduction

The high speed and resolution of state-of-the-art Light Detection and Ranging (LiDAR) sensors promise a large advantage over CCTV camera pictures for determining vehicle position within a lane. However, there is not much information available on how to use a stationary LiDAR sensor for the detection of the lateral position of passing vehicles, and the accuracy might be limited. Further reduction of accuracy and data quality are expected from the limited ability of LiDAR to detect road striping and for a larger distance to the sensor. Therefore, AHMCT investigated the use of a stationary LiDAR sensor for measuring vehicle lateral position in a multi-lane highway.

## Objectives and Requirements

The primary objective for this study was to improve data resolution and accuracy on vehicle lateral positioning with the metrics of mean deviation of the vehicle distance from the lane center and its standard deviation within a traffic lane using commercially available LiDAR sensors. In order to minimize installation cost, the LiDAR sensor's range and field of view should cover an area across multiple lanes from a single fixed location. The secondary objective was to determine the vehicle speed across multiple lanes.

Based on the primary objective, the LiDAR sensor had to meet the following requirements:

- Low cost (< \$13,000)
- Maximum sensing range > 50 meters
- Field of view > 40 degrees
- Multiple simultaneous LiDAR beams for sensing ( $\geq 16$  beams)

## State of the Art

LiDAR systems have been developed for various markets, such as mapping, aerial survey, robotics, and autonomous vehicle applications. A product survey was conducted on commercially available LiDAR systems to find a suitable system base of LiDAR systems' cost, performance, and specifications (size, weight, field of view [FOV], maximum range, and accuracy). In addition, a literature review was performed to search for suitable commercial or open

source software that could post-process the LiDAR point cloud to extract the vehicle position with respect to the lane.

## LiDAR Systems Hardware

Velodyne Lidar (<https://velodynelidar.com/>), Ouster (<https://ouster.com/>), and Blickfeld (<https://www.blickfeld.com/>) manufacture LiDAR systems suitable for our applications. Ouster has recently acquired Velodyne Lidar in February 2023.<sup>9</sup> The Velodyne Lidar's VLP16<sup>10</sup> and VLP32 and Ouster's Rev6 OS1-32, Rev6 OS1-64, Rev6 OS1-128, and Rev7 OS1-64<sup>11</sup> LiDAR met our requirements. These LiDAR systems have 16 to 128 individual LiDAR sensors internally scanning 360 degrees at 15 Hz or higher simultaneously. Figure A2.1 shows a simplified block diagram of a multi-beam 360 degree LiDAR scanning system. The point cloud data stream is presented in individual frames for a single 360 degree scan. The cost of the systems range from \$4,000 to \$13,000, depending on the number of laser beams and measurement rate. A higher number of LiDAR beams and measurement rate yield a denser point cloud and result in higher accuracy vehicle lateral position estimate. Detailed LiDAR system specifications are available on the manufacturers' websites.

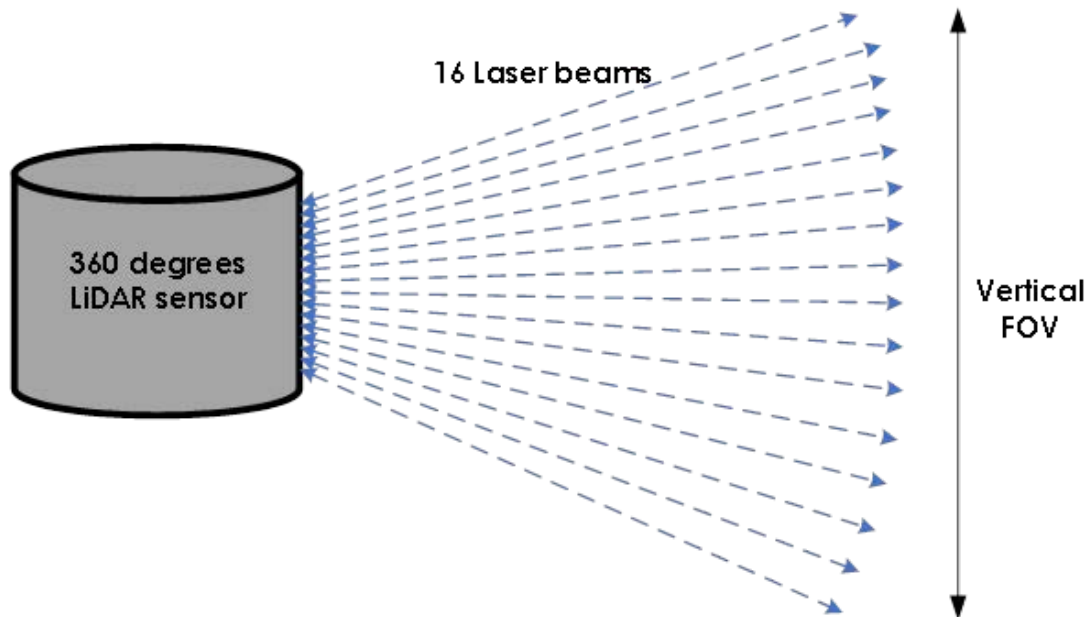


**Figure A2.1: Multi-beams 360 degree LiDAR sensor**

---

<sup>9</sup> <https://investors.ouster.com/news/news-details/2023/Ouster-and-Velodyne-Complete-Merger-of-Equals-to-Accelerate-Lidar-Adoption/default.aspx>

<sup>10</sup> <https://velodynelidar.com/products/puck/>

<sup>11</sup> <https://ouster.com/products/scanning-lidar/os1-sensor/>

The Blickfeld Qb2<sup>12</sup> is based on Blickfeld's proprietary solid-state software-defined LiDAR technology and has a fixed FOV of 90 X 45 degrees. Depending on the mounting LiDAR sensor height, the Qb2 can cover two to three lanes of highway. The Qb2 could produce a dense point cloud to estimate the vehicle position with the lane.

## Software

We have performed a literature review on point cloud objection detection and tracking software from:

- Open-source projects,
- Journal publications,
- Commercial software packages: Velodyne VDK and Bluecity.

### Commercial Software

The Ouster Gemini<sup>13</sup> software, used in conjunction with Ouster LiDAR sensors, can count and track customers and analyze human traffic flow. According to Ouster, Gemini can provide accurate 3D tracking of people and vehicles. Gemini is available for demonstration and evaluation. The Ouster Gemini webpage shows videos of the software tracking people walking in a room and providing their walking speed and location. However, Ouster's webpages do not show any example of vehicle tracking. Tracking vehicles at highway speed would require hands-on evaluation of the software with their LiDAR sensor.

The Velodyne Lidar Vella Development Kit (VDK) and BlueCity software are compatible with Velodyne Lidar's LiDAR sensors. According to Velodyne Lidar, their BlueCity perception software can detect and identify vehicles, bicycles and pedestrians with their locations in real-time. Their webpage shows a video of the system being used at a road intersection. The video demonstrates that the software can track vehicle movement (location and speed) on a four-way intersection. In the video, the software tracks well for slow moving traffic in an intersection. BlueCity software's capability of tracking highway speed vehicle remain to be tested. Velodyne Lidar VDK LiDAR perception software provide developer software libraries for obstacle detection and tracking, object classification, velocity measurement, and semantic scene segmentation.<sup>14</sup> Using VDK would reduce software development time. VDK is designed to be

---

<sup>12</sup> <https://www.blickfeld.com/lidar-sensor-products/qb2/>

<sup>13</sup> <https://ouster.com/software/gemini/>

<sup>14</sup> <https://www.automotiveworld.com/news-releases/velodyne-lidar-introduces-vella-development-kit-for-building-autonomous-solutions/>

used with Velodyne Lidar's LiDAR sensor and custom autonomous applications. The VDK system costs about \$9,000.

The Blickfeld Percept software,<sup>15</sup> used in conjunction with Blickfeld's LiDAR sensors, can perform movement-based detection, object classifications (person, bicycle, and vehicle), object counting, and tracking of objects including velocity information. The software can show the paths of tracked objects in the x-y plane. Blickfeld's website shows videos of the software tracking vehicles and pedestrians. However, we do not know if it can track vehicles' highway speed and its accuracy. Hands-on evaluations are required.

## Open Source Software

Searches were conducted on large open source projects, github.com, and paperswithcode.com for relevant software that may be employed for vehicle detection and tracking. LiDAR sensor interface and point cloud reader software were included in the searches. LiDAR sensor interface software are used for collecting data in the field.

Velodyne Lidar sensors are often used in various autonomous and robotics projects. Robotic Operating System (ROS) is an open source project with large community support. The ROS<sup>16</sup> is a set of software libraries and tools that includes drivers for sensors and advanced algorithms. ROS driver support for Velodyne,<sup>17</sup> Ouster,<sup>18</sup> and Blickfeld<sup>19</sup> LiDAR sensors are available. There are other open source Velodyne Lidar data readers<sup>20, 21</sup> available from github.com.

Our search did not yield any open source software that may be directly applied to our specific use case. However, there are a few exiting open source software solutions developed for autonomous vehicle obstacle detection and object detection. For example, ROS multi\_object\_tracking\_lidar package,<sup>22</sup> AutoLidarPerception/segmenters\_lib,<sup>23</sup> and Autoware Foundation<sup>24</sup> software support object detection, tracking, and LiDAR point cloud segmentation. Chiu et al. presented a methods that combines LiDAR and camera images data for object detection and tracking (Chiu et al., 2021). They have provided their

---

<sup>15</sup> <https://www.blickfeld.com/lidar-sensor-products/percept/>

<sup>16</sup> <https://www.ros.org/>

<sup>17</sup>

[http://wiki.ros.org/velodyne/Tutorials/Getting%20Started%20with%20the%20Velodyne%20VLP\\_16](http://wiki.ros.org/velodyne/Tutorials/Getting%20Started%20with%20the%20Velodyne%20VLP_16)

<sup>18</sup> <https://github.com/ouster-lidar/ouster-ros>

<sup>19</sup> <https://docs.blickfeld.com/cube/latest/external/ros/driver-v1/README.html>

<sup>20</sup> <https://github.com/zimpha/Velodyne-VLP-16>

<sup>21</sup> <https://github.com/DiantaoTu/VLP-reader>

<sup>22</sup> [http://wiki.ros.org/multi\\_object\\_tracking\\_lidar](http://wiki.ros.org/multi_object_tracking_lidar)

<sup>23</sup> [https://github.com/AutoLidarPerception/segmenters\\_lib](https://github.com/AutoLidarPerception/segmenters_lib)

<sup>24</sup> <https://autoware.org/>

software code on github.com.<sup>25</sup> However, the software algorithm developed are based on 360 degree LiDAR sensor mounted horizontally at vehicle height. The performance of these software solutions applied to point cloud collection with LiDAR sensor high above the roadway would require extensive testing.

## Research Publications Reviews

Researchers at the Institute of Transportation Studies (ITS) at the University of California, Irvine (UCI) conducted extensive research in using LiDAR technology for freeway traffic monitoring, including vehicle classifications and tracking. Li et al. used LiDAR to classify truck body type using deep learning (Li et al., 2021). In their research, the LiDAR sensor array was mounted in horizontal orientation on a highway shoulder of highway to collect point cloud data. Then, they used a reconstruction procedure to combine and register multiple frames of point clouds to create denser point cloud representation of vehicle objects for truck classification. Ritchie et al. investigated the use of side-fired LiDAR for vehicle classification including trucks, motorized vehicle, bicycle, and pedestrian detection at traffic intersections (Ritchie et al., 2022). Their study included feasibility of real-time detection LiDAR based vehicle objects and the use of LiDAR to estimate vehicle trajectories. Xia et al. developed a novel method to classify and filter static and dynamic background points from roadside LiDAR sensor traffic surveillance point cloud (Xia et al., 2022). AHMCT researchers and Caltrans met with UCI ITS researchers to gain a better understanding of on-going LiDAR traffic monitoring research and for possible collaboration in the future. Utilizing UCI ITS' existing research would reduce the software development time for vehicle lateral position determination. Zhang et al., researchers at Newcastle University, presented their method of using roadside LiDAR to count vehicle and measure vehicle speed (Zhang et al., 2020). They presented a method to detect vehicle clusters points in the point cloud, and a centroid-based tracking procedure to identify clusters for each vehicle.

## Use of LiDAR technology for driver behavior evaluation

Experiments performed at UC Davis using different LiDAR sensor mounting heights and orientation with a Velodyne Lidar VLP16 sensor is shown in Figure A2.1. The experiment's objective was to determine the best LiDAR mounting location and orientation for estimating the vehicle lateral positions as

---

<sup>25</sup> [https://github.com/eddyhkchiu/mahalanobis\\_3d\\_multi\\_object\\_tracking](https://github.com/eddyhkchiu/mahalanobis_3d_multi_object_tracking)

well as achieving best coverage using a single sensor. The sample LiDAR data were collected for evaluation of various post-processing methods.



**Figure A2.1: Velodyne VLP16 LiDAR sensor with a 30 degree tilt from horizontal**

## *Proof of Concept*

A Velodyne VLP16 was mounted five feet above a pickup truck bed. The pickup truck provided a movable platform for the LiDAR sensor for quick experiment setup and data collection as well as protection of operators from highway traffic hazards. The test vehicles were then park on a highway shoulder and over pass bridge with the with the VLP16 sensor in the horizontal (with slight tilt) and vertical orientation. Four different LiDAR sensor location and orientation combination configurations were used to collect sample data. Table A2.1 shows four different experiment configurations, the name, and the descriptions.

Figure A2.2 shows a sample point cloud from a VLP16 LiDAR sensor in C1 configuration. Figure A2.2 shows the side, top, and rear view of a single LiDAR point cloud frame. The Figure A2.2 point cloud consists of a semi-tractor trailer (highlighted in a rectangle with red dashed line) and highway road surface. C1 configuration provides a dense point cloud of the vehicle side facing the sensor. Depending on the vehicle longitudinal position relative to the sensor, the point density from the front or the rear of the vehicle is much less. In addition, tall vehicles, such as semi-trailer trucks traveling near the LiDAR sensor, could block the laser beams from gathering data on vehicles traveling in lanes further away from the LiDAR. If the LiDAR is mounted on the median inside of

the shoulder, the LiDAR blockage by semi-trailer trucks could be minimized since semi-trailer trucks are less likely to travel in lane 1. Having a dense point cloud of the side of the vehicle would result in accurate lateral position calculation of vehicle side surface. However, the thin point cloud of the vehicle front or rear would result in poor estimation of vehicle width dimension. Thus, the vehicle center lateral position estimation would have poor accuracy.

**Table A2.1: LiDAR experiment configuration descriptions and their name**

<b>Configuration Name</b>	<b>Configuration descriptions</b>
<b>C1</b>	LiDAR Sensor at roadside with 15 to 20 feet height above roadway surface and LiDAR orientated horizontally with ~15 degree tilt
<b>C2</b>	LiDAR Sensor at roadside with 15 to 20 feet height above roadway surface and LiDAR orientated vertically
<b>C3</b>	LiDAR Sensor on an overpass with ~30 feet height above roadway surface and LiDAR orientated vertically
<b>C4</b>	LiDAR on an overpass with ~30 feet height above roadway surface and LiDAR orientated horizontally with ~35 degree tilt



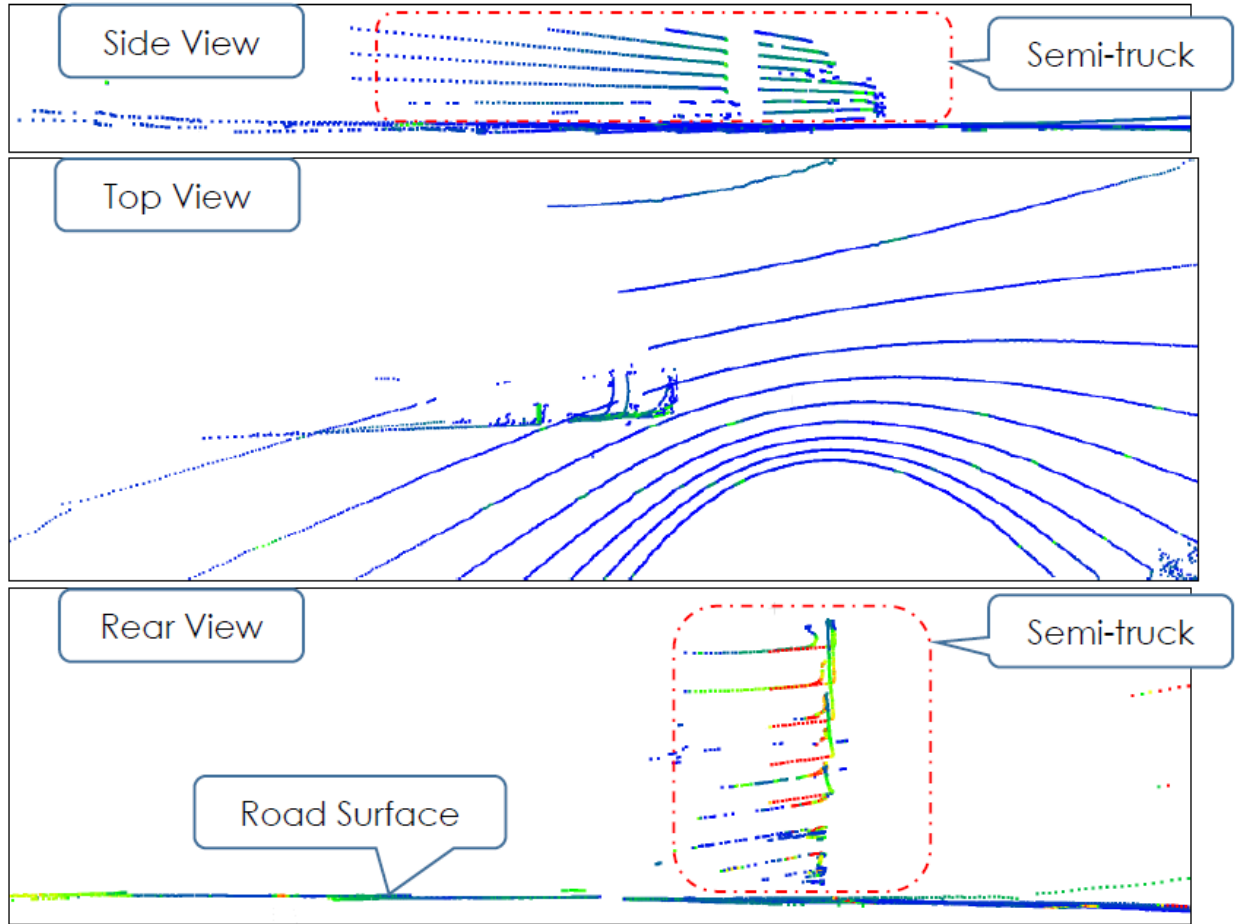


**Figure A2.2: Example of a single frame point cloud from C1 (Top image shows roadside view; middle image shows top view; bottom image shows roadway view along the direction of vehicle travel.)**

Figure A2.3 shows a sample point cloud from a VLP16 LiDAR sensor in C2 configuration. Figure A2.3 shows the side, top, and rear view of a single LiDAR point cloud frame. The Figure A2.3 point cloud consists of a front portion of a pickup truck (highlighted in a rectangle with red dashed line) and highway road surface. The C2 configuration provides a dense point cloud of the vehicle top and side facing the sensor. Depending on a vehicle's longitudinal position, the number of points from the vehicle front or the rear is very small. Similar to the C1 configuration, tall vehicles, such as semi-trailer truck traveling near the LiDAR sensor, could block the laser beams from gathering data on vehicle traveling in lanes further away from the LiDAR. C2 configuration longitudinal roadway coverage is short (~ 30 ft); the longitudinal coverage increases with sensor height and distance to the roadway. Similar to the C1 configuration, the LiDAR blockage by semi-trailer truck could be minimized if the system is mounted on the median inside of the shoulder. The dense point cloud of the side of the vehicle would result in accurate lateral position calculation of

vehicle side surface. However, the thinner point cloud of the vehicle top would result in poorer estimation of vehicle width. Based on the sample point cloud, vehicle center lateral position estimation would be better than in the C1 configuration.

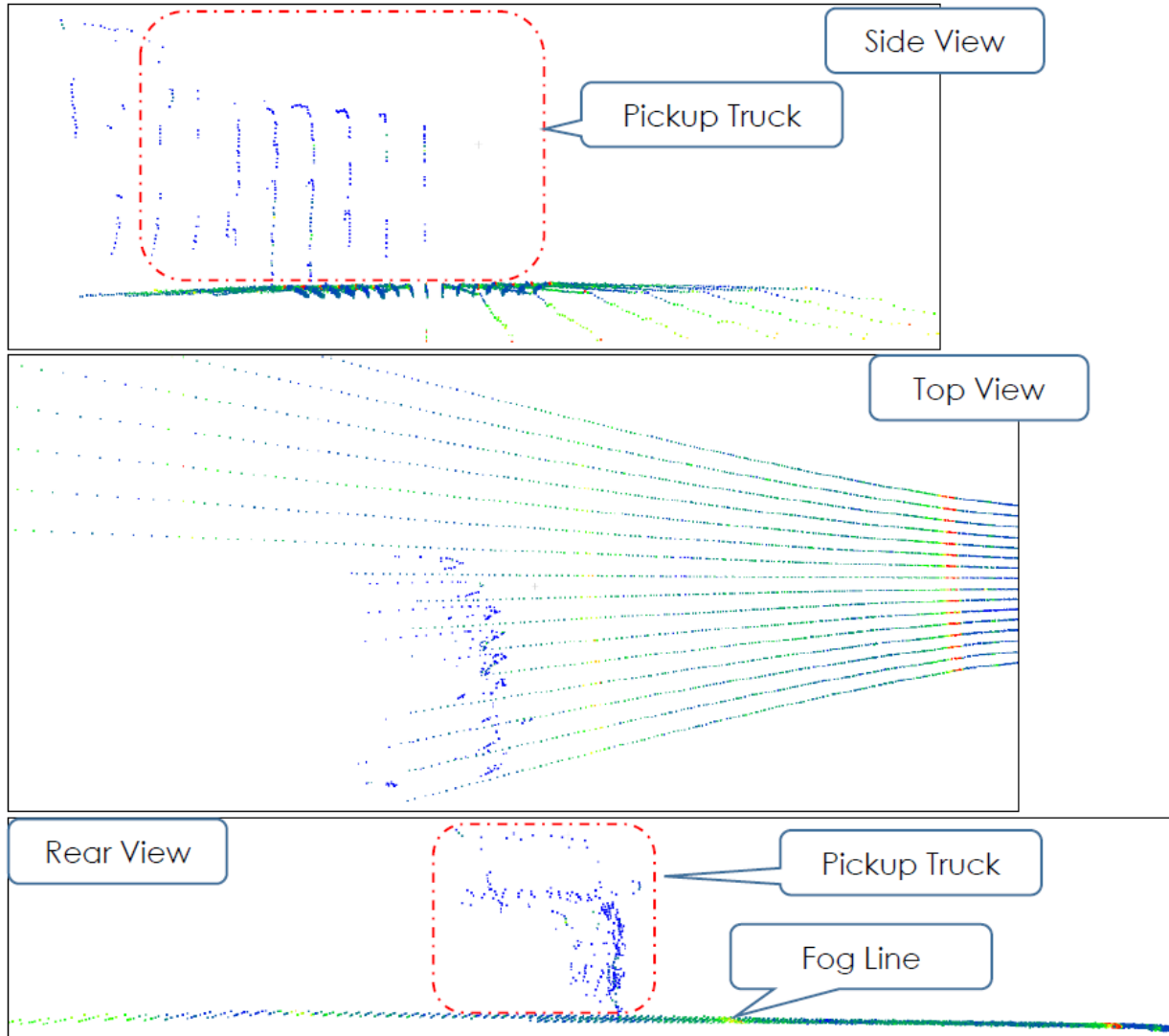


**Figure A2.3: Example of a single frame point cloud from C3 (Top image shows roadside view; middle image shows top view; bottom image shows roadway view along the direction of vehicle travel)**

Figure A2.4 shows a sample point cloud from a VLP16 LiDAR sensor in C3 configuration. The Figure A2.4 point cloud consists of a sedan (highlighted in a rectangle with red dashed line) and highway road surface. C3 configuration provides a large area of coverage along the highway. C3 configuration gathers dense longitudinal vehicle profile points. It may be best suited for measuring vehicle speed. The C3 configuration resulting point cloud does not support vehicle position estimation well.

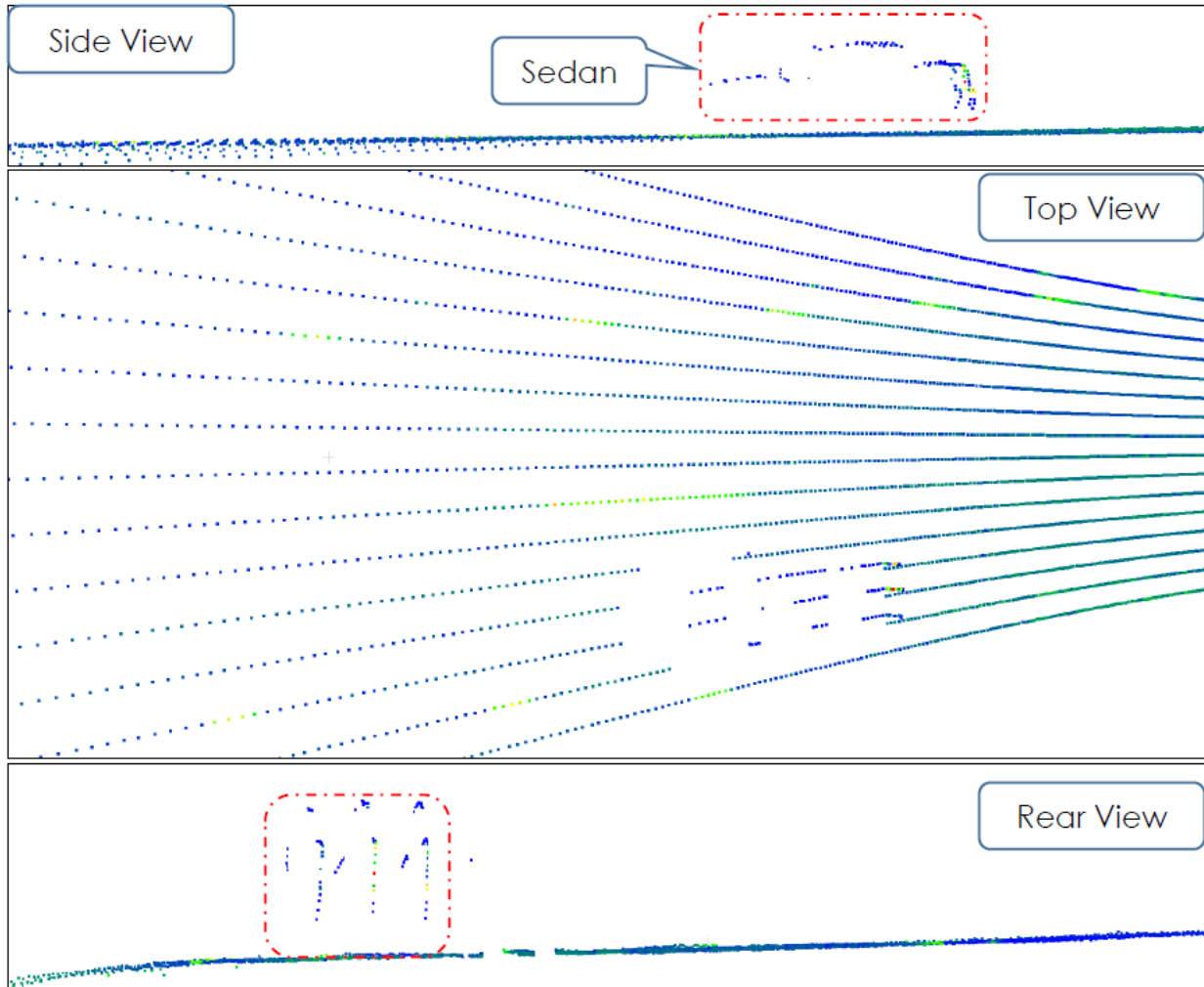


**Figure A2.4: Example of a single frame point cloud from C3 (Top image shows roadside view; middle image shows top view; bottom image shows roadway view along the direction of vehicle travel)**

Figure A2.5 shows a sample point cloud from a VLP16 LiDAR sensor in C4 configuration. The VLP16 sensor was mounted horizontal with -35 degree tilt and about 30 feet above the road surface. Figure A2.5 shows a point cloud consisting of two vehicles (highlighted in rectangles with red dashed line) and a two-lane highway road surface. The direction of travel is indicated by two red arrows. The locations of the fog lines are shown by red dots in the top view. Reducing LiDAR sensor tilt angle would increase the coverage area longitudinal to the roadway. However, point density on the vehicle would reduce with increasing longitudinal coverage. The C4 setup resulted in 56 ft coverage along the highway. The point cloud shown in Figure A2.5 was cropped  $\pm 30$  degree from the 360 degree point cloud. The traffic was moving away from the LiDAR sensor. The C4 configuration provides a dense point cloud of the vehicle top surface and thinner point cloud of vehicle sider surface facing

toward the LiDAR as shown in Figure A2.5. In addition, the C4 configuration provides a clear line of sight to vehicle top surface for two lanes. AHMCT researchers expect the C4 configuration would cover up to four lanes. However, the LiDAR blockage by tall semi-trailer truck could still happen in some cases. Dense point cloud of the vehicle top surface would facilitate accuracy lateral position calculation of vehicle assuming that the majority of the vehicles has bilateral symmetry along the direction of travel axis. Figure A2.5 shows that C4 configuration also provides dense points on the rear vehicle surface. Depending on the vehicle shape, these point cloud points could aid the vehicle lateral position estimation.

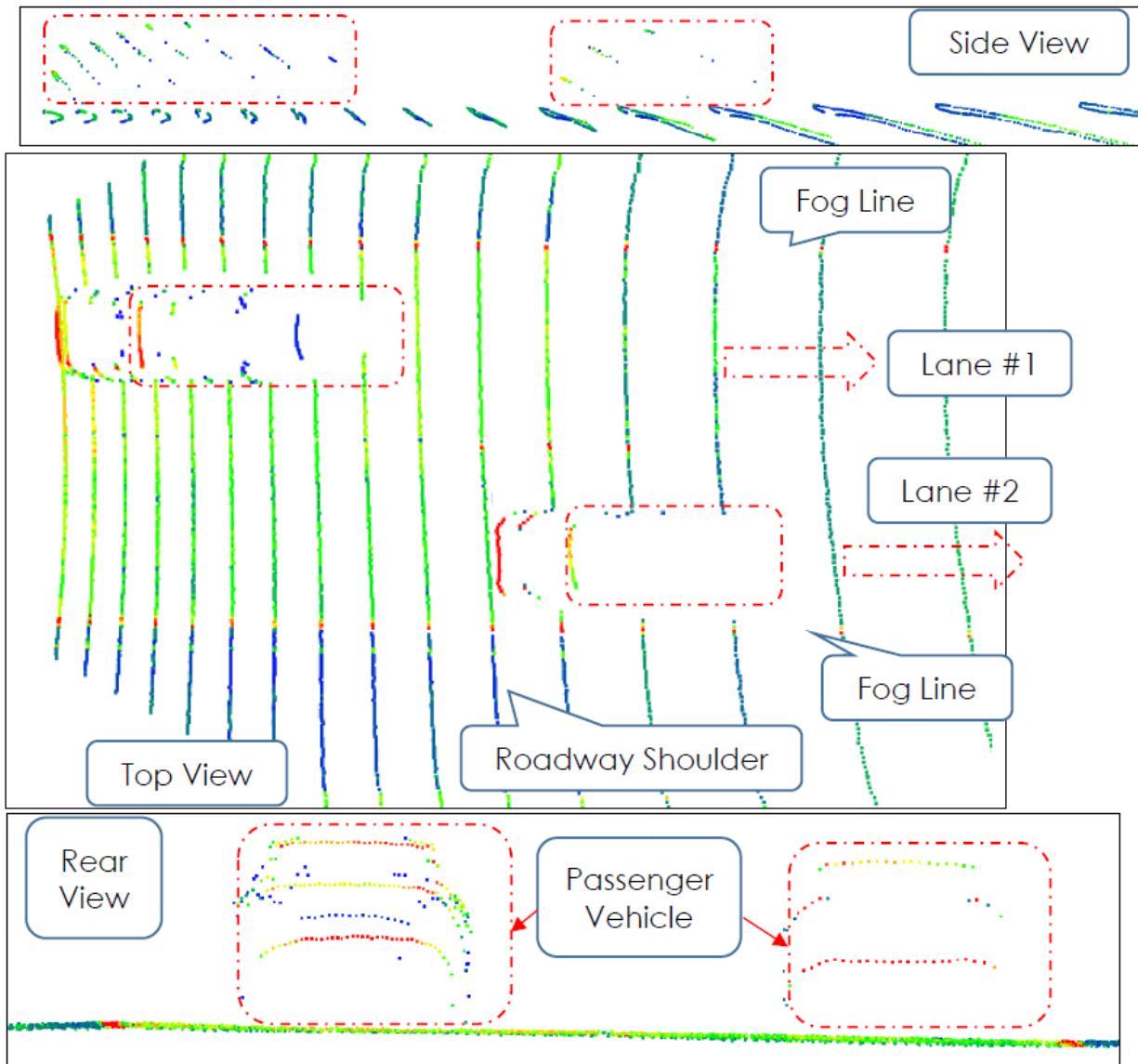


**Figure A2.5: Example of a single frame point cloud from C4 (Top image shows roadside view; middle image shows top view; bottom image shows roadway view along the direction of vehicle travel)**

Nevertheless, the C4 configuration may not be suitable for vehicle speed estimation. Based on the current maximum LiDAR sensor frame rate (15 Hz), tilt angle (longitudinal range), and vehicle speed, the LiDAR sensor can only capture the same passenger vehicles in only two to three frames. In many cases, a partial vehicle was captured in LiDAR frames. LiDAR sensors with more laser beams and higher frame rate would provide improvement. Alternatively, an additional LiDAR sensor in the C3 configuration could provide better vehicle speed estimates.

## **Post-processing Concept**

Based on our experimental results, we concluded that the C4 configuration was best suited for measuring vehicle lateral position. Figure A2.6 illustrates a high level block diagram of a proposed point cloud post-processing logic to extract vehicle lateral position. Software was not developed in this stage.

The proposed post-processing logic assumed that the vehicles have bilateral symmetry along the direction of travel axis. First, the point cloud XYZ-axes are aligned with direction of travel (x-axis), roadway lateral direction (y-axis), and vertical (z-axis, up being positive). Then, the LiDAR data stream is broken down into individual frames of point cloud data as shown in Figure A2.5. In the example data frame shown in Figure A2.6, there are two vehicles in the LiDAR's field of view simultaneously. The x-axis value is ignored or set to zero, resulting in a set of 2D points and reduction of a 3D to a 2D problem. Then, the points on the highway pavement surface are filtered out based on the z-axis value. Using established clustering algorithms, points on individual vehicle can be separated from points on other vehicles. After that, various established algorithms and methods may be applied to extract the vehicle center position. For example, convex hull software libraries could be used to extract the outline of the vehicle. The center (median y-value) of the vehicle outline would be the vehicle center. Alternatively, the median y-value of the top few layers of points on vehicle could be used vehicle center position. The red star in the Figure A2.6 represents the theoretical vehicle center estimated from different methods. Geometric correction may be needed to be applied to correct for the tilting of the vehicle due to a small cross slope of the roadway.

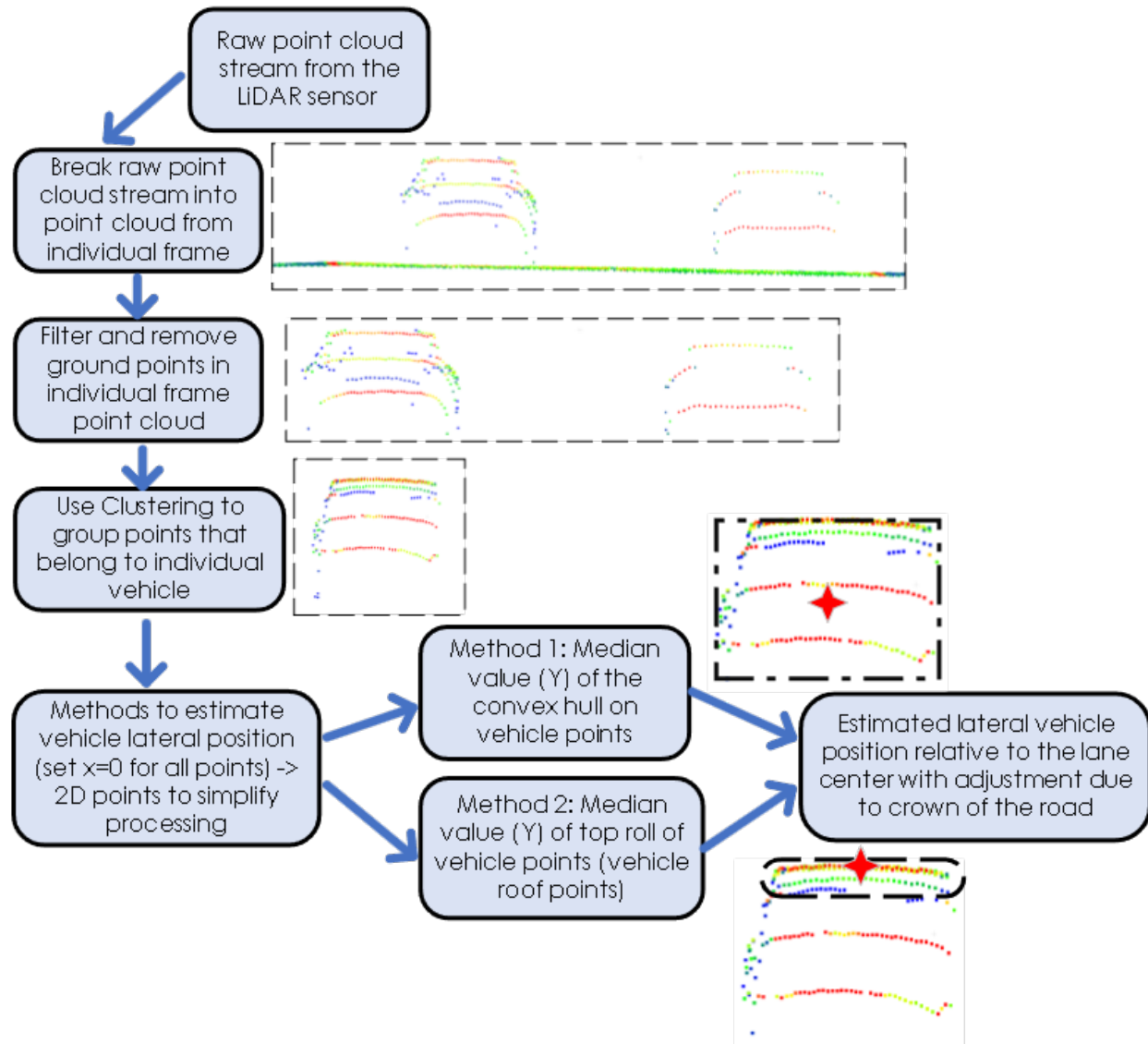


**Figure A2.6: High level conceptual point cloud post-processing steps**

## Challenges

The post-processing concept is a simplified version of the solution. However, the practical solution would have higher complexity. There are challenges to pick the best frame for vehicle position extraction. Each unique vehicle may be captured two to three times in different longitudinal positions within the LiDAR sensor's FOV. In some cases, the partial vehicle body is captured by the LiDAR. Different methods are needed to select the best frame data to use for position calculation. One simple method would be based on the number of points captured on the vehicle body. It is also important to prevent measuring the same vehicle position twice and affecting the overall statistics.

## General findings and future work

- All commercially available software from different LiDAR manufacturers are only compatible with their own hardware. Some of the software are designed for intersection traffic monitoring. Evaluation is needed to determine if the software can detect/track vehicles at highway speed and the estimated vehicle lateral position accuracy.
- UCI ITS researchers have extensive experience with using LiDAR for traffic monitoring and vehicle classification. Collaboration with them would reduce software development time.
- Significant software development with open source software would be needed to put together open source software to achieve our desired results.
- Vehicle position accuracy is unknown with either commercial software or open source software libraries.
- Evaluation of commercial software for their effectiveness and position estimate accuracy is necessary.
- Employing LiDAR sensors with more laser beams ( $\geq 32$ ) with a higher point measurement rate to increase data resolution may result in better lateral position estimate accuracy.
- Proof of concept software development would determine if the proposed post-process concept is viable on real data from live traffic.
- Additional experimentation is required to optimize the longitudinal coverage (sensor tilt angle) and point density on the vehicle to capture the full vehicle body within a single LiDAR frame.

# Appendix C – Survey on orange striping perception

## Survey questions

### **Build NCC: Temporary Orange Lane Striping Feedback Survey Caltrans and SANDAG Build NCC**

Caltrans and SANDAG Build NCC crews are constructing highway improvements and upgrades along Interstate 5 (I-5) between Palomar Airport Road in Carlsbad and State Route 78 (SR 78) in Oceanside. This project installed orange striping to contrast the regular white striping for lanelines during construction throughout April 2022. This survey will assess your perception of the effectiveness of the orange contrasted striping to increase awareness and safety in work zones.

1. \* How often do you drive on Interstate 5 anywhere between Lomas Santa Fe Drive and State Route 78 (SR 78)?
  - a) At least once a week
  - b) At least once a month
  - c) Less than once a month
  
2. \* Did you notice the orange contrasted striping in the construction work zone between Palomar Airport Road and SR 78?
  - a) Yes
  - b) No
    - Skip to Q8 if No
  
3. Did the orange contrasted striping increase your awareness of being in a road construction work zone?
  - a) Yes
  - b) No



4. Did you notice a difference in the northbound and the southbound orange contrasted lane line striping?
  - a) Yes
  - b) No
5. If you noticed a difference, which orange contrasted lane line striping did you prefer?



- a) Orange along both sides of the white lane line in the northbound direction
  - b) Orange preceding the white lane line in the southbound direction
  - c) No preference
6. Please select your level of agreement to the following statements:
 

\*Likert Scale (Strongly agree, Agree, Neither agree or disagree, Disagree, Strongly disagree)

    - a. The orange contrasted striping caused me to drive at a more reasonable or safe speed in the work zone.
    - b. The orange contrasted lane line striping makes it easier than traditional white lane line striping to stay in my lane.
  7. Did you have prior knowledge that the striping would be orange contrasted before driving through the work zone?

- a) Yes – I was aware of the orange contrasted striping on this section of I-5.
  - b) No – I had no knowledge of the orange contrasted striping before entering the work zone.
8. \* Would you like to see orange contrasted lane line striping used in more road construction work zones?
- a) Yes
  - b) No
9. \* Have you driven through the work zone between Palomar Airport Road and SR 78 at night?
- a) Yes
  - b) No
    - If No, skip to Q11
10. If yes, what is your opinion of the orange contrasted striping at night?
- a) Prefer the orange contrasted lane line striping
  - b) Prefer traditional white lane line striping
  - c) No preference
11. Please select your age group.
- a) 18 – 19 years old
  - b) 20 to 24 years old
  - c) 25 to 39 years old
  - d) 40 to 54 years old
  - e) 55 to 64 years old
  - f) 65 to 74 years old
  - g) 75+ years old
  - h) Prefer not to answer.
12. Where do you live?
- a) San Diego County

- b) Orange County
- c) Los Angeles County
- d) Baja California, Mexico
- e) Other

13.\* What kind of vehicle do you drive most commonly in the respective area?

- a) Passenger car/Sedan
- b) Commercial Vehicle
- c) Van
- d) SUV
- e) Pickup Truck
- f) Motorcycle

14. What is your gender?

- a) Male
- b) Female
- c) Other
- d) Prefer Not to Say

15. Do you have any additional feedback to provide?

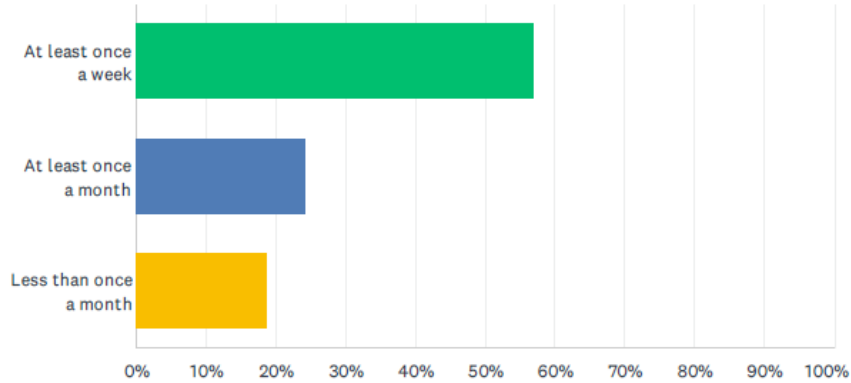
- a) [text box]

(\* denotes mandatory questions.)

# Survey results

Q1 How often do you drive on Interstate 5 anywhere between Lomas Santa Fe Drive and State Route 78 (SR 78)?

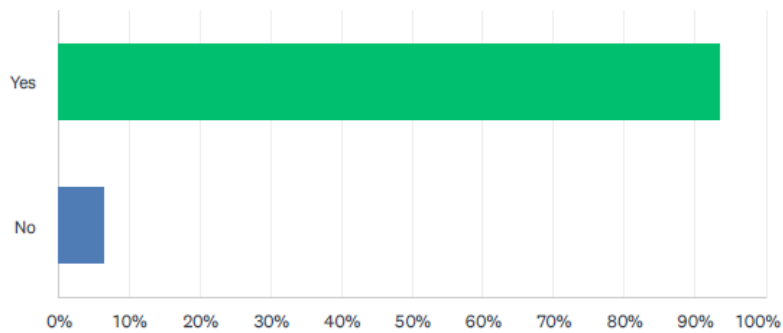
Answered: 1,185 Skipped: 0



ANSWER CHOICES	RESPONSES
At least once a week	56.96% 675
At least once a month	24.30% 288
Less than once a month	18.73% 222
TOTAL	1,185

Q2 Did you notice the orange contrasted striping in the construction work zone between Palomar Airport Road and SR 78?

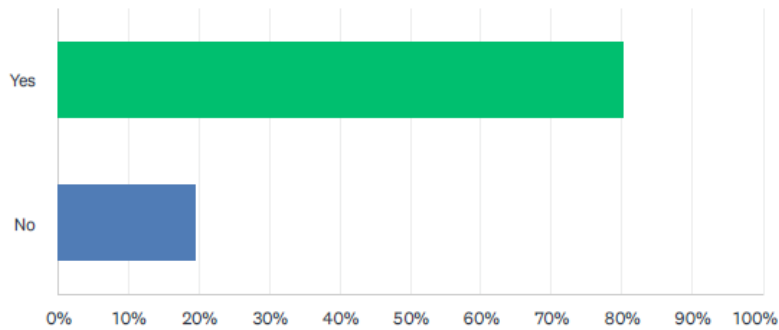
Answered: 1,185 Skipped: 0



ANSWER CHOICES	RESPONSES
Yes	93.67% 1,110
No	6.33% 75
TOTAL	1,185

### Q3 Did the orange contrasted striping increase your awareness of being in a road construction work zone?

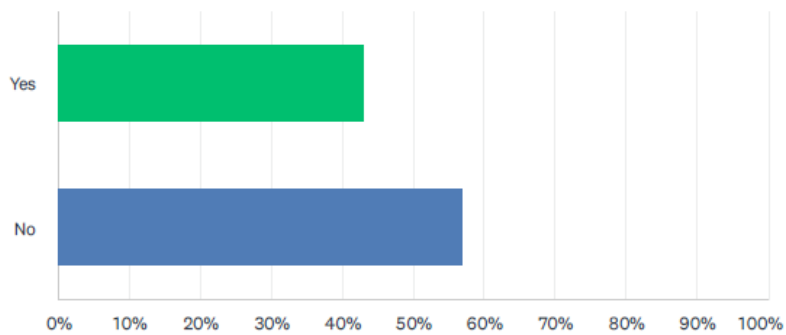
Answered: 1,093 Skipped: 92



ANSWER CHOICES	RESPONSES	
Yes	80.42%	879
No	19.58%	214
TOTAL		1,093

### Q4 Did you notice a difference in the northbound and the southbound orange contrasted laneline striping?

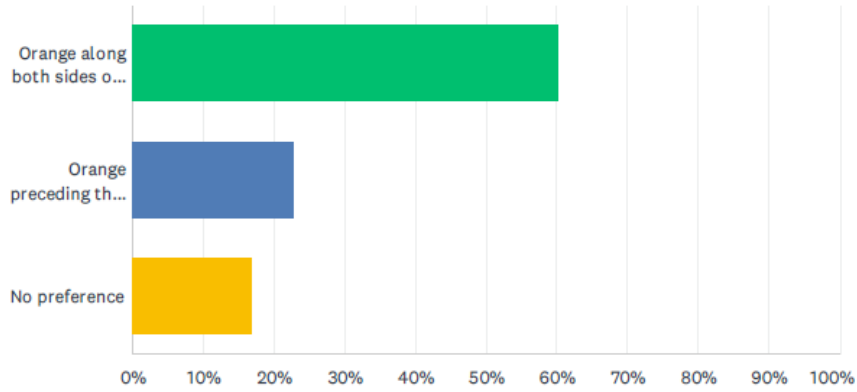
Answered: 1,087 Skipped: 98



ANSWER CHOICES	RESPONSES	
Yes	43.15%	469
No	56.85%	618
TOTAL		1,087

### Q5 If you noticed a difference, which orange contrasted laneline striping did you prefer?

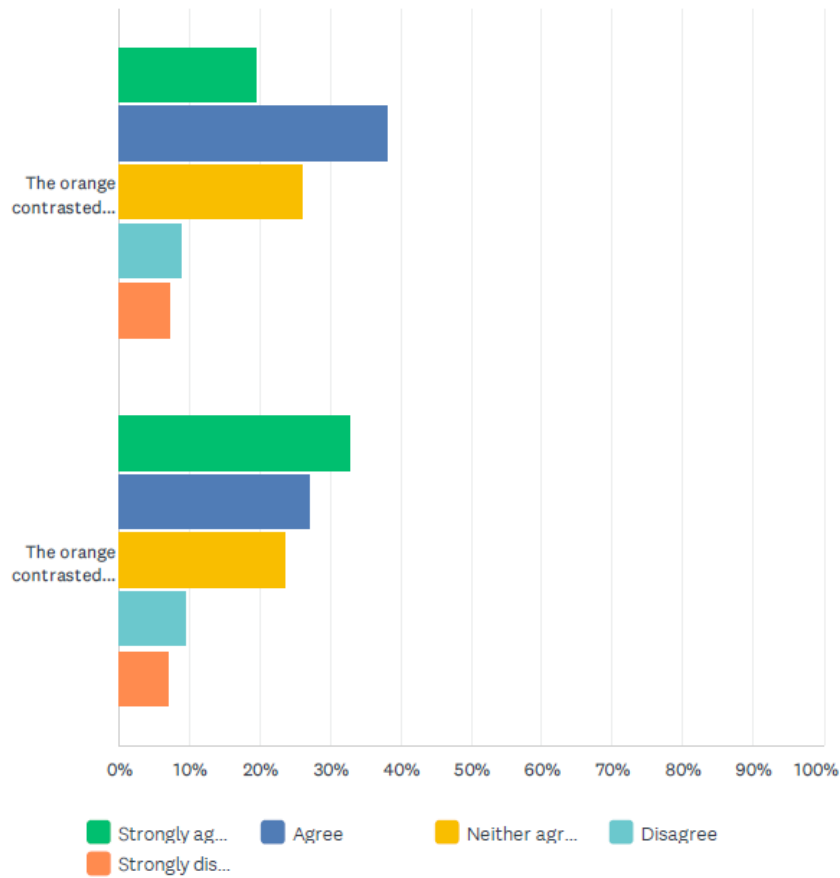
Answered: 465 Skipped: 720



ANSWER CHOICES	RESPONSES	
Orange along both sides of the white laneline in the northbound direction	60.43%	281
Orange preceding the white laneline in the southbound direction	22.80%	106
No preference	16.77%	78
<b>TOTAL</b>		<b>465</b>

Q6 Please select your level of agreement to the following statements:

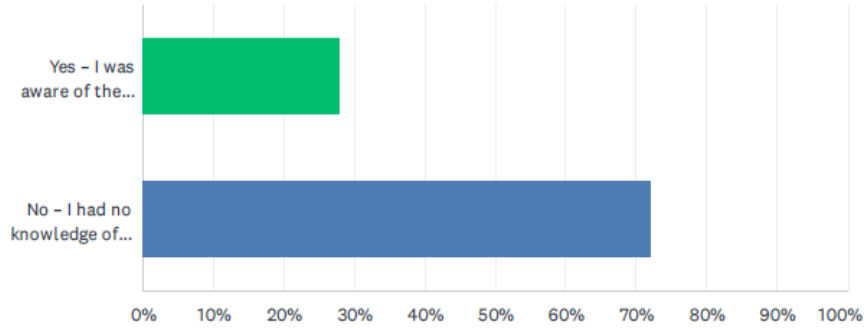
Answered: 1,079 Skipped: 106



	STRONGLY AGREE	AGREE	NEITHER AGREE OR DISAGREE	DISAGREE	STRONGLY DISAGREE	TOTAL
The orange contrasted striping caused me to drive at a more reasonable or safe speed in the work zone.	19.67% 212	38.13% 411	25.97% 280	9.00% 97	7.24% 78	1,078
The orange contrasted laneline striping makes it easier than traditional white laneline striping to stay in my lane.	32.81% 353	27.04% 291	23.61% 254	9.57% 103	6.97% 75	1,076

### Q7 Did you have prior knowledge that the striping would be orange contrasted before driving through the work zone?

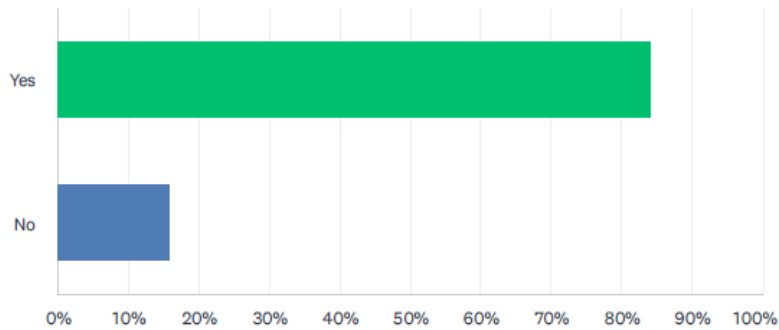
Answered: 1,067 Skipped: 118



ANSWER CHOICES	RESPONSES	
Yes – I was aware of the orange contrasted striping on this section of I-5.	27.93%	298
No – I had no knowledge of the orange contrasted striping before entering the work zone.	72.07%	769
<b>TOTAL</b>		<b>1,067</b>

### Q8 Would you like to see orange contrasted striping used in more road construction zones?

Answered: 1,142 Skipped: 43

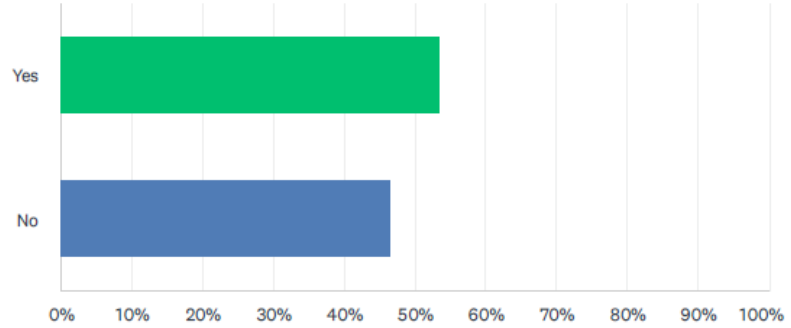


ANSWER CHOICES	RESPONSES	
Yes	84.33%	963
No	15.67%	179
<b>TOTAL</b>		<b>1,142</b>



### Q9 Have you driven through the work zone between Palomar Airport Road and SR 78 at night?

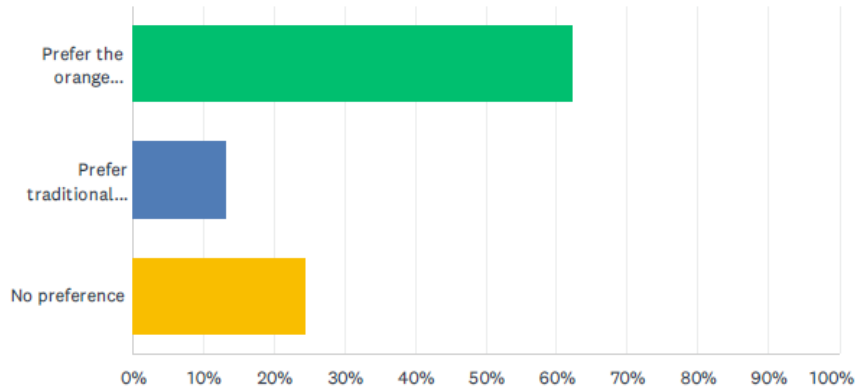
Answered: 1,142 Skipped: 43



ANSWER CHOICES	RESPONSES	
Yes	53.59%	612
No	46.41%	530
TOTAL		1,142

### Q10 If yes, what is your opinion of the orange contrasted striping at night?

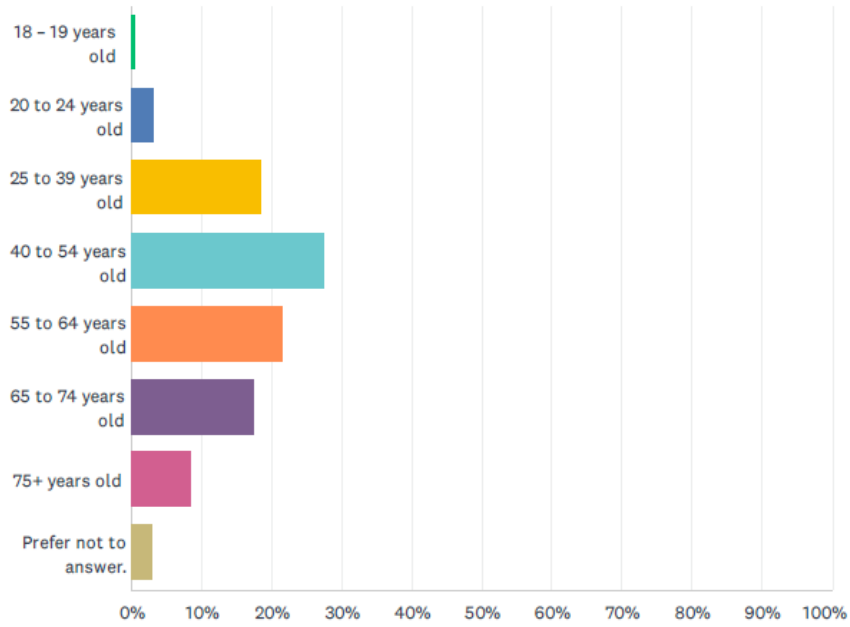
Answered: 608 Skipped: 577



ANSWER CHOICES	RESPONSES	
Prefer the orange contrasted laneline striping	62.34%	379
Prefer traditional white laneline striping	13.16%	80
No preference	24.51%	149
TOTAL		608

## Q11 Please select your age group.

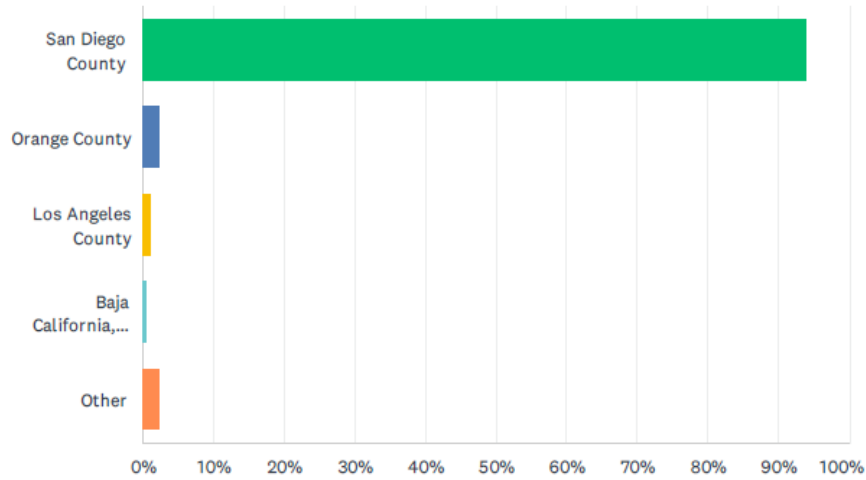
Answered: 1,136 Skipped: 49



ANSWER CHOICES	RESPONSES	
18 – 19 years old	0.44%	5
20 to 24 years old	3.17%	36
25 to 39 years old	18.49%	210
40 to 54 years old	27.55%	313
55 to 64 years old	21.48%	244
65 to 74 years old	17.52%	199
75+ years old	8.45%	96
Prefer not to answer.	2.90%	33
<b>TOTAL</b>		<b>1,136</b>

## Q12 Where do you live?

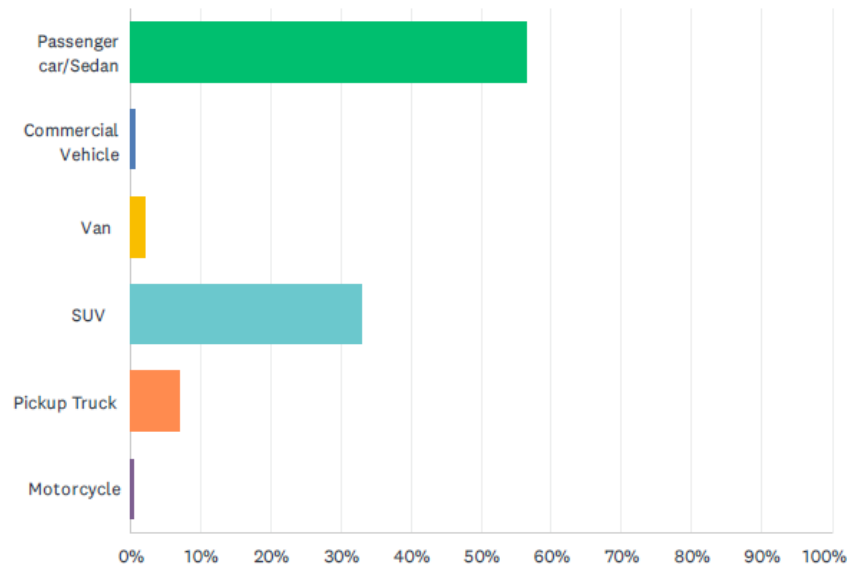
Answered: 1,136 Skipped: 49



ANSWER CHOICES	RESPONSES	
San Diego County	93.93%	1,067
Orange County	2.38%	27
Los Angeles County	1.06%	12
Baja California, Mexico	0.35%	4
Other	2.29%	26
<b>TOTAL</b>		<b>1,136</b>

### Q13 What kind of vehicle do you drive most commonly in the respective area?

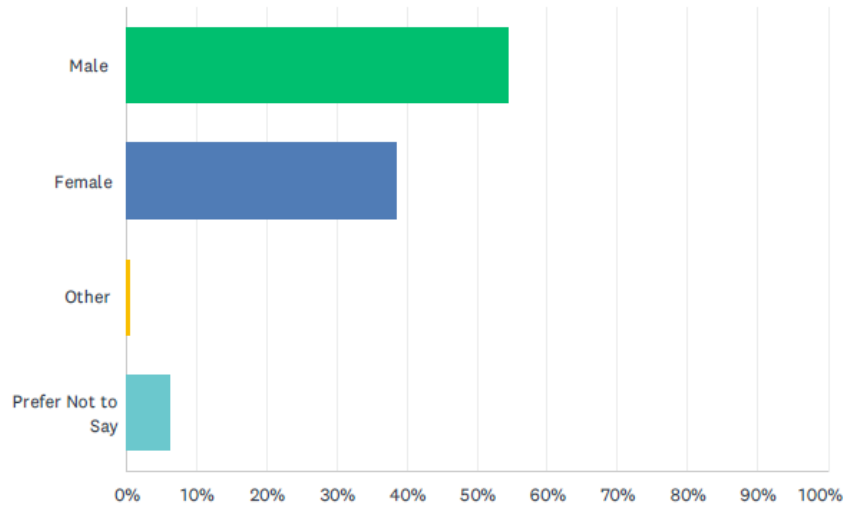
Answered: 1,136 Skipped: 49



ANSWER CHOICES	RESPONSES	
Passenger car/Sedan	56.43%	641
Commercial Vehicle	0.70%	8
Van	2.11%	24
SUV	33.10%	376
Pickup Truck	7.13%	81
Motorcycle	0.53%	6
<b>TOTAL</b>		<b>1,136</b>

# Q14 What is your gender?

Answered: 1,132 Skipped: 53



ANSWER CHOICES	RESPONSES	
Male	54.68%	619
Female	38.69%	438
Other	0.53%	6
Prefer Not to Say	6.10%	69
TOTAL		1,132